

# FACTORIZATIONS OF DIFFEOMORPHISMS OF COMPACT SURFACES WITH BOUNDARY

ANDY WAND

ABSTRACT. We study diffeomorphisms of compact, oriented surfaces, developing methods of distinguishing those which have positive factorizations into Dehn twists from those which satisfy the weaker condition of right veering. We use these to construct open book decompositions of Stein-fillable 3-manifolds whose monodromies have no positive factorization.

## 1. INTRODUCTION

Let  $\Sigma$  be a compact, orientable surface with nonempty boundary. The (restricted) mapping class group of  $\Sigma$ , denoted  $\Gamma_\Sigma$ , is the group of isotopy classes of orientation preserving diffeomorphisms of  $\Sigma$  which restrict to the identity on  $\partial\Sigma$ . The goal of this paper is to study the monoid  $Dehn^+(\Sigma) \subset \Gamma_\Sigma$  of products of right Dehn twists. In particular, we are able to show:

**Theorem 1.1.** *There exist open book decompositions which support Stein fillable contact structures but whose monodromies cannot be factorized into positive Dehn twists.*

This result follows from much more general results which we develop concerning  $Dehn^+(\Sigma)$ . We develop necessary conditions on the images of properly embedded arcs under these diffeomorphisms, and also necessary conditions for elements of the set of curves which can appear as twists in some positive factorization of a given  $\varphi \in \Gamma_\Sigma$ . The first of these can be thought of as a refinement of the *right veering* condition, which dates at least as far back as Thurston's proof of the left orderability of the braid group, and which was introduced into the study of contact structures by Honda, Kazez, and Matic in [HKM]. In that paper, it is shown that the monoid  $Veer(\Sigma) \subset \Gamma_\Sigma$  of right-veering diffeomorphisms (see Section 2 for definitions) strictly contains  $Dehn^+(\Sigma)$ . Our methods allow one to easily distinguish certain elements of  $Veer(\Sigma) \setminus Dehn^+(\Sigma)$ .

Central to much of current research in contact geometry is the relation between the monodromy of an open book decomposition and geometric properties of the contact structure, such as tightness and fillability. The starting point is the remarkable theorem of Giroux [Gi], demonstrating a one-to-one correspondence between oriented contact structures on a 3-manifold  $M$  up to isotopy and open book decompositions of  $M$  up to positive stabilization. It has been shown by Giroux [Gi], Loi and Peirgallini [LP], and Akbulut and Ozbagci [AO], that any open book with monodromy which can be factorized into positive Dehn twists supports a Stein-fillable contact structure, that every Stein-fillable contact structure is supported by *some* open book with monodromy which can be factored into positive twists, and in [HKM] that a contact structure is tight if and only if the monodromy of each

supporting open book is right-veering. The question of whether *each* open book which supports a Stein-fillable contact structure must be positive, answered in the negative by our Theorem 1.1, has been a long-standing open question.

Section 2 introduces some conventions and definitions, and provides motivation for what is to come. Section 3 introduces the concept of a *right position* for the monodromy image of a properly embedded arc in  $\Sigma$ , and compatibility conditions for right positions on collections of arc images under a given monodromy. More importantly, we show that a monodromy can have a positive factorization only if the images of any collection of nonintersecting properly embedded arcs in  $\Sigma$  admit right positions which are pairwise compatible. We use this to construct simple examples of open books whose monodromies, though right veering (see Section 2 for a precise definition), have no positive factorization.

In Section 4 we use these results to address the question of under what conditions various isotopy classes of curves on a surface can be shown not to appear as Dehn twists in any positive factorization of a given monodromy. We obtain various necessary conditions under certain assumptions on the monodromy.

Finally, in Section 5, we construct explicit examples of open book decompositions which support Stein fillable contact structures yet whose monodromies have no positive factorizations. For the construction we demonstrate a method of modifying a certain mapping class group relation (the lantern relation) into an ‘immersed’ configuration, which we then use to modify certain open books with positively factored monodromies (which therefore support Stein fillable contact manifolds) into stabilization-equivalent open books (which support the same contact structures) whose monodromies now have non-trivial negative twisting. We then apply the methods developed in the previous sections to show that in fact this negative twisting is essential.

As this work was being written, Baker, Etnyre, and Van Horn-Morris [BEV] were able to construct similar examples of non-positive open books supporting Stein fillable contact structures, all of which use the same surface,  $\Sigma_{2,1}$ , involved in our construction. Their method for demonstrating non-positivity is on the one hand substantially shorter, but on the other is quite restrictive, being entirely specific to this surface, and also requiring complete knowledge of the Stein fillings of the contact manifold in question, which is known only for a small class of contact manifolds.

We would like to thank Danny Calegari for many helpful comments on a previous version of this paper, and Rob Kirby for his support and encouragement throughout the much extended period over which it was completed. A revision was done while at the Max Planck Institute for Mathematics.

## 2. PRELIMINARIES

Throughout,  $\Sigma$  denotes a compact, orientable surface with nonempty boundary. The (restricted) mapping class group of  $\Sigma$ , denoted  $\Gamma_\Sigma$ , is the group of isotopy classes of orientation preserving diffeomorphisms of  $\Sigma$  which restrict to the identity on  $\partial\Sigma$ . In general we will not distinguish between a diffeomorphism and its isotopy class.

Let  $SCC(\Sigma)$  be the set of simple closed curves on  $\Sigma$ . Given  $\alpha \in SCC(\Sigma)$  we may define a self-diffeomorphism  $D_\alpha$  of  $\Sigma$  which is supported near  $\alpha$  as follows. Let a neighborhood  $N$  of  $\alpha$  be identified by oriented coordinate charts with the

annulus  $\{a \in \mathbb{C} \mid 1 \leq \|a\| \leq 2\}$ . Then  $D_\alpha$  is the map  $a \mapsto e^{-i2\pi(\|a\|-1)}a$  on  $N$ , and the identity on  $\Sigma \setminus \alpha$ . We call  $D_\alpha$  the *positive Dehn twist* about  $\alpha$ . The inverse operation,  $D_\alpha^{-1}$ , is a *negative* Dehn twist. We denote the mapping class of  $D_\alpha$  by  $\tau_\alpha$ . It can easily be seen that  $\tau_\alpha$  depends only on the isotopy class of  $\alpha$ .

We call  $\varphi \in \Gamma_\Sigma$  *positive* if it can be factored as a product of positive Dehn twists, and denote the monoid of such mapping classes as  $Dehn^+(\Sigma)$ .

An open book decomposition  $(\Sigma, \varphi)$ , where  $\varphi \in \Gamma_\Sigma$ , for a 3-manifold  $M$ , with binding  $K$ , is a homeomorphism between  $((\Sigma \times [0, 1]) / \sim_\varphi, (\partial\Sigma \times [0, 1]) / \sim_\varphi)$  and  $(M, K)$ . The equivalence relation  $\sim_\varphi$  is generated by  $(x, 0) \sim_\varphi (\varphi(x), 1)$  for  $x \in \Sigma$  and  $(y, t) \sim_\varphi (y, t')$  for  $y \in \partial\Sigma$ .

**Definition 2.1.** For a surface  $\Sigma$  and positive mapping class  $\varphi$ , we define the *positive extension*  $p.e.(\varphi) \subset SCC(\Sigma)$  as the set of all  $\alpha \in SCC(\Sigma)$  such that  $\tau_\alpha$  appears in some positive factorization of  $\varphi$ .

A recurring theme of this paper is to use properly embedded arcs  $\gamma_i \hookrightarrow \Sigma$  to understand restrictions on  $p.e.(\varphi)$  which can be derived from the monodromy images  $\varphi(\gamma_i)$  in  $\Sigma$  (relative to the arcs themselves). Our general method is as follows: Suppose that  $P$  is some property of pairs  $(\varphi(\gamma), \gamma)$  (which we abbreviate by referring to  $P$  as a property of the image  $\varphi(\gamma)$ ) which holds for the case  $\varphi$  is the identity, and is preserved by positive Dehn twists. Suppose then that  $\alpha \in p.e.(\varphi)$ ; then there is a positive factorization of  $\varphi$  in which  $\tau_\alpha$  is a twist. Using the well known braid relation, we can assume  $\tau_\alpha$  is the *final* twist, and so the monodromy given by  $\tau_\alpha^{-1} \circ \varphi$  is also positive. It follows that  $P$  holds for  $(\tau_\alpha^{-1} \circ \varphi)(\gamma)$  as well.

As a motivating example, consider a pair of arcs  $\gamma, \gamma' : [0, 1] \hookrightarrow \Sigma$  which share an endpoint  $\gamma(0) = \gamma'(0) = x \in \partial\Sigma$ , isotoped to minimize intersection. Following [HKM], we say  $\gamma'$  is ‘to the right’ of  $\gamma$ , denoted  $\gamma' \geq \gamma$ , if either the pair is isotopic, or if the tangent vectors  $(\dot{\gamma}'(0), \dot{\gamma}(0))$  define the orientation of  $\Sigma$  at  $x$ . The property of being ‘to the right’ of  $\gamma$  (at  $x$ ) is then a property of images  $\varphi(\gamma)$  which satisfies the conditions of the previous paragraph. We conclude that, if  $\varphi(\gamma)$  is to the right of  $\gamma$ , then  $\alpha \in p.e.(\varphi)$  only if  $(\tau_\alpha^{-1} \circ \varphi)(\gamma)$  is to the right of  $\gamma$ .

The main motivation for the use of properly embedded arcs to characterize properties of mapping classes is the well-known result that a mapping class of a surface with boundary is completely determined by the images of a set of properly embedded disjoint arcs whose complement is a disc (an application of the ‘Alexander method’, see e.g. [FM]). The most well-known example of such a property is what is now generally known as *right veering*:

**Definition 2.2.** [HKM] Let  $\varphi$  be a mapping class in  $\Gamma_\Sigma$ ,  $\gamma \hookrightarrow \Sigma$  a properly embedded arc with endpoint  $x \in \partial\Sigma$ . Then  $\varphi$  is *right veering* if, for each such  $\gamma$  and  $x$ , the image  $\varphi(\gamma)$  is to the right of  $\gamma$  at  $x$ .

We denote the set of isotopy classes of right veering diffeomorphisms as  $Veer(\Sigma) \subset \Gamma_\Sigma$ .

The right veering property can perhaps best be thought of as a necessary condition of positivity, and (by [HKM]), using the Giroux correspondence, also a necessary condition for tightness of the supported contact structure. It was however shown in that paper that right veering is far from a sufficient condition; indeed, that *any* open book decomposition may be stabilized to a right veering one.

The failure of right veering to capture either tightness or positivity is at least partially due to two obvious shortcomings. Firstly, we observe that right veering

‘only sees one arc at a time’. Referring back to the original motivation of the Alexander method, we would rather a property which can see arbitrary collections of (disjoint) arcs. Secondly, right veering is ‘localized’ to the boundary; in particular negative twisting in the interior of a surface may be hidden by positivity nearer to the boundary. The goal of Section 3 is to introduce a substantial refinement of right veering which takes into account each of these issues.

As an initial step, we consider what it should mean for two arcs to have ‘the same’ images under  $\varphi$ . An obvious candidate is the following:

**Definition 2.3.** Let  $\gamma$  be a properly embedded arc in  $\Sigma$ ,  $\varphi \in \text{Veer}(\Sigma)$ . Define the *step-down*  $\mathcal{C}_{\varphi(\gamma)}$  as the embedded multi-curve on  $\Sigma$  obtained by slicing  $\varphi(\gamma)$  along  $\gamma$ , and re-attaching the endpoints as in Figure 1.

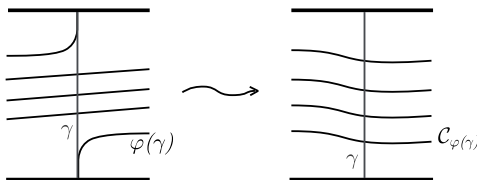


FIGURE 1. Construction of step-down

The stepdown thus allows us to relate distinct arcs to a common object, a multicurve. We want to say that a pair of arcs has in some sense ‘the same’ image if they have the same stepdown:

**Definition 2.4.** Let  $\gamma_1, \gamma_2$  be properly embedded arcs in  $\Sigma$ , and  $\varphi \in \text{Veer}(\Sigma)$ . We say the pair  $\gamma_1, \gamma_2$  is *parallel* under  $\varphi$  if  $\mathcal{C}_{\varphi(\gamma_1)}$  is isotopic to  $\mathcal{C}_{\varphi(\gamma_2)}$ .

As it stands, however, this condition is far too strict to be of any practical use. Our approach then is to ‘localize’ these ideas by decomposing the monodromy images of arcs into segments which we may then compare across distinct arc images, as will be made clear in the following section.

### 3. RIGHT POSITION

In this section, we develop the idea of a *right position* for the diffeomorphic image of a properly embedded arc in  $\Sigma$ , and develop consistency conditions which allow us to prove:

**Theorem 3.1.** *Let  $\Sigma$  be a compact surface with boundary,  $\varphi \in \Gamma_\Sigma$  admit a positive factorization into Dehn twists, and  $\{\gamma_i\}_{i=1}^n, n \geq 1$ , be a collection of non-intersecting, properly embedded arcs in  $\Sigma$ . Then  $\{(\varphi, \gamma_i)\}_{i=1}^n$  admit consistent right positions.*

#### 3.1. Definitions and examples.

**Definition 3.2.** Suppose  $\gamma \hookrightarrow \Sigma$  is a properly embedded arc with boundary  $\{c, c'\}$ , and  $\varphi \in \text{Veer}(\Sigma)$ , with  $\varphi(\gamma)$  isotoped to minimize  $\gamma \cap \varphi(\gamma)$ . Let  $A$  be a subset of the positively oriented interior intersections in  $\gamma \cap \varphi(\gamma)$  (sign conventions are illustrated in Figure 2). Then the set  $\{c, c'\} \cup A$  is a *right position*  $\mathcal{P} = \mathcal{P}(\varphi, \gamma)$  for the pair  $(\varphi, \gamma)$

Note that we are thinking of the set  $I$  of positively oriented interior intersections in  $\gamma \cap \varphi(\gamma)$  as depending only on the data of  $\gamma$  and the isotopy class  $\varphi$ , and thus independent of isotopy of  $\gamma$  and  $\varphi(\gamma)$  as long as intersection minimality holds. In particular, the integer  $|I|$  clearly depends only on this data. We may label elements of  $I$  with indices  $1, \dots, |I|$  increasing along  $\gamma$  from distinguished endpoint  $c$ . Right positions for the pair  $(\varphi, \gamma)$  are thus in 1-1 correspondence with subsets of the set of these indices.

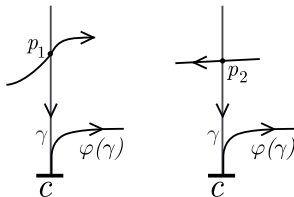


FIGURE 2.  $p_1$  is a positive,  $p_2$  a negative, point of  $\gamma \cap \varphi(\gamma)$

Associated to a right position is the set  $H(\mathcal{P}) := \{[v, v'] \subset \varphi(\gamma) \mid v, v' \in \mathcal{P}\}$ . We denote these segments by  $h_{v,v'}$ , or, if only a single endpoint is required, simply use  $h_v$  to denote a subarc starting from  $v$  and extending as long as the context requires. In this case direction of extension along  $\varphi(\gamma)$  will be clear from context.

Right position can thus be thought of as a way of decomposing the image  $\varphi(\gamma)$  into ‘horizontal’ segments  $H(\mathcal{P})$ , separated by the points  $\mathcal{P}$  (Figure 3). Note that for any right-veering  $\varphi$ , and any properly embedded arc  $\gamma$ ,  $(\varphi, \gamma)$  has a trivial right position consisting of the points  $\partial(\gamma)$ , and so there is a single horizontal segment  $h_{c,c'} = \varphi(\gamma)$ . Of course if  $I$  is nonempty, there are  $2^{|I|} - 1$  non-trivial right positions. Intuitively, the points in  $\mathcal{P}$  play a role analogous to the initial (boundary) points of the arc, allowing us to localize the global ‘right’ness of an arc image through the decomposition into horizontal segments (this will be made more precise further on in the paper).

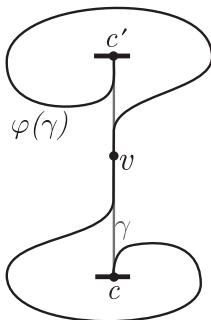


FIGURE 3.  $\mathcal{P} = \{c, v, c'\}$  is a right position of  $(\varphi, \gamma)$ . There are three distinct horizontal segments:  $h_{c,v}$ ,  $h_{v,c'}$ , and  $h_{c,c'}$

We are interested in using right position to compare *pairs* of arcs; the idea being that, if  $\varphi$  is positive, we expect to be able to view any pair of horizontal segments as either unrelated, or as belonging to the ‘same’ horizontal segment.

To get started, we need to be able to compare horizontal segments. To that end, we have:

**Definition 3.3.** Suppose  $\gamma_i$ ,  $i = 1, \dots, 4$  are properly embedded arcs in a surface  $\Sigma$ . A *rectangular region* in  $\Sigma$  is the image of an immersion of the standard disc  $[0, 1] \times [0, 1]$ , such that the image of each side is a subset of one of the  $\gamma_i$ , and corners map to intersections  $\gamma_i \cap \gamma_j$ .

**Definition 3.4.** Let  $\gamma_1, \gamma_2$  be distinct, properly embedded arcs in  $\Sigma$ ,  $\varphi \in \text{Veer}(\Sigma)$ , and  $\mathcal{P}_i = \mathcal{P}_i(\varphi, \gamma_i)$  a right position for  $i = 1, 2$ . We say that  $h_v \in H(\mathcal{P}_1)$  and  $h_w \in H(\mathcal{P}_2)$  are *initially parallel (along  $B$ )* if there is a rectangular region  $B$  in  $\Sigma$  bounded by  $\gamma_1, h_w, \gamma_2, h_v$ , such that, if each of  $h_v$  and  $h_w$  is oriented *away* from its respective vertical point, then the orientations give an orientation of  $\partial B$  (see Figure 4). We refer to  $v$  and  $w$  as the *endpoints* of the region, and the remaining two corners *midpoints*.

*Remark 3.5.* It is helpful to think of the rectangular region  $B$  along which two segments are initially parallel as the image under the covering map  $\rho : \tilde{\Sigma} \rightarrow \Sigma$  of an *embedded* disc in the universal cover. As such, we will draw these regions as embedded discs whenever doing so does not result in any loss of essential information.

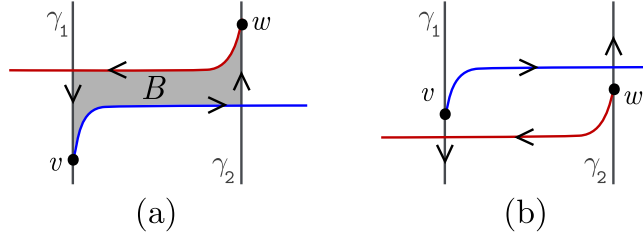


FIGURE 4. (a)  $h_v$  and  $h_w$  are initially parallel along  $B$ . (b)  $h_v$  and  $h_w$  are *not* initially parallel.

So, to say that a pair of horizontal segments is ‘unrelated’ is to say that they are not initially parallel. It is left to clarify what we expect of initially parallel segments  $h_v$  and  $h_w$ . The idea is to extend the notion of being parallel up to a second pair of vertical points  $v' w'$ , and thus to the horizontal segments  $h_{v,v'}$   $h_{w,w'}$ , such that the pair is ‘completed’; i.e. if we switch the orientations so that  $h_{v'}$  and  $h_{w'}$  are taken as extending in the opposite direction, then  $h_{v'}$  and  $h_{w'}$  are themselves initially parallel, and the rectangular regions complete one another to form a ‘singular annulus’ (Figure 5) (notice that there is no restriction on intersections of the regions beyond those given by the properties of the boundary arcs). To be precise:

**Definition 3.6.** Let  $\gamma_i, \mathcal{P}_i$ ,  $i = 1, 2$  be as in the previous definition. Suppose horizontal segments  $h_v$  and  $h_w$  are initially parallel along  $B$ , with corners  $v, w, y_1, y_2$ , where  $y_i \in \gamma_i$ . Then the pair  $h_v, h_w$  are *completed* if there are points  $v' \in \mathcal{P}_1, w' \in \mathcal{P}_2$ , which we call the *endpoints*, such that the arcs  $\gamma_1, \gamma_2, h_{v,v'}, h_{w,w'}$  bound a second rectangular region  $B'$ , with corners  $v', w', y_1, y_2$  (Figure 6). We say the pair  $h_v, h_w$  are *completed along  $B'$* . Note that, turning the picture upside-down, the arcs  $h_{v',v}$  and  $h_{w',w}$  are initially parallel along  $B'$ , and completed along  $B$ .

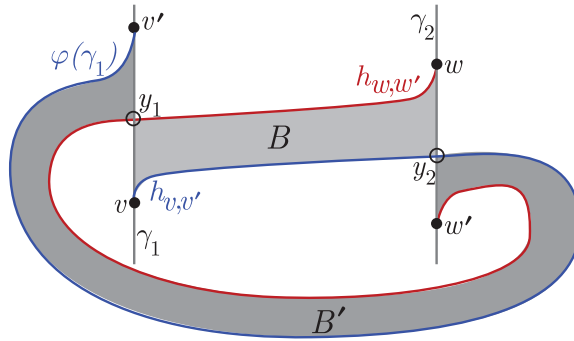


FIGURE 5. Horizontal segments  $h_{v,v'}$ ,  $h_{w,w'}$  complete one another, forming the boundary of a ‘singular annulus’.

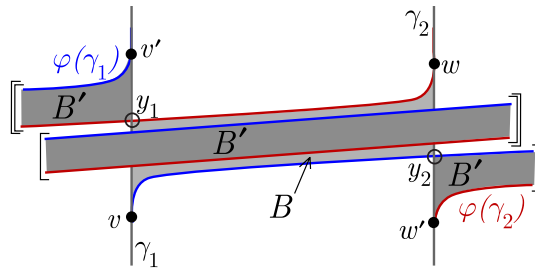


FIGURE 6. The horizontal segments  $h_v, h_w$  are completed by points  $v', w'$ . Strands which terminate in like brackets are meant to be identified along arcs which are not drawn; a similar convention will be used throughout the paper.

*Remark 3.7.* Throughout the paper, we will draw vertical points as solid dots, midpoints as circles.

As justification of the term ‘singular annulus’, note that if initially parallel  $h_v$  and  $h_w$  are completed then the resolution of the midpoints  $y_1$  and  $y_2$  as in Figure 7 transforms the ‘singular’  $B \cup B'$  into an immersed annulus.

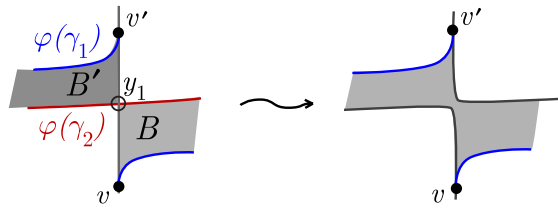


FIGURE 7. resolution of  $y_1$

We have come to the key definition of this section:

**Definition 3.8.** Let  $\{\gamma_i\}_{i=1}^n$ ,  $n \geq 1$ , be a collection of non-intersecting, properly embedded arcs in  $\Sigma$ ,  $\varphi \in \text{Veer}(\Sigma)$ , and  $\mathcal{P}_i = \mathcal{P}_i(\varphi, \gamma_i)$  a right position for each  $i$ . We say the  $\mathcal{P}_i$  are *consistent* if for all  $j \neq k$ , each pair of horizontal segments

$h \in H(\mathcal{P}_j)$  and  $g \in H(\mathcal{P}_k)$  is completed if initially parallel. For the case  $n = 2$ , we say  $(\varphi, \gamma_1)$  and  $(\varphi, \gamma_2)$  are a *right pair* if they admit consistent right positions  $\mathcal{P}_1$  and  $\mathcal{P}_2$ .

*Example 3.9.* The pair  $(\varphi, \gamma_1), (\varphi, \gamma_2)$  in Figure 8(a), with the right positions indicated, is a right pair, with two completed pairs of horizontal arcs, as indicated in (b). It is straightforward to verify that there are no other initially parallel segments.

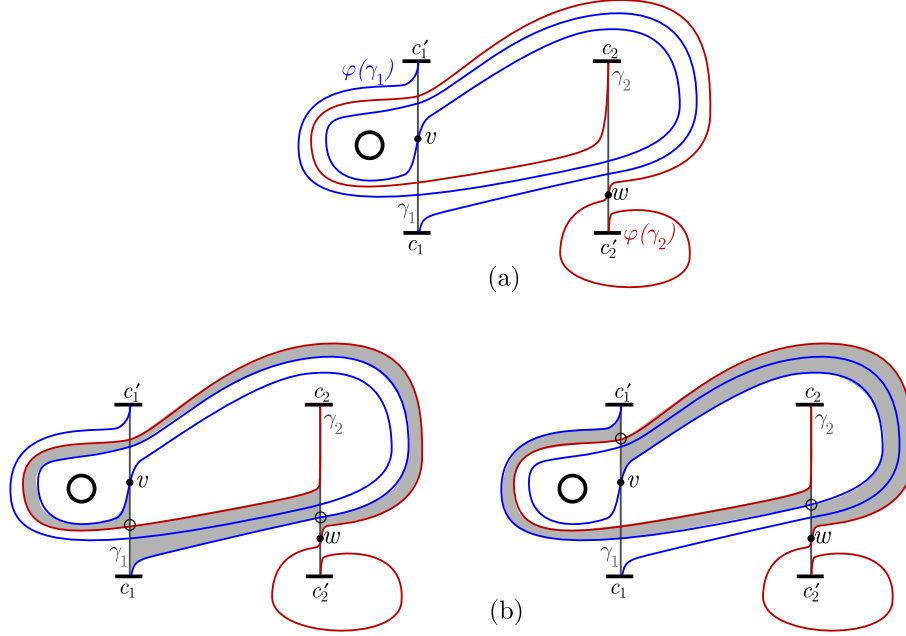


FIGURE 8. (a): The pair  $(\varphi, \gamma_1), (\varphi, \gamma_2)$  is a right pair. The pairs of completing discs are shaded in (b).

The pair in Figure 9, however, is not a right pair: Suppose  $\mathcal{P}_1$  and  $\mathcal{P}_2$  are consistent right positions. Then  $h_{c_1}$  and  $h_{c_2}$  are initially parallel along  $B$ , so there must be  $v \in \mathcal{P}_1$  and  $w \in \mathcal{P}_2$  satisfying the compatibility conditions. The only candidates are  $c_1'$  and  $c_2'$ , and these do not give completed horizontal segments. By Theorem 3.1, this is sufficient to conclude that the mapping class has no positive factorization.

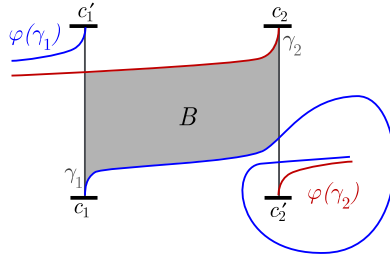


FIGURE 9. The pair  $(\varphi, \gamma_1), (\varphi, \gamma_2)$  is *not* a right pair.



Finally, consider the open book decomposition indicated in Figure 10, where the monodromy  $\varphi$  is  $\tau_\alpha^{-1}\tau_{\beta_1}^{n_1}\tau_{\beta_2}^{n_2}\tau_{\beta_3}\tau_{\beta_4}$  (we have drawn the case  $n_1 = 1$ ). Using the shaded initially parallel region, observe that the pair  $(\varphi, \gamma_1)$  and  $(\varphi, \gamma_2)$  are not a right pair; indeed, for any  $n_1, n_2 > 0$  this will clearly remain true, as the picture will only be modified by twists about the boundary component parallel to  $\beta_2$ . In particular,  $\varphi$  has no positive factorization for any  $n_1$  and  $n_2$ . On the other hand, it is a simple exercise to show that for any positive  $n_1$  and  $n_2$  each boundary component is ‘protected’; i.e. each properly embedded arc with endpoint on the boundary component under consideration maps to the right at that point (it suffices to check for the either of the boundary components parallel to  $\beta_3$  or  $\beta_4$ ). In particular, each such monodromy is right-veering. See e.g. [L] for a more in-depth examination of this example.

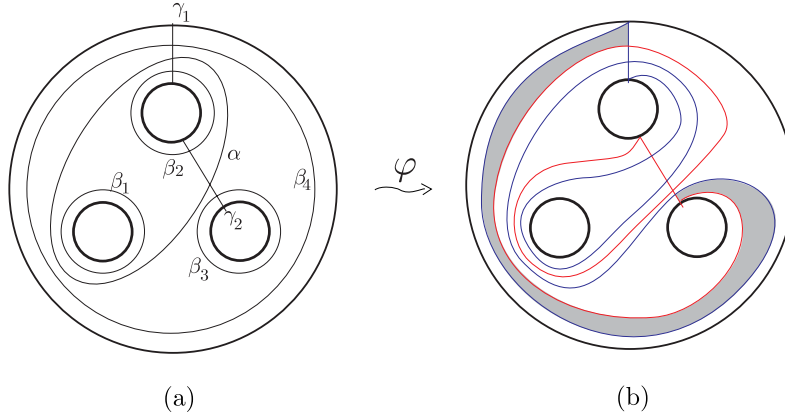


FIGURE 10. (a) Surface and curves for the open book decomposition  $(\Sigma_{0,4}, \tau_\alpha^{-1}\tau_{\beta_1}^{n_1}\tau_{\beta_2}^{n_2}\tau_{\beta_3}\tau_{\beta_4})$ . (b) The pair  $(\varphi, \gamma_1)$  (in blue), and  $(\varphi, \gamma_2)$  (in red) is *not* a right pair, but  $\varphi$  is right veering for all  $m, n \geq 1$ .

**3.2. The right position associated to a factorization.** Suppose we have a surface  $\Sigma$ , a mapping class  $\varphi \in \Gamma_\Sigma$  given as a factorization  $\omega$  of positive Dehn twists, and a set  $\{\gamma_i\}_{i=1}^n$  of pairwise non-intersecting, properly embedded arcs in  $\Sigma$ . While each such arc admits at least one, and possibly many, right positions, the goal of this subsection is to give an algorithm which associates to  $\omega$  a unique right position, denoted  $\mathcal{P}_\omega(\gamma_i)$  for each  $i$ , such that the set  $\{\mathcal{P}_\omega(\gamma_i)\}_{i=1}^n$  is consistent (Definition 3.8). Note that existence of such an algorithm proves Theorem 3.1.

We begin with the case of a single arc  $\gamma$ , and construct  $\mathcal{P}_\omega(\gamma)$  by induction on the number of twists  $m$  in  $\omega$ .

**Base step:  $m = 1$**  Suppose  $\varphi = \tau_\alpha$ , for some  $\alpha \in SCC(\Sigma)$ . We begin by isotoping  $\alpha$  so as to minimize  $\alpha \cap \gamma$ . Label  $\alpha \cap \gamma = \{x_1, \dots, x_p\}$ , with indices increasing along  $\gamma$ . We then define the right position  $\mathcal{P}(\tau_\alpha, \gamma)$  associated to the factorization  $\tau_\alpha$  to be the points  $\{c = v_0, v_1, \dots, v_{p-1}, c' = v_p\}$ , where  $\{c, c'\} = \partial(\gamma)$ , and, for  $0 < i < p$ ,  $v_i$  lies in the connected component of  $\gamma \setminus \text{support}(\tau_\alpha)$  between  $x_i$  and  $x_{i+1}$  (Figure 11).

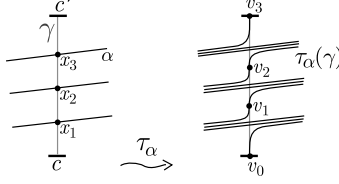


FIGURE 11. The base case: the right position  $\mathcal{P}(\tau_\alpha, \gamma)$  associated to a single Dehn twist.

As an aside, note that, in this case, if  $\bar{h}_{v_i, v_j}$  denotes the closed curve obtained from the horizontal segment  $h_{v_i, v_j}$  by adding the segment along  $\gamma$  from  $v_i$  to  $v_j$ , then  $\bar{h}_{v_i, v_{i+1}} \simeq \alpha$  for  $0 \leq i < p$ . Compare this with the *stepdown* of Definition 2.3.

Now, this construction has as input only the isotopy class of  $\alpha$ , so we have:

**Lemma 3.10.** *The right position  $\mathcal{P}_{\tau_\alpha}(\gamma)$  defined in **base step** depends only on the isotopy class of  $\alpha$ .*

**3.2.1. Description of the inductive step.** For the inductive step, we demonstrate an algorithm which has as input a surface  $\Sigma$ , mapping class  $\varphi \in \text{Veer}(\Sigma)$ , properly embedded arc  $\gamma \hookrightarrow \Sigma$ , right position  $\mathcal{P}(\varphi, \gamma)$ , and  $\alpha \in \text{SCC}(\Sigma)$ . The output then will be a unique right position  $\mathcal{P}^\alpha = \mathcal{P}^\alpha(\tau_\alpha \circ \varphi, \gamma)$ . A key attribute of the algorithm will be that, while  $\alpha$  is given as a particular representative of its isotopy class  $[\alpha]$ , the resulting right position  $\mathcal{P}^\alpha$  will be independent of choice of representative.

To keep track of things in an isotopy-independent way, we consider *triangular regions* in  $\Sigma$ :

**Definition 3.11.** Suppose  $\gamma$  and  $\gamma'$  are properly embedded arcs in a surface  $\Sigma$  such that  $\partial(\gamma) = \partial(\gamma')$ , isotoped to minimize intersection. Then for  $\alpha \in \text{SCC}(\Sigma)$ , a *triangular region*  $T$  (of the triple  $(\gamma, \gamma', \alpha)$ ) is the image of an immersion  $f : \Delta \looparrowright \Sigma$ , where  $\Delta$  is a 2-simplex with vertices  $t_1, t_2, t_3$  and edges  $t_1t_2, t_2t_3, t_3t_1$ , such that  $f(t_1t_2) \subset \gamma$ ,  $f(t_2t_3) \subset \gamma'$ , and  $f(t_3t_1) \subset \alpha$ .

**Definition 3.12.** A triangular region  $T$  for the ordered triple  $(\alpha, \gamma, \gamma')$  is

- *essential* if  $\alpha$  can be isotoped relative to  $T \cap \alpha$  so as to intersect  $\gamma$  and  $\gamma'$  in a minimal number of points (Figure 15(a)).
- *upward (downward)* if bounded by  $\alpha, \gamma, \gamma'$  in clockwise (counterclockwise) order (Figure 15(b)).

We begin with a brief description of the algorithm, with an illustrative example in Figure 12. Let  $\alpha$  be a representative of  $[\alpha]$  which minimizes  $\alpha \cap \gamma$  and  $\alpha \cap \varphi(\gamma)$ , so in particular all triangular regions for the triple  $(\alpha, \gamma, \varphi(\gamma))$  are essential. Furthermore, chose  $\text{support}(D_\alpha)$  so as not to intersect any point of  $\gamma \cap \varphi(\gamma)$  (Figure 12(a)) (recall that  $D_\alpha$  refers to the Dehn twist about fixed  $\alpha \in [\alpha]$ , while  $\tau_\alpha$  is its mapping class). Consider then the image  $D_\alpha(\varphi(\gamma))$ , which differs from  $\varphi(\gamma)$  only in  $\text{support}(D_\alpha)$  (Figure 12(b)). Now, the only bigons bounded by the arcs  $D_\alpha(\varphi(\gamma))$  and  $\gamma$  contain vertices which were in upward triangles in the original configuration. In particular, there is an isotopy of  $D_\alpha(\varphi(\gamma))$  over (possibly some subset of) these bigons which minimizes  $\gamma \cap \tau_\alpha(\varphi(\gamma))$  (the issue of exactly when a proper subset of the bigons suffices is taken up below, in Section 3.2.2). There is thus an inclusion map  $i$  of those points of  $\mathcal{P}$  which are *not* in upward triangles into the set of positive intersections of  $\gamma \cap \tau_\alpha(\varphi(\gamma))$ , whose image is therefore a right position (Figure 12(c)).

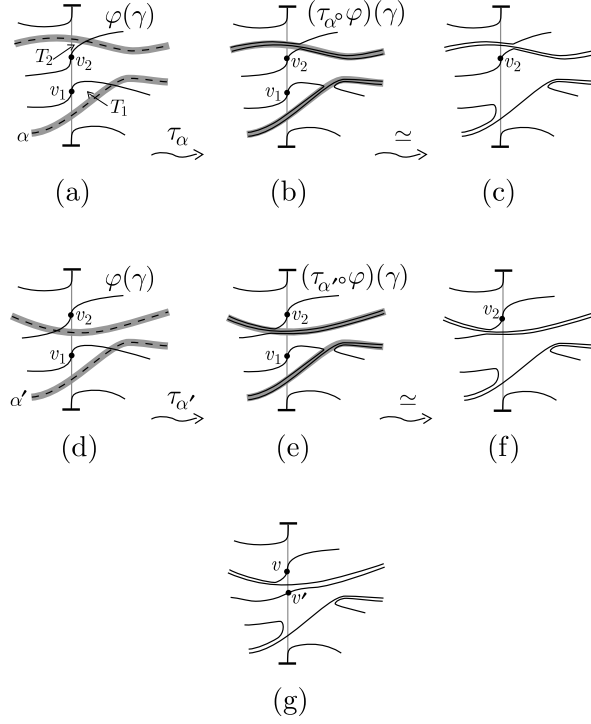


FIGURE 12. Top row: (a) The setup for the above discussion. Triangular region  $T_1$  is upward, while  $T_2$  is downward. The support of the twist  $\tau_\alpha$  is shaded. (b) The result of  $\tau_\alpha$ . There is a single bigon, in which  $v_1$  is a vertex. (c) The result of isotoping  $\tau_\alpha(\varphi(\gamma))$  over this bigon so as to minimize intersection with  $\gamma$ . Bottom row: Same as the top, but with  $\alpha'$ . Note that while the images  $\tau_\alpha(\varphi(\gamma))$ ,  $\tau_{\alpha'}(\varphi(\gamma))$  are of course isotopic, the right positions of (c) and (f) differ. Finally, (g) indicates the isotopy-independent right position (i.e. the points  $v$  and  $v'$ , along with  $\partial\gamma$ ) which our algorithm is meant to pick out.

Note however that, as described, this resulting right position is *not* independent of the choice of  $\alpha$  - indeed, if  $T_1$  is any downward triangle, we may isotope the given  $\alpha$  over  $T_1$  (e.g. go from Figure 12(a) to Figure 12(d)) to obtain  $\alpha' \in [\alpha]$  such that  $\alpha' \cap \gamma$  and  $\alpha' \cap \varphi(\gamma)$  are also minimal. The algorithm of the previous paragraph then determines a distinct right position for  $(\tau_{\alpha'} \circ \varphi, \gamma)$  (Figure 12(f)). Motivated by this observation, we refine the algorithm by adding *all* points of  $\gamma \cap \tau_\alpha(\varphi(\gamma))$  which would be obtained by running the algorithm for any allowable isotopy of  $\alpha$  (Figure 12(g)). As we shall see, this simply involves adding a single point for each downward triangle in the original configuration.

**3.2.2. Details of the inductive step.** This subsection gives the technical details necessary to make the algorithm work as advertised, and extracts and proves the various properties we will require the algorithm and its result to have.

We begin with some results concerning triangular regions. Let  $\gamma, \gamma'$  be properly embedded, non-isotopic arcs in  $\Sigma$ , with  $\partial(\gamma) = \partial(\gamma')$ , isotoped to minimize intersection. Our motivating example, of course, is the case  $\gamma' = \varphi(\gamma)$ , so we orient the arcs as in Figure 2. Let  $\mathcal{G}$  denote their union. A *vertex* of  $\mathcal{G}$  is thus an intersection point  $\gamma \cap \gamma'$ . Let  $\alpha \in SCC(\Sigma)$  be isotoped so as not to intersect any vertex of  $\mathcal{G}$ . A *bigon* in this setup is an immersed disc  $B$  bounded by the pair  $(\alpha, \gamma)$  or by  $(\alpha, \gamma')$ . Similarly, a *bigon chain* is a set  $\{B_i\}_{i=1}^n$  of bigons bounded exclusively by one of the pairs  $(\alpha, \gamma), (\alpha, \gamma')$ , for which the union  $\bigcup\{\alpha \cap \partial(B_i)\}_{i=1}^n$  is a connected segment of  $\alpha$  (Figure 13(a)). Finally, we say points  $p, p' \in \alpha \cap \mathcal{G}$  are *bigon-related* if they are vertices in a common bigon chain.

Suppose then that  $T$  is a triangular region in this setup, with vertex  $v \in \gamma \cap \gamma'$ . We define the *bigon collection associated to  $T$* , denoted  $\mathcal{B}_T$ , as the set of points  $\{p \in \alpha \cap \mathcal{G} \mid p \text{ is bigon-related to a vertex of } T\}$  (Figure 13(b)). Note that, if a vertex of  $T$  is not a vertex in any bigon, the vertex is still included in  $\mathcal{B}_T$ , so that, for example, the bigon collection associated to an essential triangle  $T$  is just the vertices of  $T$ .

Now, the point  $v$  divides each of  $\gamma, \gamma'$  into two segments, which we label  $\gamma_+, \gamma_-, \gamma'_+, \gamma'_-$  in accordance with the orientation. For each bigon collection  $\mathcal{B}$  associated to a triangle with vertex  $v$ , we define  $\sigma_v(\mathcal{B}) := (|\mathcal{B} \cap \gamma_+|, |\mathcal{B} \cap \gamma_-|, |\mathcal{B} \cap \gamma'_+|, |\mathcal{B} \cap \gamma'_-|) \in (\mathbb{Z}_2)^4$ , where intersection numbers are taken mod 2 (Figure 13(b)).

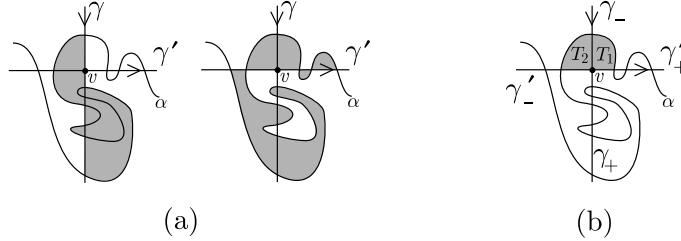


FIGURE 13. (a) The shaded regions are distinct maximal bigon chains. (b) As each chain from (a) has a vertex in each of the triangular regions  $T_1, T_2$ , the bigon collection  $\mathcal{B}_{T_1} = \mathcal{B}_{T_2}$  includes each intersection point of each chain. In this example,  $\sigma_v(\mathcal{B}_{T_1}) = (0, 1, 1, 0)$ , so the collection is downward. Note that  $T_1$  is an essential downward triangular region (Definition 3.12), while  $T_2$  is non-essential.

Finally, we label a bigon collection  $\mathcal{B}$  as *upward* (with respect to  $v$ ) if  $\sigma_v(\mathcal{B}) \in \{(1, 0, 1, 0), (0, 1, 0, 1)\}$ , *downward* if  $\sigma_v(\mathcal{B}) \in \{(1, 0, 0, 1), (0, 1, 1, 0)\}$ , *non-essential* otherwise (Figure 13(b)). Compare with Definition 3.12,

**Lemma 3.13.** *Let  $\alpha \in [\alpha]$  be such that  $\alpha \cap \gamma$  and  $\alpha \cap \varphi(\gamma)$  are minimal, and  $v \in \varphi(\gamma) \cap \gamma$ . Then the number of essential triangles with vertex  $v$  in the triple  $(\gamma, \varphi(\gamma), \alpha)$  depends only on the isotopy class  $[\alpha]$ .*

*Proof.* Let  $\alpha$  be an arbitrary representative of  $[\alpha]$  (in particular  $\alpha \cap \gamma$  and  $\alpha \cap \varphi(\gamma)$  are not necessarily minimal), and  $v$  a vertex. We define an equivalence relation on the set of triangular regions with vertex  $v$  by  $T_1 \sim T_2 \Leftrightarrow \mathcal{B}_{T_1} = \mathcal{B}_{T_2}$ . In particular, there is a 1-1 correspondence between  $\{\text{triangular regions with vertex } v\} / \sim$  and the set of bigon collections associated to triangular regions with vertex  $v$ .

Now, if  $\alpha'$  is another representative of the isotopy class  $[\alpha]$ , we may break the isotopy into a sequence  $\alpha = \alpha_1 \simeq \dots \simeq \alpha_n = \alpha'$ , where each isotopy  $\alpha_i \simeq \alpha_{i+1}$  is either a bigon birth, a bigon death, or does not affect either of  $|\alpha \cap \gamma|$  and  $|\alpha \cup \varphi(\gamma)|$ . Note that, if  $\mathcal{B}$  is upward or downward, an isotopy  $\alpha_i \simeq \alpha_{i+1}$  which does not cross  $v$  does not affect  $\sigma_v(\mathcal{B})$ , while an isotopy  $\alpha_i \simeq \alpha_{i+1}$  which crosses  $v$  changes  $\sigma_v(\mathcal{B})$  by addition with  $(1, 1, 1, 1)$ . In either case, the classification is preserved; i.e. we can keep track of an essential upward (downward) bigon collection through each isotopy. Furthermore, any two distinct bigon collections will have distinct images under each such isotopy (a bigon birth/death cannot cause two maximal bigon chains to merge). We therefore have an integer  $a(v)$ , defined as the number of essential bigon collections  $\mathcal{B}$  associated to triangular regions with vertex  $v$ , which depends only on  $[\alpha]$

Finally, if we take  $\alpha'$  to be a representative of  $[\alpha]$  which intersects  $\gamma$  and  $\varphi(\gamma)$  minimally, then  $\{\text{triangular regions with vertex } v\} / \sim$  is by definition just the set of essential triangular regions with vertex  $v$ , and has size  $a(v)$ . □

**Lemma 3.14.** *Let  $\alpha$  be a fixed representative of the isotopy class  $[\alpha]$  which has minimal intersection with  $\gamma \cap \varphi(\gamma)$ , and  $v \in \gamma \cap \varphi(\gamma)$  a vertex of an upward triangle  $T$ . Then  $v$  is not a vertex of any downward triangular region  $T'$  for  $\alpha$ .*

*Proof.* Consider the neighborhood of  $v$  as labeled in Figure 14. As  $T$  is upward, it must be  $T_1$  or  $T_3$ , while  $T'$  must be  $T_2$  or  $T_4$ . Without loss of generality then suppose  $T = T_1$  is a triangular region. But then neither of  $T_2, T_4$  can be triangular regions without creating a bigon, violating minimality. □

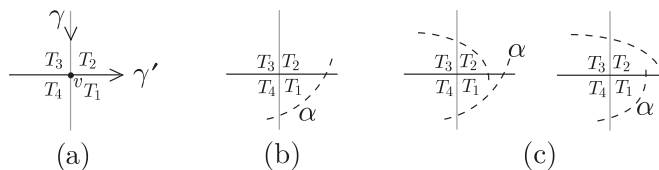


FIGURE 14. (a) A neighborhood of  $v$ . (b) The upward triangle  $T_1$ . (c) As  $\alpha$  has no self-intersection,  $T_2$  cannot be a triangular region without creating a bigon.

It follows from Lemmas 3.13 and 3.14 that we may unambiguously refer to a vertex of an essential triangular region as downward, upward, or neither, in accordance with any essential triangular region of which it is a vertex. In particular, if  $\alpha$  has minimal intersection with  $\gamma, \varphi(\gamma)$ , then all triangular regions are essential. Henceforth we will drop the adjective ‘essential’. Figure 15(b) and (c) give examples of the various types of vertices.

**Definition 3.15.** Suppose  $T$  is a triangular region with vertex  $v \in \gamma \cap \varphi(\gamma)$ . Isotope  $\alpha$  over  $T$  to obtain another triangular region  $T'$  of the same type (upward/downward) as  $T$  with vertex  $v$ , as in Figure 16. Note that if  $T$  contains sub-regions with vertex  $v$  then the process involves isotoping the innermost region first, and proceeding to  $T$  itself. We call such an isotopy a *shift over  $v$* .

We require a final pair of definitions before we bring the pieces together:

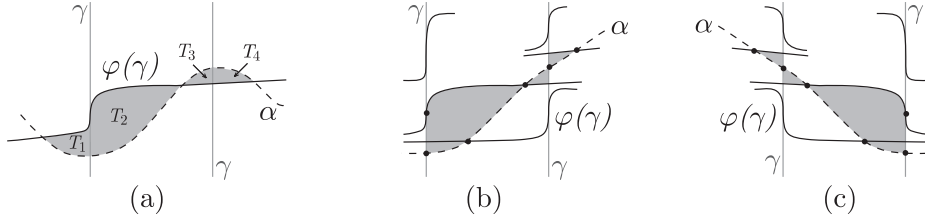


FIGURE 15. (a) If the shaded region is a maximal bigon chain, then  $T_1$  and  $T_4$  are essential triangular regions for  $(\alpha, \gamma, \gamma')$ ,  $T_2$  and  $T_3$  are not. (b) Upward triangular regions and vertices. (c) Downward triangular regions and vertices.

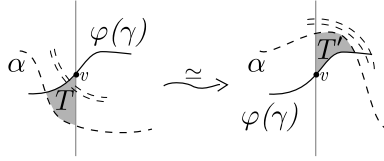


FIGURE 16. A shift over a vertex  $v$ .

**Definition 3.16.** Let  $\gamma$  be a properly embedded arc in  $\Sigma$ ,  $\varphi \in \Gamma_\Sigma$ . Suppose  $\gamma, \varphi(\gamma)$ , and  $\alpha$  are isotoped to minimize intersection. Let  $\alpha \in SCC(\Sigma)$  be a fixed representative of its isotopy class which has minimal intersection with  $\gamma$  and  $\varphi(\gamma)$ . Choose  $support(D_\alpha)$  to be disjoint from  $\gamma \cap \varphi(\gamma)$ . Then let  $i_\alpha : (\gamma \cap \varphi(\gamma)) \hookrightarrow (\gamma \cap D_\alpha(\varphi(\gamma)))$  be the obvious inclusion. Note that  $D_\alpha(\varphi(\gamma))$  will not in general have minimal intersection with  $\gamma$ .

**Definition 3.17.** Let  $\gamma$  and  $\varphi$  be as in the previous definition, and  $v \in \gamma \cap \varphi(\gamma)$  a positively oriented intersection point. If there is a representative  $\alpha \in SCC(\Sigma)$  of the isotopy class  $[\alpha]$  such that the image  $D_\alpha(\varphi(\gamma))$  which differs from  $\varphi(\gamma)$  only in a support neighborhood of  $\alpha$  can be isotoped to minimally intersect  $\gamma$  while fixing a neighborhood of  $i_\alpha(v)$ , we say  $v$  and  $i_\alpha(v)$  are *fixable under* the mapping class  $\tau_\alpha$ . Similarly, for a factorization  $\omega = \tau_{\alpha_n} \cdots \tau_{\alpha_1}$  of  $\varphi$ , we say  $v \in \varphi(\gamma) \cap \gamma$  is *fixable under*  $\omega$  if  $v$  is fixable under each successive  $\tau_{\alpha_i}$ . Various examples are gathered in Figure 17.

*Observation 3.18.* Using this terminology, we have the following characterization of the right position  $\mathcal{P}_\omega(\gamma)$  which the reader may or may not find helpful: The right position  $\mathcal{P}_\omega(\gamma)$  is a maximal subset of the positive intersections in  $\gamma \cap \varphi(\gamma)$  such that each point of  $\mathcal{P}_\omega(\gamma)$  is fixable under  $\omega$ , and is in fact the unique such position up to a choice involved in the coarsening process (described in detail in the proof of Lemma 3.21).

As a simple example, Figure 18 illustrates distinct right positions of a pair  $(\varphi, \gamma)$  associated to distinct factorizations of a mapping class  $\varphi$ .

We are now ready to precisely describe the inductive step. Let  $\mathcal{P} = \mathcal{P}(\varphi, \gamma)$  be a right position, and let  $\alpha \in SCC(\Sigma)$ . We construct the right position  $\mathcal{P}^\alpha = \mathcal{P}^\alpha(\tau_\alpha \circ \varphi, \gamma)$  in two steps. Firstly, we coarsen  $\mathcal{P}$  by removing all points which are not fixable by  $\tau_\alpha$ . This new right position, being fixable under  $\tau_\alpha$ , defines a right

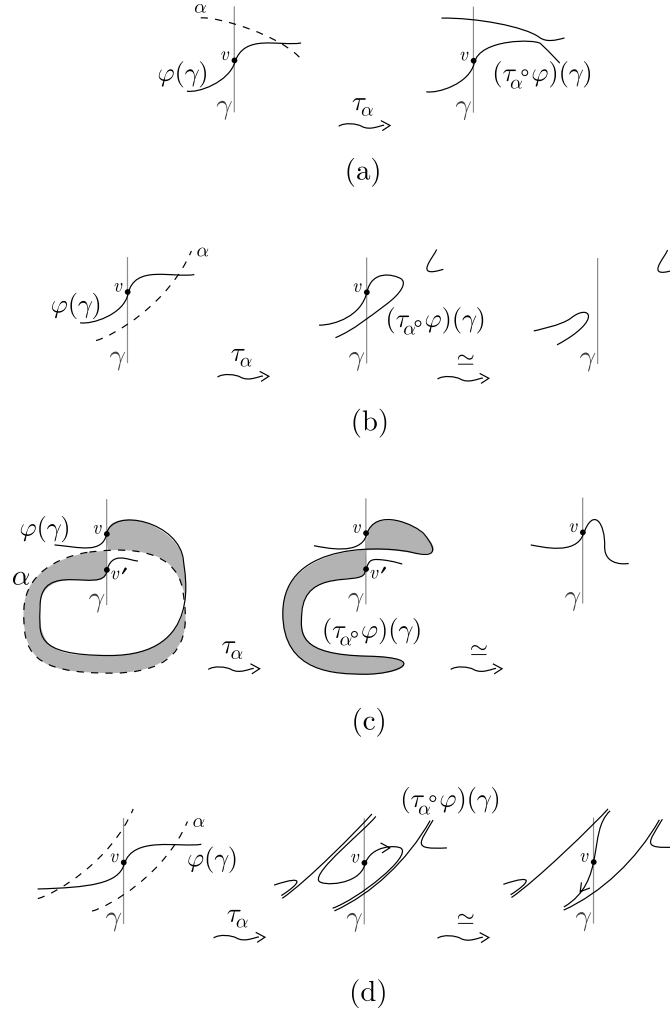


FIGURE 17. (a) A downward point is fixable. (b) An upward point is *not* fixable, unless (c) there is another upward triangle sharing the other two vertices. Note that, in this case, while either of the points  $v, v'$  is individually fixable, the pair is not simultaneously fixable. Finally, (d) illustrates the reason for demanding that a *neighborhood* of the point be fixed - though the intersection-minimizing isotopy may be done without removing the intersection point  $v$ , there is no fixable neighborhood, and so  $v$  is not fixable.

position for  $\gamma, \tau_\alpha(\varphi(\gamma))$ . Secondly we refine this new position by adding points so as to have each new fixable point of  $\gamma \cap \tau_\alpha(\varphi(\gamma))$  accounted for.

3.2.3. *The coarsening  $\mathcal{P} \rightsquigarrow \mathcal{P}'$ .* The coarsening process takes the given right position  $\mathcal{P}$  and a curve  $\alpha \in SCC(\Sigma)$ , and returns a right position  $\mathcal{P}' = \mathcal{P}'(\varphi, \gamma) \subset \mathcal{P}$ . The intuitive idea is that we will remove a minimal subset of  $\mathcal{P}$  such that the remaining points are fixable by  $\tau_\alpha$ , thus allowing an identification of  $\mathcal{P}$  with a subset

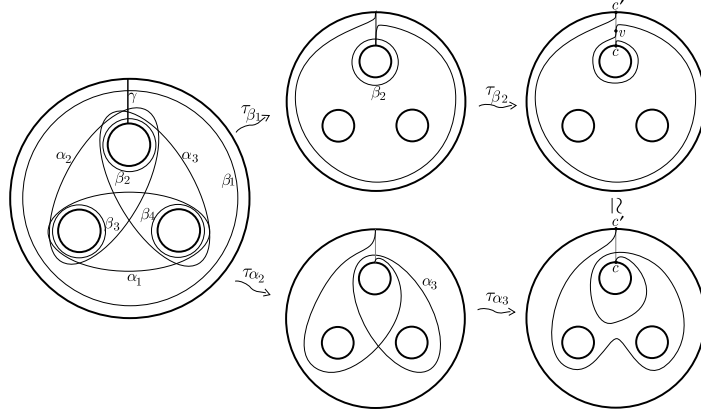


FIGURE 18. On the left are the curves of the well-known lantern relation on  $\Sigma_{0,4}$  - setting  $\omega_1 = \tau_{\beta_4}\tau_{\beta_3}\tau_{\beta_2}\tau_{\beta_1}$ ,  $\omega_2 = \tau_{\alpha_3}\tau_{\alpha_2}\tau_{\alpha_1}$ , the lantern relation tells us that  $\omega_1, \omega_2$  are factorizations of a common  $\varphi \in \Gamma_\Sigma$ . Clearly, for the arc  $\gamma$  indicated, the intersection point  $v \in \varphi(\gamma) \cap \gamma$  in the upper right figure is fixable under  $\omega_1$ . However, as is clear from the lower sequence of figures,  $v$  is *not* fixable under the factorization  $\omega_2$ . Thus the right position  $\mathcal{P}(\omega_1, \gamma)$  contains the point  $v$  as well as the endpoints of  $\gamma$ , while  $\mathcal{P}(\omega_2, \gamma)$  contains only the endpoints of  $\gamma$ .

of  $\gamma \cap \tau_\alpha(\varphi(\gamma))$ . Of course we must do so in a way which depends only on the isotopy class of  $\alpha$ .

We begin by choosing a representative  $\alpha$  of the isotopy class  $[\alpha]$  which has minimal intersection with  $\gamma$  and  $\varphi(\gamma)$ . Choose  $\text{support}(D_\alpha)$  to be disjoint from  $\mathcal{P}$ . Now, the only bigons bounded by the arcs  $D_\alpha(\varphi(\gamma))$  and  $\gamma$  correspond to upward triangular regions of the original triple  $(\gamma, \varphi(\gamma), \alpha)$ . Thus, any isotopy which minimizes  $\tau_\alpha(\varphi(\gamma)) \cap \gamma$  must isotope  $D_\alpha(\varphi(\gamma))$  over some subset of the upward triangular regions. The coarsening must therefore consist of a removal of a subset of the upward points of  $\mathcal{P}$ . We want to determine which of these points are fixable under  $\tau_\alpha$ .

**Lemma 3.19.** *Suppose that  $v \in \mathcal{P}$  is a vertex of an upward triangular region  $T$ . Then if  $v$  is fixable under  $\tau_\alpha$ , then there is another upward triangular region  $T'$  such that  $T, T'$  share the vertices of  $T$  other than  $v$  (Figure 17(c)).*

*Proof.* Let  $a$  be the vertex of  $T$  at  $\alpha \cap \gamma$  and  $p$  the remaining vertex (Figure 19(a)). As  $v$  is upward, there is a bigon in the image, corresponding to  $T$ , bounded by  $(\tau_\alpha(\varphi(\gamma))$  and  $\gamma$ , with vertices  $v$  and  $a$  (Figure 19(b)). Therefore, if  $v$  is to be fixed through an isotopy of  $\tau_\alpha(\varphi(\gamma))$  which minimizes  $\tau_\alpha(\varphi(\gamma)) \cap \gamma$ , then  $a$  must be a vertex of a second bigon also bounded by  $\tau_\alpha(\varphi(\gamma))$  and  $\gamma$ , with vertices  $a$  and  $v'$  for some  $v' \in \tau_\alpha(\varphi(\gamma)) \cap \gamma$  (Figure 19(c)). By minimality of intersections in the original configuration, this new bigon then corresponds to a second upward triangle  $T'$  with vertices  $a, v', p'$  in the original configuration (Figure 19(d)). As  $v$  is fixable, the bigons must cancel, and we have  $p = p'$ , as desired (Figure 17(c) indicates the configuration). Note that, while each of  $v, v'$  is fixable, the pair is not *simultaneously* fixable.  $\square$



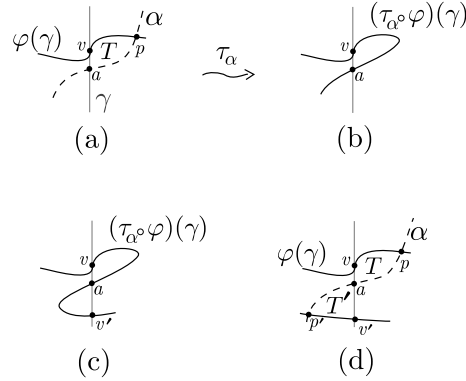


FIGURE 19. Figures for Lemma 3.19.

We refer to such a twist as *surgering out*  $\alpha$  from  $\varphi(\gamma)$  relative to  $\gamma$ . Also,

**Lemma 3.20.** *If triangular regions  $T$  and  $T'$  share exactly two vertices, then these vertices are the two which lie on the closed curve  $\alpha$ .*

*Proof.* Let the triples  $(v_1, p_1, a_1)$ ,  $(v_2, p_2, a_2)$  be the vertices of upward triangles  $T_1$  and  $T_2$ , where  $v_i \in \gamma \cap \varphi(\gamma)$ ,  $p_i \in \alpha \cap \varphi(\gamma)$ , and  $a_i \in \alpha \cap \gamma$ , and suppose  $T_1$  and  $T_2$  have exactly two vertices in common. Essential triangular regions can have no edges in common, so they can have two vertices in common only if the vertices lie along a closed curve given by the union of the two edges defined by the pair of vertices. In particular, as  $\alpha$  is the only closed curve in the construction, the points in common must be  $p_1 = p_2$  and  $a_1 = a_2$ .  $\square$

Motivated by Lemmas 3.19 and 3.20, we introduce an equivalence relation  $\sim$  on the set of upward triangular regions, such that  $T \sim T'$  if and only if they share exactly two vertices. Now, any such equivalence class  $\Omega$  comprises of  $m$  triangular regions, each of which has a unique vertex in  $\gamma \cap \varphi(\gamma)$ . These vertices (and thus the elements of  $\Omega$ ) may be ordered along  $\varphi(\gamma)$  from the distinguished endpoint  $c$ . We then define a new right position  $\mathcal{P}'$  for the pair  $(\gamma, \varphi)$  by removing the last (in the sense of the previous sentence) point of  $\mathcal{P}$  from each equivalence class in which each triangular region has a vertex in  $\mathcal{P}$ .

**Lemma 3.21.** *Let  $\mathcal{P}' \subset \mathcal{P}$  be as defined in the previous paragraph. Then  $\mathcal{P}'$  satisfies the following properties:*

- (1) *Each point of  $\mathcal{P}'$  is fixable under  $\tau_\alpha$*
- (2)  *$\mathcal{P}'$  is a maximal subset of  $\mathcal{P}$  for which property (1) holds.*
- (3)  *$\mathcal{P}'$  depends only on the isotopy class of  $\alpha$ .*

*Proof.* Let  $\Omega$  be an equivalence class of upward triangles. We distinguish two subcases, depending on whether each element of  $\Omega$  has a vertex in  $\mathcal{P}$  or not. To emphasize the distinction, we call a point  $p \in \gamma \cap \varphi(\gamma)$  a *vertical point* if  $p$  is in  $\mathcal{P}$ , non-vertical otherwise.

- (1) (Each element of  $\Omega$  has a vertex in  $\mathcal{P}$ ) Let  $T \in \Omega$ . Using Lemma 3.20, the equivalence class of  $T$  is formed of triangles sharing the points along  $\alpha$  (a typical equivalence class of three triangles is shown in the left side of Figure 20(a) - note that for either choice of  $\alpha$ , exactly two of the three regions are

embedded). Suppose then that  $\Omega$  contains  $m$  triangular regions. As noted in the proof of Lemma 3.19, at most  $m - 1$  vertical points from the vertices of elements of  $\Omega$  are simultaneously fixable under  $\tau_\alpha$ , and conversely, *any* set of  $m - 1$  vertical points from these is fixable. In particular, if each triangle in the class has a vertex in  $\mathcal{P}$ , the removal of a single vertical point is a necessary and sufficient refinement of the vertical points involved in the equivalence class so as to satisfy properties (1) and (2). Clearly the resulting set  $\mathcal{P}'$  obtained by repeating this refinement on each equivalence class is independent (as an unordered set) of the actual choice of which vertical point to remove, and so property (3) is satisfied.

- (2) ( $\Omega$  contains some element which does not have a vertex in  $\mathcal{P}$ ) If there is a triangle in the class which does not have a vertex in  $\mathcal{P}$ , then all of the above goes through for the neighborhood of the non-vertical point  $p$  of  $\varphi(\gamma) \cap \gamma$ ; i.e., the twist  $\tau_\alpha$ , along with any isotopy of the image  $\tau_\alpha(\gamma)$  necessary to minimize intersections can be done relative to a neighborhood of each vertical point, so that there is no coarsening necessary. Again, property (3) follows immediately. □

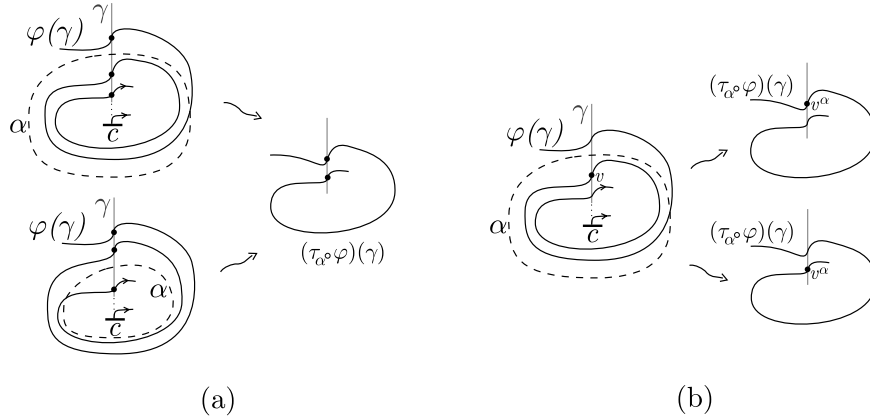


FIGURE 20. (a) For the case that each element of an equivalence class has a vertical vertex,  $\alpha$  can be isotoped so as to fix all but any single vertical point - the result is independent of the choice of which subset to fix. (b) An upward equivalence class of triangles whose set of vertices contain non-consecutive (along  $\gamma$ ), non-vertical points of  $\gamma \cap \varphi(\gamma)$  (here separated by the vertical point  $v$ ). There is therefore a choice of vertical point in the image. Our convention will be to choose the lower figure.

3.2.4. *The inclusion map  $i_\alpha$ .* Now, let  $\alpha$  be a specific representative of the isotopy class  $[\alpha]$  which has minimal intersection with  $\gamma$  and  $\varphi(\gamma)$ . We again consider the effect of the Dehn twist  $D_\alpha$  restricted to a supporting neighborhood of the twist chosen so as not to intersect any point of  $\gamma \cap \varphi(\gamma)$ . As  $D_\alpha(\varphi(\gamma))$  will not (in the presence of upward triangular regions) have minimal intersection with  $\gamma$ , the image

of the inclusion  $i_\alpha(\mathcal{P}) \subset (\gamma \cap D_\alpha(\varphi(\gamma)))$  (Definition 3.16) will not in general be a right position. Indeed,  $i_\alpha$  is no longer well-defined as a map into  $\tau_\alpha(\varphi(\gamma))$  once this has been isotoped to minimize intersections with  $\gamma$ .

One may get around this by fixing conventions: if  $\Omega$  is an equivalence class of  $m$  upward triangles, let  $\{x_1, \dots, x_m\}$  be the collection of its vertices in  $\gamma \cap \varphi(\gamma)$ , indexed in order along  $\varphi(\gamma)$  from  $c$ . By Lemma 3.21, the image of the  $\{x_j\}$  under  $i_\alpha$  will be a collection of  $m$  points in  $\gamma \cap D_\alpha(\varphi(\gamma))$ , and exactly one of these intersections must be removed by the intersection-minimizing isotopy. The resulting set of  $m-1$  simultaneously fixable points in  $\gamma \cap \tau_\alpha(\varphi(\gamma))$  is independent of this choice; we label these points  $\{y_1, \dots, y_{m-1}\}$ , ordered along  $\tau_\alpha(\varphi(\gamma))$  from  $c$ . Then, if  $x_j \in \mathcal{P}$  for each  $j$ , set  $i_\alpha(x_j) = y_j$  for  $j < m$ . Otherwise, let  $k := \max\{j \mid x_j \notin \mathcal{P}\}$ , and set  $i_\alpha(x_j) = y_j$  for  $j < k$ , and  $i_\alpha(x_j) = y_{j-1}$  for  $j > k$  (Figure 20).

With these conventions:

**Lemma 3.22.** *For any  $\alpha \in [\alpha]$ , the image  $i_\alpha(\mathcal{P}')$  is a right position for  $(\tau_\alpha \circ \varphi, \gamma)$ . Moreover,  $i_\alpha(\mathcal{P}')$  is simultaneously fixable under  $\tau_\alpha$ .*

*Proof.* We again consider the effect of the Dehn twist  $\tau_\alpha$  restricted to a supporting neighborhood of the twist chosen so as not to intersect any point of  $\gamma \cap \varphi(\gamma)$ . Observe then that in the image, the only bigons bounded by the curves  $\gamma$  and  $D_\alpha(\varphi(\gamma))$  correspond to essential upward triangles in the original configuration. Each singleton equivalence class contributes a single, isolated bigon, while classes with multiple elements contribute canceling pairs of bigons. In particular,  $\gamma \cap \tau_\alpha(\varphi(\gamma))$  may be minimized by an isotopy of  $\tau_\alpha(\varphi(\gamma))$  over one bigon from each class. This isotopy fixes a neighborhood of each of the points  $\mathcal{P}'$ . □

3.2.5. *The refinement  $i_\alpha(\mathcal{P}') \rightsquigarrow \mathcal{P}^\alpha$ .* For the final step, we wish to refine a given  $i_\alpha(\mathcal{P}')$  by adding points to obtain the desired right position  $\mathcal{P}^\alpha$  for  $(\tau_\alpha \circ \varphi, \gamma)$  so that  $\mathcal{P}^\alpha$  depends only on  $[\alpha]$ .

So, let  $\alpha$  be a given representative of the isotopy class  $[\alpha]$  such that the sets  $\alpha \cap \gamma, \alpha \cap \varphi(\gamma)$  are minimal. By Lemma 3.22 we have an identification of  $\mathcal{P}'$  as a subset  $i_\alpha(\mathcal{P}')$  of the positive intersections of  $\tau_\alpha(\varphi(\gamma)) \cap \gamma$ , and thus as a right position for  $(\tau_\alpha \circ \varphi, \gamma)$ .

As we are after an isotopy-independent result, we shall require that  $\mathcal{P}^\alpha$  include each point which is fixed by *any* representative of  $[\alpha]$  which satisfies the intersection-minimality conditions. So, let  $v \in \mathcal{P}'$  be a downward point. Then for each vertical downward triangular region  $T$  with vertex  $v$ , let  $a$  be the vertex  $\alpha \cap \gamma$ . We label the positive intersection of  $\gamma$  with  $\tau_\alpha(\varphi(\gamma))$  corresponding to  $a$  by  $d_{a,v} \in (\tau_\alpha \circ \varphi)(\gamma) \cap \gamma$  (Figure 21), and call the set of all such points  $V_v$ . We refer to  $i_\alpha(v) \cup V_v \subset \mathcal{P}^\alpha$  as *the refinement set corresponding to  $v$* . Note that, for distinct  $v, v'$ , the sets  $V_v, V_{v'}$  are not necessarily disjoint, but as we only require that each such point be accounted for, this does not affect the construction. We now define the right position  $\mathcal{P}^\alpha$  of  $(\tau_\alpha \circ \varphi, \gamma)$  as the union of all the refinement sets of each point,  $\mathcal{P}^\alpha := i_\alpha(\mathcal{P}') \cup \{V_v \mid v \in \mathcal{P}'\}$ .

Finally,

**Lemma 3.23.** *The right position  $\mathcal{P}^\alpha$  of  $(\tau_\alpha \circ \varphi, \gamma)$  given by the refinement process is exactly the set  $\bigcup_{\alpha \in [\alpha]} i_\alpha(\mathcal{P}')$ . In particular,  $\mathcal{P}^\alpha$  depends only on the isotopy class of  $\alpha$ .*

*Proof.* We will show that  $\mathcal{P}^\alpha = \bigcup_{\alpha \in [\alpha]} i_\alpha(\mathcal{P}')$  by showing that each of these sets are equivalent to the set  $W := \{v \in \gamma \cap (\tau_\alpha \circ \varphi)(\gamma) \mid v \text{ is fixable under } \tau_\alpha \text{ with preimage (under } i_\alpha) v' \in \mathcal{P}\}$ . Now, by construction, for any  $\alpha \in [\alpha]$  or  $v' \in \mathcal{P}$ , each element of  $i_\alpha(\mathcal{P}')$  or  $V_{v'}$  is in  $W$ , so we only need to show that, for arbitrary  $\alpha$ , each  $v \in W$  is in both  $\mathcal{P}^\alpha$  and  $\bigcup_{\alpha \in [\alpha]} i_\alpha(\mathcal{P}')$ .

So, let  $v \in W$ , with preimage  $v'$ , and  $\alpha$  a fixed representative of  $[\alpha]$ . There are two cases:

- (1) ( $v'$  is downward) Suppose  $v \notin i_\alpha(\mathcal{P}')$ . Then there is  $\alpha' \in [\alpha]$ , given by a shift of  $\alpha$  over  $v$ , such that  $v \in i_{\alpha'}(\mathcal{P}')$ . Then  $v$  is in the refinement set  $V_{v'}$  in the right position  $\mathcal{P}^\alpha$ , and also in  $i_{\alpha'}(\mathcal{P}')$ .
- (2) ( $v'$  is not downward) Then  $v' \in \mathcal{P}'$ , and so  $v \in i_\alpha(\mathcal{P}')$  for any  $\alpha$ .

□

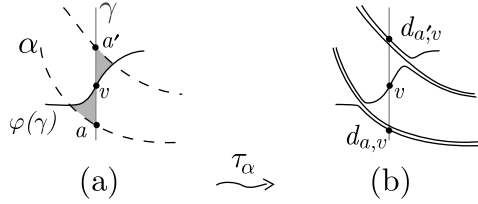


FIGURE 21. Construction of the set  $V_v$  for downward  $v \in \mathcal{P}'$ . Figure (a) is the setup in  $\mathcal{P}'$ , (b) shows the result of the refinement for  $\mathcal{P}^\alpha$  by vertical points  $V_v = \{d_{a,v}, d_{a',v}\}$  on  $\tau_\alpha(\varphi(\gamma))$ .

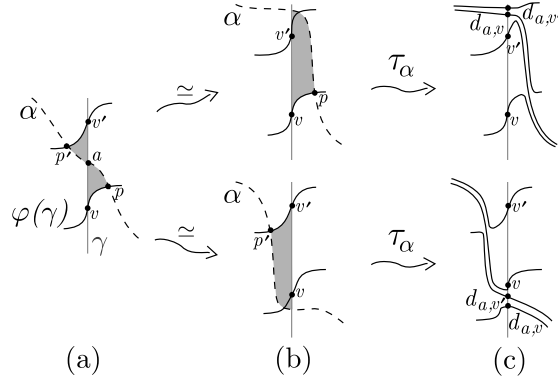


FIGURE 22.  $\mathcal{P}^\alpha$  is independent of isotopy of  $\alpha$  in the refinement process. (a) is the initial setup, with  $p, p' \in \alpha \cap \varphi(\gamma)$ , (b) indicates distinct isotopies, and (c) is the resulting  $\mathcal{P}^\alpha$  for each choice. While the labeling is different, the right positions are equivalent.

### 3.2.6. The associated right position $\mathcal{P}_\omega$ .

**Definition 3.24.** Let  $\varphi \in \Gamma_\Sigma$  be given as a positive factorization  $\omega$ . The unique right position associated to the pair  $\omega, \gamma$  by the algorithm detailed in this section is the *right position associated to  $\omega$* , denoted  $\mathcal{P}_\omega(\gamma)$ .

Finally, we need to extend the associated right position to each pair  $\gamma_i, \varphi(\gamma_i)$  for an arbitrary set  $\{\gamma_i\}$  of nonintersecting properly embedded arcs. We have:

**Lemma 3.25.** *Let  $\{\gamma_i\}$  be a set of pairwise non-intersecting properly embedded arcs in  $\Sigma$ . The algorithm as given above extends to an algorithm which assigns a unique right position  $\mathcal{P}_\omega(\gamma_i)$  to each pair  $\gamma_i, \varphi(\gamma_i)$ .*

*Proof.* This follows directly from independence of the algorithm from the choice of representative of the isotopy class of  $\alpha$ , and the observation that we may always find some representative of  $\alpha$  which intersects each of  $\gamma_i$  and  $\varphi(\gamma_i)$  minimally (by e.g. an inductive sequence of removing bigons which contain no other bigons - alternately, but at the expense of losing self-containment, of course one could simply choose everything to be geodesic for some hyperbolic metric).  $\square$

**3.3. Consistency of the associated right positions.** The goal of this subsection is to show that any two right positions  $\mathcal{P}_\omega(\gamma_1), \mathcal{P}_\omega(\gamma_2)$  associated to a positive factorization  $\omega$  are consistent (Definition 3.8). Theorem 3.1 will follow from this result coupled with Lemma 3.25.

Our method to show consistency will be to use the right positions to ‘localize’ the situation. Recall from the previous section (in particular Lemma 3.23) that, if  $\mathcal{P} \rightsquigarrow \mathcal{P}^\alpha$  denotes the inductive step of the algorithm, then, using the notation of that section, given a point  $z \in \mathcal{P}^\alpha$ , there is a representative  $\alpha$  of  $[\alpha]$  such that  $z$  is in the image of the inclusion map  $i_\alpha$ . In particular, this identification of  $z$  as  $i_\alpha(v)$ , for some  $v \in \mathcal{P}$ , will hold for any isotopy of  $\alpha$  which does not involve a shift over  $v$ . Thus, having fixed  $\alpha$  up to this constraint, we may consider  $v$  as having properties analogous to the endpoints of  $\gamma$ ; i.e. it is fixed by  $\tau_\alpha$ , and  $\alpha$  cannot be isotoped so as to cross it. We refer to  $v$  as the *preimage* of  $z$ .

Suppose then that we have a *pair* of nonintersecting properly embedded arcs on a surface with a given monodromy, with right positions  $\mathcal{P}_1$  and  $\mathcal{P}_2$ . Then, for a Dehn twist  $\tau_\alpha$ , the inductive step of the algorithm gives a pair  $\mathcal{P}_1^\alpha, \mathcal{P}_2^\alpha$ . Consider a *pair* of points, one from each of  $\mathcal{P}_i^\alpha$ . We need to show that for each such pair, the horizontal segments originating at the pair of points are completed if initially parallel. We call a pair satisfying this condition *consistent*.

Now, if there is an isotopy of  $\alpha$  such that each point in a given pair of points is in the image of the associated inclusion map  $i_\alpha$ , we call the pair a *simultaneous image*. The idea is that the horizontal segments originating at such a pair have well-defined preimages in  $\mathcal{P}_1$  and  $\mathcal{P}_2$ , so we only have to understand the ‘local picture’ consisting of the images under  $\tau_\alpha$  of each such pair.

In keeping with analogy of fixable points as boundary points, we generalize the notion of ‘to the right’ (as presented in [HKM]) to paths with common endpoint on the interior of a properly embedded arc  $\gamma$ . We will say that an isotopy  $\eta_t, t \in [0, 1]$ , of path  $\eta$  *respects* path  $\eta'$  if, for all  $s \in [0, 1]$ , the interior of path  $\eta_s$  contains neither endpoint of  $\eta'$ .

**Definition 3.26.** Let  $\gamma$  be a properly embedded arc in  $\Sigma$ ,  $\eta, \eta' : [0, 1] \hookrightarrow \Sigma$  paths in  $\Sigma$  with common endpoint  $\eta(0) = \eta'(0) = x \in \gamma$ , such that each intersects  $\gamma$  minimally, and then isotoped (relative to the endpoints and respecting each other) to minimize intersection with each other. Further suppose that each lies to the same side of  $\gamma$  (i.e. if we fix a lift  $\tilde{\gamma}$  in the universal cover  $\tilde{\Sigma}$  of  $\Sigma$ , and lifts  $\tilde{\eta}, \tilde{\eta}'$  with endpoints  $\tilde{x} \in \tilde{\gamma}$  then  $\tilde{\eta}, \tilde{\eta}'$  lie in the same connected component of  $\tilde{\Sigma} \setminus \tilde{\gamma}$ ). We say  $\eta'$  is *to the right* of  $\eta$  (at  $x$ ), denoted  $\eta' \geq \eta$ , if either the pair is homotopic (relative

to the endpoints), or if the tangent vectors  $(\dot{\eta}'(0), \dot{\eta}(0))$  define the orientation of  $\Sigma$  at  $x$  (Figure 23(a)). Similarly we say  $\eta$  is *to the left* of  $\eta'$ , denoted  $\eta' \leq \eta$ .

We also need a slightly stronger notion of comparative rightness:

**Definition 3.27.** Let  $\gamma, \eta, x$  be as in the previous definition, and suppose  $\Delta : [0, 1] \hookrightarrow \Sigma$  is an embedded arc in  $\Sigma$  with endpoints  $\Delta(0) = x$ , and  $\Delta(1) = y \in \gamma'$ , for  $\gamma'$  another properly embedded arc in  $\Sigma$ , disjoint from  $\gamma$ . Then if there is a triangular region for the triple  $(\eta, \Delta, \gamma')$  in which  $x$  and  $y$  are vertices, we say  $\eta$  is *parallel along*  $\Delta$ . If  $\eta \geq \Delta$  ( $\eta \leq \Delta$ ) and  $\eta$  and  $\Delta$  are *not* parallel along  $\eta'$ , then we say  $\eta$  is *strictly to the right (left)* of  $\Delta$  (Figure 23(b)).

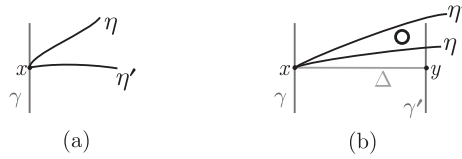


FIGURE 23. (a) Arc  $\eta'$  is to the right of  $\eta$  at  $x$ . (b) Arc  $\eta$  is parallel along  $\Delta$ , while  $\eta'$  is strictly to the left of  $\Delta$ .

*Observation 3.28.* Note that, for a pair of horizontal segments  $h_v$  and  $h_w$ , the property of being initially parallel along a rectangular region  $B$  implies that each is parallel along the unique (up to isotopy) ‘diagonal’ arc  $\Delta$  with endpoints  $v$  and  $w$  and contained in  $B$ . Conversely, if  $h_v$  and  $h_w$  are each parallel along and to the right of an arc  $\eta$  with endpoints  $v$  and  $w$ , there is a rectangular region along which the segments are initially parallel (given by the union of the triangular regions of Definition 3.27).

As for the utility of these definitions, let  $\mathcal{P}_i \rightsquigarrow \mathcal{P}_i^\alpha$  denote the inductive step of the algorithm, and consider a simultaneously fixable pair  $v \in \mathcal{P}_1, w \in \mathcal{P}_2$ . If the images  $\tau_\alpha(h_v)$  and  $\tau_\alpha(h_w)$  are initially parallel along rectangular region  $B$  with diagonal  $\Delta$ , then we may compare  $\Delta$  with the preimages  $h_v$  and  $h_w$ . Clearly, for either of  $h_v$  and  $h_w$ , the property of being strictly to the right of  $\Delta$  is preserved by  $\tau_\alpha$ , and so incompatible with the images being initially parallel along  $B$ . Moreover, if one of the pair, say  $h_v$ , is to the left of  $\Delta$ , then if  $h_w$  is to the right of  $\Delta$ , as it has no intersection with  $h_v$  it must be *strictly* to the right of  $\Delta$ , which as above gives a contradiction. We summarize:

**Lemma 3.29.** *Let  $v \in \mathcal{P}_1(\varphi, \gamma_1)$  and  $w \in \mathcal{P}_2(\varphi, \gamma_2)$  be simultaneously fixable under  $\tau_\alpha$ . Fix  $\alpha \in [\alpha]$ , and let  $u = i_\alpha(v) \in \mathcal{P}_1^\alpha$  and  $z = i_\alpha(w) \in \mathcal{P}_2^\alpha$ . Suppose that  $h_u$  and  $h_z$  are initially parallel along  $B$ , with diagonal  $\Delta$ . Then:*

- (1) *If  $h_v \geq \Delta$ , then  $h_v$  is parallel along  $\Delta$ .*
- (2)  *$h_v \geq \Delta \Leftrightarrow h_w \geq \Delta$  (and so  $h_v \leq \Delta \Leftrightarrow h_w \leq \Delta$ )*

We now have everything we need to show that the algorithm preserves consistency. We begin with a check that, under certain conditions, initially parallel images of initially parallel and completed segments are themselves completed. To be precise:

**Lemma 3.30.** *Let  $\mathcal{P}_i$  be consistent right positions for  $(\varphi, \gamma_i)$ ,  $i = 1, 2$ . Suppose  $v \in \mathcal{P}_1$  and  $w \in \mathcal{P}_2$  are fixable under  $\tau_\alpha$ , and horizontal segments  $h_v$  and  $h_w$  initially parallel along a rectangular region  $B$  with diagonal  $\Delta$ , and completed along a region  $B'$  with diagonal  $\Delta'$  to points  $v'$  and  $w'$ . Then,*

- (1) *If neither of  $v$  and  $w$  are downward (Definition 3.12), and  $h_{i_\alpha(v)}$  and  $h_{i_\alpha(w)}$  are initially parallel along  $\tau_\alpha(\Delta)$ , then  $h_{i_\alpha(v)}$  and  $h_{i_\alpha(w)}$  are completed.*
- (2) *Suppose at least one of  $v$  and  $w$  is downward, and let  $V_v$  and  $V_w$  denote the refinement classes from the refinement step of the algorithm. Then for any  $u \in V_v$  and  $z \in V_w$ , if the horizontal segments  $h_u$  and  $h_z$  are initially parallel along (a parallel translate of)  $\Delta$  (here a ‘parallel translate’ of  $\Delta$  just refers to an isotopy which allows the endpoints to move along the arcs  $\gamma_i$ ), then they are completed.*

*Proof.* For claim (1), note that, for any allowable  $\alpha \in [\alpha]$  (i.e.  $\alpha$  has minimal intersection with the  $\gamma_i$  and their images),  $\alpha$  intersects  $B$  in arcs as in Figure 24(a). In particular, if neither initial point is downward, then any arc of  $\alpha \cap B$  either connects parallel edges, or is the edge of an upward triangle in either  $(\gamma_1, \varphi(\gamma_2), \alpha)$  (so  $y_1$  is a vertex), or  $(\gamma_2, \varphi(\gamma_1), \alpha)$  (so  $y_2$  is a vertex).

Suppose firstly that neither  $y_i$  is a vertex of an upward triangle. Then for any allowable  $\alpha$ , all arcs  $\alpha \cap B$  connect parallel edges, and so all four corners of  $B$  are fixable. We thus may view these as the corners of the initially parallel region containing  $\tau_\alpha(\Delta)$  (observe that this is well-defined when its endpoints are fixable) in the image, and so need only check the completing region  $B'$ . Observe that any arc of  $B' \cap \alpha$  either connects parallel edges, or is the edge of a downward triangle in which  $v'$  or  $w'$  is a vertex (Figure 24(b)). It follows then that  $h_{i_\alpha(v)}$  and  $h_{i_\alpha(w)}$  are completed by points  $u' \in V_{v'}$  and  $z' \in V_{w'}$ .

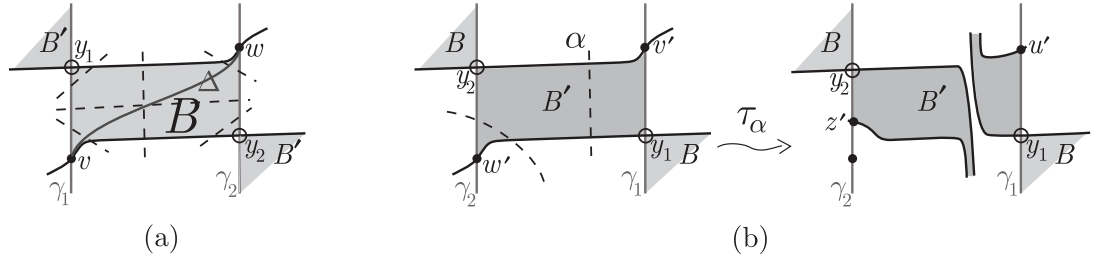


FIGURE 24. (a) Dashed lines illustrate possible intersections  $\alpha \cap B$ .  
 (b) If the corners  $y_i$  are not upward, the completing disc is preserved.

We may then assume that any point of  $\alpha \cap h_v$  is a vertex of an upward triangle with vertex  $y_2$  (and similarly for  $\alpha \cap h_w$  and  $y_1$ ). Suppose then that  $y_2$  is a vertex of an upward triangular region of the triple  $(\alpha, \gamma_2, \varphi(\gamma_1))$ . Following the argument of Lemma 3.21, the image  $\tau_\alpha(h_v)$  can be initially parallel along  $\tau_\alpha(\Delta)$  only if there are a pair of triangular regions  $T_1$  and  $T_2$  in the triple  $(\gamma_2, \varphi(\gamma_1), \alpha)$  with two vertices in common (Figure 25(a)); i.e.  $\tau_\alpha$  is a ‘surgering out’ of  $\alpha$  relative to  $\gamma_2$  (using the terminology of the coarsening step of the algorithm). It is then straightforward to check that consistency is preserved: If the surgery can be done so as to fix the edges of  $B'$ , this is of course trivial. Otherwise, either an  $\alpha$  is surgered out of *each* of the

arc-images along the edges of  $B'$ , thus fixing endpoints and preserving the region, or  $B'$  itself is contained in a neighborhood of  $\alpha$ , in which case the surgery must remove a pair of regions with common endpoints, which again preserves consistency.

To see this explicitly, we may separate the claim into 4 cases as follows: if we let  $p$  denote the vertex at  $\gamma_2 \cap \varphi(\gamma_1)$  of  $T_2$  (Figure 25(a)), then we may distinguish whether  $p$  is on the edge of  $B'$  along  $\varphi(\gamma_1)$  (call this edge  $e_{\varphi(\gamma_1)}$ ), and then also whether it is on the edge of  $B'$  along  $\gamma_2$  (which we refer to as  $e_{\gamma_2}$ ). We see then that, if  $p \in e_{\gamma_2}$ , then there is an isotopy of  $\alpha$  such that  $\tau_\alpha$  fixes each edge of  $B'$  (Figure 25(b) shows the case  $p \notin e_{\varphi(\gamma_1)}$ , (c) shows  $p \in e_{\varphi(\gamma_1)}$ ), while if  $p \in e_{\varphi(\gamma_1)}$  and  $p \notin e_{\gamma_2}$ , then  $\tau_\alpha$  surgers out a subarc of each edge of  $B'$  (Figure 25(d)). For the remaining case (Figure 25(e)), if  $p \notin \partial B'$ , then  $B'$  is contained in a neighborhood of  $\alpha$ . As  $h_w$  is also assumed parallel along  $\Delta$ , we find that  $h_{v'}$  and  $h_{w'}$  are constrained to be initially parallel along a further region (call this  $B_1$ , which for consistency is completed by some  $B'_1$ ) again contained in a neighborhood of  $\alpha$ . The surgery then has the effect of removing  $B'$  and  $B_1$ , and connecting the midpoints of  $B$  with those of  $B_1$  via canceling bigon pairs. We thus have  $B$  completed by  $B'_1$  in the image.

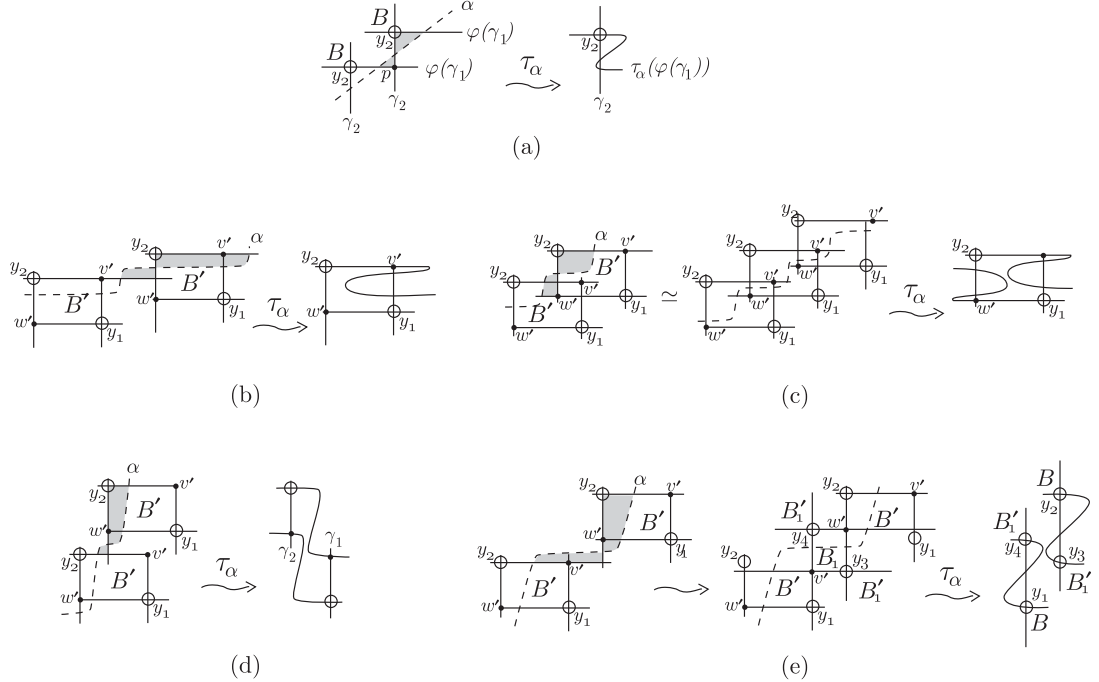


FIGURE 25. (a) Surgering  $\alpha$  from  $\varphi(\gamma_1)$  relative to  $\gamma_2$ . The figure is in the universal cover; all lifts of a given object are given the same label as the object itself. (b)  $p \in e_{\gamma_2}, p \notin e_{\varphi(\gamma_1)}$ . (c)  $p \in e_{\gamma_2} \cap e_{\varphi(\gamma_1)}$ . We have added the extra step of isotoping  $\alpha$  so that the twist more clearly fixes all of the edges of  $B'$ . (d)  $p \notin e_{\gamma_2}, p \in e_{\varphi(\gamma_1)}$ . (e)  $p \notin e_{\gamma_2} \cup e_{\varphi(\gamma_1)}$ . Again we have added an extra step, this time extending the picture to see the region  $B_1$  (with midpoints  $y_3$  and  $y_4$ ) as described in the proof.



For claim (2), in addition to the intersections of  $\alpha$  with  $B$  and  $B'$  as in the previous case, we must deal with the case that our initial points  $v$  and  $w$  are downward. So, let  $p \in \alpha \cap h_v$  be a vertex in a downward triangle  $T$  with vertex  $v$ . We first observe that, as  $h_u$  is assumed parallel along  $\Delta$ , for each such  $T$  there is a complementary region  $T'$  of the triple  $(\alpha, \gamma_2, \varphi(\gamma_1))$ , such that  $T$  and  $T'$  share the vertex  $\alpha \cap \varphi(\gamma_1)$  (Figure 26(a)).

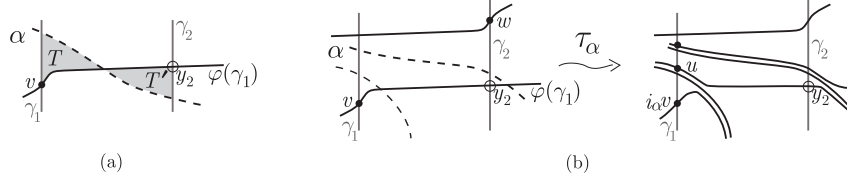


FIGURE 26. (a) If  $v$  is downward, then to preserve parallelity of  $h_{i_\alpha v}$  along  $\Delta$ ,  $\alpha$  must extend from the downward region  $T$  to form a complementary region  $T'$ . (b) For an arbitrary point  $u$  in  $V_v$  such that  $h_u$  is parallel along  $\Delta$ , we may isotope  $\alpha$  to fix  $y_2$ .

In the case that  $u = i_\alpha v$ , we may then use these complementary regions to assume  $\alpha$  is shifted over  $y_2$  so that  $h_v \cap \partial B$  is fixed by  $\tau_\alpha$ . In particular,  $y_2$  itself is fixed, and so we only need check that the images are completed, which follows from the proof of case (1) above.

Finally, we are left with arbitrary  $u \in V_v$ . Note firstly that (by definition) such a  $u$  corresponds to the corner  $x \in \alpha \cap \gamma_1$  of a downward triangle  $T$  of the triple  $(\alpha, \gamma_1, \varphi(\gamma_1))$ . We may assume  $\alpha$  is isotoped such that the edge of  $T$  along  $\gamma_1$  is contained in  $\partial B$ . We are assuming  $h_u$  is parallel to  $\Delta$ , so as above we may further assume  $\alpha$  isotoped such that  $y_2$  is fixed (Figure 26(b)). The same arguments hold for  $z \in V_w$ , so  $h_u$  and  $h_z$  are again initially parallel along a region with corners  $y_1$  and  $y_2$ , which is again completed by the argument of part (1).  $\square$

We are now able to show that the algorithm preserves consistency. We split the statement into two lemmas, beginning with the case of a simultaneous image pair:

**Lemma 3.31.** *Let  $\mathcal{P}_i$ ,  $i = 1, 2$  be consistent, and let  $u \in \mathcal{P}_1^\alpha$  and  $z \in \mathcal{P}_2^\alpha$  be a simultaneous image. Then if  $h_u$  and  $h_z$  are initially parallel, they are completed.*

*Proof.* Suppose  $h_u$  and  $h_z$  are initially parallel along rectangular region  $B$  with diagonal  $\Delta$ . As usual, we label the remaining two corners of  $B$  by  $y_i \in \gamma_i$ . Let  $\alpha \in [\alpha]$  be fixed such that  $u$  and  $z$  are in the image of  $i_\alpha$ . Denote the preimages by  $v \in \mathcal{P}_1$  and  $w \in \mathcal{P}_2$ , so  $i_\alpha(v) = u$  and  $i_\alpha(w) = z$ . Using Lemma 3.29, there are two cases:

- (1)  $h_v, h_w \leq \Delta$ . We again fix a neighborhood  $U(\alpha)$  of  $\alpha$ , and consider the isotopy  $D_\alpha(h_v) \rightsquigarrow h_{i_\alpha(v)}$  which minimizes intersections of  $\tau_\alpha(h_v)$  with  $\gamma$  and  $\Delta$ . We let  $p$  be the initial (along  $h_v$  from  $v$ ) point of  $\alpha \cap h_v$ , and  $p'$  the first point of  $\partial(\nu(\alpha)) \cap h_v$  along  $h_v$  from  $p$  (Figure 27). Now, the only bigons bounded by  $D_\alpha(h_v)$  and  $\gamma$  or  $\Delta$  correspond to triangular regions in the preimage. We distinguish two subcases:

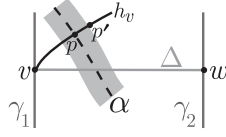


FIGURE 27. Notation for Lemma 3.31. The shaded region is a neighborhood of  $\alpha$ .

- (a) The point  $v$  is the vertex of a downward triangular region  $T$  in the triple  $(\alpha, \gamma_1, h_v)$  (Figure 28(a)). Then  $p'$  (considered now as a point of  $D_\alpha(h_v)$ ) is *not* in a bigon bounded by  $D_\alpha(h_v)$  and  $\gamma_1$  (else  $\gamma_1$  and  $h_v$  bound a bigon), so our isotopy may be done so as to fix  $p'$ . Thus, for the image  $\tau_\alpha(h_v)$  to lie along  $\Delta$ , we find that there is a triangular region  $T'$  of  $(\gamma_2, \Delta, \alpha)$  which intersects  $T$  in the vertex  $\alpha \cap \Delta$  of  $T$ . Similarly, as  $h_w \leq \Delta$ , it follows that an initial segment of  $h_w$  is within  $T'$ , and thus  $w$  is also downward. Using  $T$  and  $T'$ , we may then assume that  $\alpha$  runs from  $\gamma_1$  to  $\gamma_2$  within a neighborhood of  $\Delta$ , intersecting  $\Delta$  exactly once (Figure 29). There are then  $u' \in \mathcal{P}_1^\alpha, z' \in \mathcal{P}_2^\alpha$  corresponding to the vertices  $\alpha \cap \gamma_i$  of the associated triangles. The segments  $h_u$  and  $h_z$  are compatible, initially parallel along  $\Delta$  with completing region along the remainder of  $\alpha$  and endpoints  $u'$  and  $z'$ .

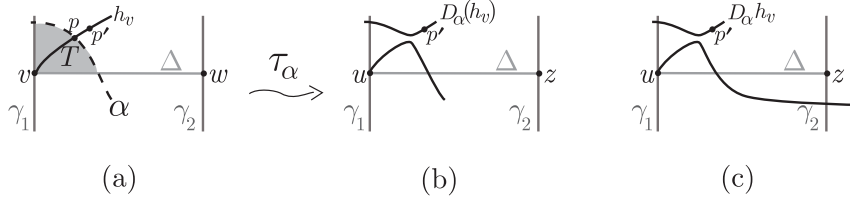


FIGURE 28. Figures for Lemma 3.31

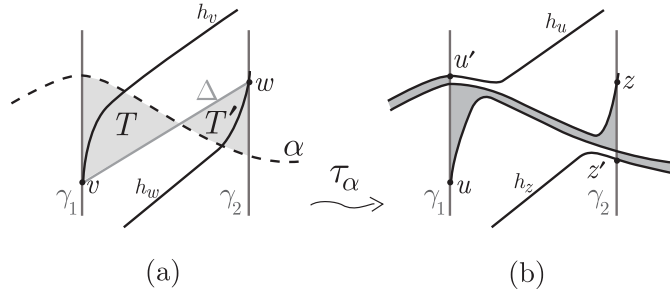


FIGURE 29. (a) If  $h_v \geq \Delta$  (at  $v$ ), then the same is true of  $h_w$  (at  $w$ ), so the pair is initially parallel along  $\Delta$ . (b) The segments  $h_u = \tau_\alpha(h_v)$  and  $h_z = \tau_\alpha(h_w)$  are compatible, with endpoints  $u', z'$ , given by the refinement procedure, corresponding to the points  $\alpha \cap \gamma_i$

- (b) The points  $v$  and  $p$  are not vertices in a downward triangular region of  $(\alpha, \gamma_1, h_v)$  (Figure 30(a)). By part (a),  $w$  is also not in a downward triangular region (of  $(\alpha, \gamma_2, \Delta)$ ). Now,  $h_u$  is assumed parallel along  $\Delta$ , so we consider the respective triangular region  $T$  in  $((\tau_\alpha \circ \varphi)(\gamma_1), \Delta, \gamma_2)$  (Figure 30(c)). As the point  $w$  is not downward, all arcs of  $\alpha \cap T$  connect  $h_u$  to  $\Delta$  or  $\gamma_2$ . In particular,  $h_v = \tau_\alpha^{-1}(h_u)$  is parallel along  $\tau_\alpha^{-1}(\Delta)$ . The same holds for the complementary triangular region  $T'$  in  $((\tau_\alpha \circ \varphi)(\gamma_2), \Delta, \gamma_1)$ . Now,  $B = T \cup T'$ , so we find the preimages  $h_v$  and  $h_w$  initially parallel along a region with diagonal  $\tau_\alpha^{-1}$  (Figure 31 gives a typical situation). The result then follows from Lemma 3.30.

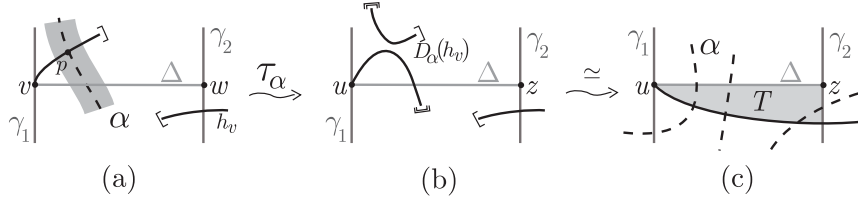


FIGURE 30. (a) The points  $v$  and  $p$  are not vertices in a downward triangular region. (b) The image under  $D_\alpha$ . (c) The triangular region  $T$  in  $((\tau_\alpha \circ \varphi)(\gamma_1), \Delta, \gamma_2)$ , and some possible components of  $\alpha \cap T$ .

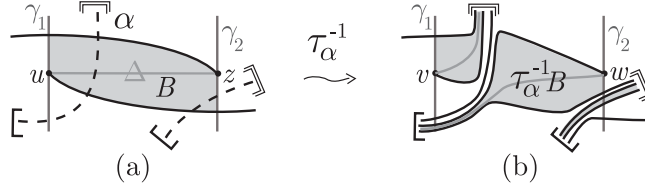


FIGURE 31. (a) Some possible components of  $\alpha \cap B$ . (b) Segments  $h_v$  and  $h_w$  are initially parallel along  $\tau^{-1}(B)$

- (2)  $h_v, h_w \geq \Delta$  By Lemma 3.29,  $h_v$  and  $h_w$  are each parallel along  $\Delta$ . The pair is thus initially parallel along the same region  $B$ , and so completed by points  $v'$  and  $w'$ . Again, the result follows from Lemma 3.30.

□

We must also consider the case of non-simultaneous image pairs:

**Lemma 3.32.** *Let  $\mathcal{P}_i, i = 1, 2$  be consistent, and let  $u \in \mathcal{P}_1^\alpha$  and  $z \in \mathcal{P}_2^\alpha$  not be a simultaneous image. Then if  $h_u$  and  $h_z$  are initially parallel, they are completed.*

*Proof.* As discussed at the beginning of this subsection, we may assume, by shifting  $\alpha$ , that any given point in  $\mathcal{P}_2^\alpha$  is the image under  $i_\alpha$  of some  $w \in \mathcal{P}_2$ . We therefore begin by fixing  $\alpha \in [\alpha]$  such that  $z = i_\alpha(w)$  (i.e. up to isotopies which do not involve a shift over  $w$ ). By assumption, this  $\alpha$  does not fix  $u$ , so there is a point  $v \in \mathcal{P}_1$  such that  $u$  is in the refinement set  $V_v$  (Figure 32(a)). In particular,  $v$  is downward. Note that  $w$  is in the interior of the associated downward triangular region  $T$  (else

we could use  $T$  to isotope  $\alpha$  so as to fix each of  $u$  and  $z$  simultaneously). The point  $w$  is thus also downward.

We wish to adapt the proof of Lemma 3.31 to this situation. We again suppose  $h_u$  and  $h_z$  are initially parallel along  $B$  with diagonal  $\Delta$ , and label the remaining two corners of  $B$  by  $y_i \in \gamma_i$ . However, we no longer have a preimage of  $h_u$ . We may get around this difficulty as follows: Observe that, after possibly shifting  $\alpha$  over  $u$ , we may assume  $u$  is not downward in  $(y_1, h_u, \alpha)$  (Figure 32(b)), so that  $h_u$  has a well-defined ‘preimage’ path  $\sigma$  with endpoint  $x \in \gamma_1$  as in Figure 32(c). Intuitively,  $\sigma$  starts at the corner  $x = \gamma_1 \cap \alpha$  of  $T$ , follows  $\alpha$  along the length of the edge of  $T$ , then coincides with  $h_v$  up to its endpoint. Thus  $\sigma$  is a path with the property that all self intersections and/or intersections with  $h_w$  lie along its coincidence with  $\alpha$ . Let  $\Delta'$  be the (unique up to isotopy) properly embedded arc obtained from  $\Delta$  by sliding its endpoint on  $\gamma_1$  along  $\gamma_1$  to  $v$ . We proceed to analyze cases as in Lemma 3.31:

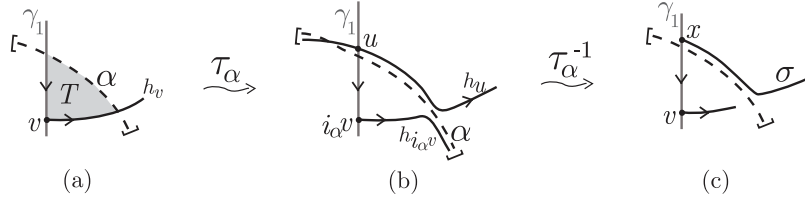


FIGURE 32. The construction of the path  $\sigma$  with basepoint  $x$  in 3.32.

- (1)  $\sigma \leq \Delta$ : Similarly to the argument of Lemma 3.29, we observe that  $h_v < \Delta'$ , and so  $h_w$  cannot be both parallel along and to the right of  $\Delta$  (at  $w$ ) without intersecting  $h_v$ . Thus  $h_w \leq \Delta$  (Figure 33(a)). The proof follows exactly as in Lemma 3.31, with  $v$  and  $h_v$  replaced by  $x$  and  $\sigma$ .
- (2)  $\sigma \geq \Delta$ : as in the argument for Lemma 3.29,  $\sigma$  cannot be *strictly* to the right of  $\Delta$ , so it is parallel along  $\Delta$ , and so by construction both  $h_v$  and  $h_w$  parallel along  $\Delta'$  (Figure 33(b),(c)). We are thus in case (2) of Lemma 3.30.

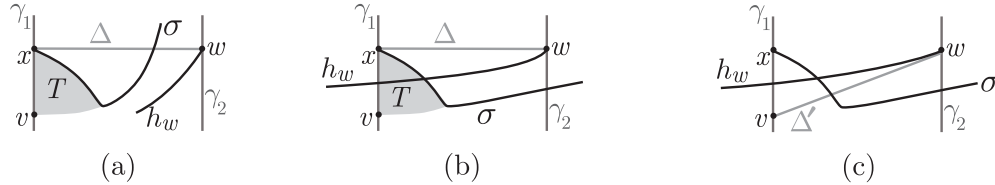


FIGURE 33. Figures for Lemma 3.32. Although in  $\Sigma$  the point  $w$  will actually lie in the region  $T$ , we keep to our convention of drawing pictures in the universal cover.

□

Finally, we bring all of the above together to prove Theorem 3.1.

*Proof.* (of Theorem 3.1) It follows from Lemmas 3.31 and 3.32 that the inductive step of the algorithm preserves consistency of right positions. It is left to show that the base step, in which  $\varphi$  is a single twist  $\tau_\alpha$ , gives consistent right positions to each pair  $\gamma_1, \gamma_2$ .

So, let  $\mathcal{P}_i$  be the right position associated to  $(\gamma_i, \tau_\alpha)$ ,  $i = 1, 2$  by the base step. We index the points and associated horizontal segments in increasing order along  $\gamma_i$  from the basepoint  $c_i$ . Suppose then that  $h_{v_j} \in H(\mathcal{P}_1)$  and  $h_{w_k} \in H(\mathcal{P}_2)$  are initially parallel horizontal segments, along region  $B$  (Figure 34(b)). As noted in the construction of the base step, each  $h_{v_j, v_{j+1}}$  is just the image of a segment of  $\gamma_1$  which has a single intersection with  $\alpha$ , with endpoints corresponding to each connected component of the fixable points  $\gamma_1 \setminus \text{support}(\tau_\alpha)$ , and similarly for each  $h_{w_j, w_{k+1}}$ . Thus, if  $n$  is the number of points of  $\mathcal{P}_1 \cap \partial B$ , then  $h_{v_j}$  and  $g_{v_k}$  are completed by the points  $v_{j+n+1}$  and  $w_{k+n+1}$ . Figure 34(b) illustrates the local picture for the case  $n = 1$ .

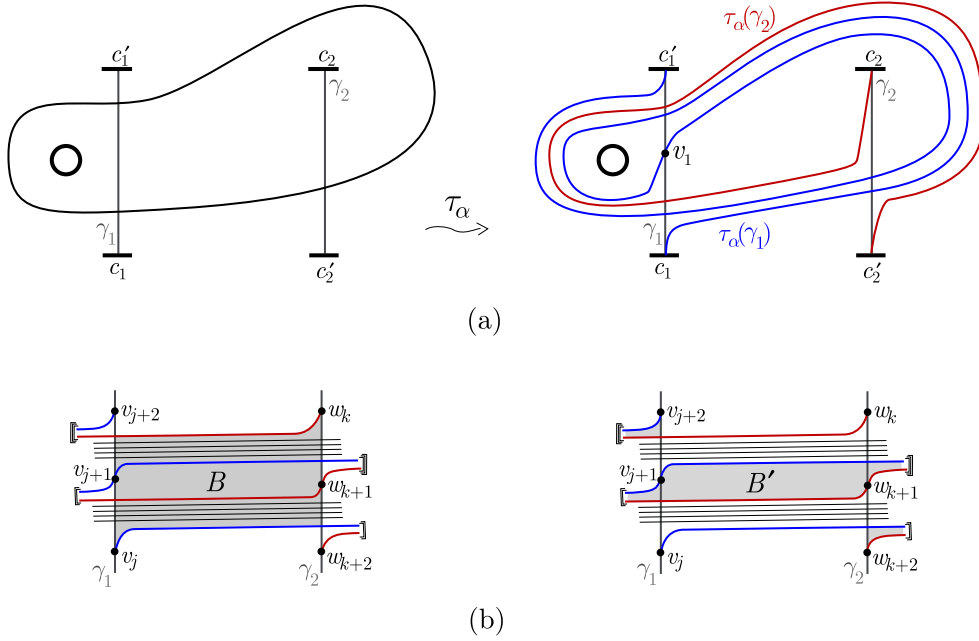


FIGURE 34. (a) An example of the right position associated to a single Dehn twist. (b) Segments  $h_{v_j}$  and  $h_{w_k}$  are initially parallel along the shaded disk in the leftmost figure, and are completed to  $v_{j+2}, w_{k+2}$  along the shaded disk in the rightmost figure

By induction, then, given a surface  $\Sigma$ , and  $\varphi \in \Gamma_\Sigma$  with positive factorization  $\omega$ , the associated right positions  $\mathcal{P}_\omega(\gamma), \mathcal{P}_\omega(\gamma')$  are consistent for any nonintersecting properly embedded arcs  $\gamma, \gamma'$ .  $\square$

#### 4. RESTRICTIONS ON $p.e.(\varphi)$

In this section, we switch focus back to the entirety of pairs of distinct properly embedded arcs  $\gamma_1, \gamma_2$  in a surface  $\Sigma$ , and the images of these arcs under right-veering  $\varphi \in \Gamma_\Sigma$ . The motivating observation here is that, as the endpoints of each arc are

by definition included in any right position, the property of the initial horizontal segments of the images being initially parallel is independent of right position, and so is a property of the pair  $\varphi(\gamma_1), \varphi(\gamma_2)$ . In particular, for *positive*  $\varphi$ , if  $\varphi(\gamma_1)$  and  $\varphi(\gamma_2)$  are initially parallel, they must admit consistent right positions  $\mathcal{P}_i(\varphi, \gamma_i)$  in which the initial segments are completed (see Example 3.9). We are interested in understanding what necessary conditions on  $\alpha \in p.e.(\varphi)$  (Definition 2.1) can be derived from the information that  $\varphi(\gamma_1)$  and  $\varphi(\gamma_2)$  are initially parallel. These are summarized in Lemma 4.4 and Theorem 4.13.

**4.1. Restrictions from initial horizontal segments.** Throughout the section, we will be considering rectangular regions  $R$  in  $\Sigma$ , and classifying various curves and arcs by their intersection with such regions. We need:

**Definition 4.1.** Let  $R$  be a rectangular region with distinguished oriented edge  $e_1$ , which we call the *base* of  $R$ . We label the remaining edges  $e_2, e_3, e_4$  in order, using the orientation on  $e_1$  (Figure 35). We classify properly embedded (unoriented) arcs on  $R$  by the indices of the edges corresponding to their boundary points, so that an arc with endpoints on  $e_i$  and  $e_j$  is of *type*  $[i, j]$  (on  $R$ ). We are only concerned with arcs whose endpoints are not on a single edge. An arc on  $R$  is then

- *horizontal* if of type  $[2, 4]$
- *vertical* if of type  $[1, 3]$
- *upward* if of type  $[1, 2]$  or  $[3, 4]$
- *downward* if of type  $[1, 4]$  or  $[2, 3]$
- *non-diagonal* if horizontal or vertical
- *type 1* if not downward

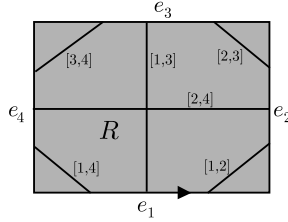


FIGURE 35. Representatives of each of the 6 possible types of arc on  $R$

**Definition 4.2.** Let  $R$  in  $\Sigma$  be an rectangular region with distinguished base as in Definition 4.1. We say  $\alpha \in SCC(\Sigma)$  is *type 1 on  $R$*  if each arc  $\alpha \cap R$  is type 1 on  $R$ .

Following Definition 4.1, we use a given pair of properly embedded arcs to define a rectangular region  $D$  of  $\Sigma$  as follows: Suppose  $\gamma_1$  and  $\gamma_2$  are disjoint properly embedded arcs, where  $\partial\gamma_i = \{c_i, c'_i\}$ , and  $\tilde{\gamma}_1$  is a given properly embedded arc with endpoints  $c'_1$  and  $c_2$ . Let  $\tilde{\gamma}_2$  be a parallel copy of  $\tilde{\gamma}_1$  with endpoints isotoped along  $\gamma_1$  and  $\gamma_2$  to  $c_1$  and  $c'_2$ . We then define  $D$  as the rectangular region bounded by  $\gamma_1, \gamma_2, \tilde{\gamma}_1, \tilde{\gamma}_2$  (the endpoints are labeled so that  $c_1$  and  $c_2$  are diagonally opposite), and base  $\tilde{\gamma}_2$ , oriented away from  $c_1$  (see Figure 36). For the remainder of this section,  $D$  will always refer to this construction. Of course, for a given pair of arcs,  $D$  is unique only up to the choice of  $\tilde{\gamma}_1$ . We also make use of the *diagonal*  $\Delta$  of

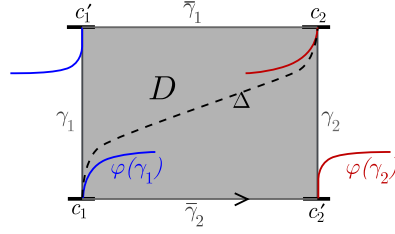


FIGURE 36. disc construction

$D$ , a representative of the unique isotopy class of arcs with boundary  $\{c_1, c_2\}$  and interior within  $D$ . In particular, the diagonal determines  $\bar{\gamma}_1$ , and vice versa.

**Definition 4.3.** We say the pair  $\varphi(\gamma_1), \varphi(\gamma_2)$  is *initially parallel (on  $D$ )* if there exists  $D$  such that  $\varphi(\gamma_1), \varphi(\gamma_2), \gamma_1, \gamma_2$  bound a rectangular region  $B \hookrightarrow D$  on which  $c_1$  and  $c_2$  are vertices. Initially parallel images are *flat* if  $D$  can be constructed such that  $\varphi(\gamma_i) \cap \bar{\gamma}_j = \emptyset$  for  $i, j \in \{1, 2\}$ .

As expected, then, the pair of arcs  $\varphi(\gamma_1), \varphi(\gamma_2)$  is initially parallel exactly when the horizontal segments  $h_{c_1}$  and  $g_{c_2}$  originating from the boundary of each pair of right positions are initially parallel. Using this, we immediately obtain:

**Lemma 4.4.** *Let  $\varphi$  be positive, and the pair  $\varphi(\gamma_1), \varphi(\gamma_2)$  initially parallel on  $D$ . Then  $\alpha \in p.e.(\varphi)$  only if  $\alpha$  is type 1 on  $D$ .*

*Proof.* Suppose otherwise - then  $\alpha \cap D$  has an arc of type  $[1, 4]$  or  $[2, 3]$  on  $D$ . Now, if  $\alpha \in p.e.(\varphi)$ , there is some positive factorization of  $\varphi$  in which  $\tau_\alpha$  is the initial Dehn twist. However, if  $\alpha \cap D$  has an arc of type  $[1, 4]$ , then  $\tau_\alpha(\gamma_1)$  is strictly to the right of  $\varphi(\gamma_1)$  (in the sense of section 2), while if the arc is of type  $[2, 3]$ , then  $\tau_\alpha(\gamma_2)$  is strictly to the right of  $\varphi(\gamma_2)$ , either of which contradicts  $\varphi(\gamma_1)$  and  $\varphi(\gamma_2)$  being initially parallel. □

Now, by Theorem 3.1, if  $\varphi$  is positive, there are consistent right positions  $\mathcal{P}_1$  and  $\mathcal{P}_2$  for any pair  $\varphi(\gamma_1), \varphi(\gamma_2)$ . If the initial horizontal segments  $h_{c_1} \in H(\mathcal{P}_1), h_{c_2} \in H(\mathcal{P}_2)$  are initially parallel, then there are  $v \in \mathcal{P}_1$  and  $w \in \mathcal{P}_2$  such that  $v$  and  $w$  are endpoints of the completed segments. Letting  $B'$  be the completing disk (Definition 3.6), we can define a new rectangular region by extending  $B'$  so that its corners lie on  $\bar{\gamma}_i$ , rather than  $\gamma_i$  :

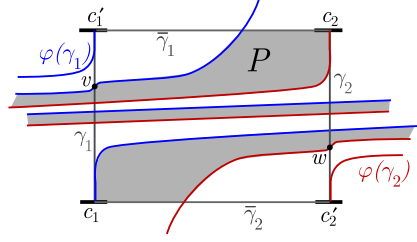
**Definition 4.5.** A *bounded path* in  $(\Sigma, D, \varphi)$  is a rectangular region  $P$  bounded by  $\bar{\gamma}_i$  and  $\varphi(\gamma_i), i = 1, 2$ , with corners  $c_1$  and  $c_2$  in common with  $D$  (Figure 37).

**Lemma 4.6.** *If  $\varphi(\gamma_1)$  and  $\varphi(\gamma_2)$  are initially parallel, for positive  $\varphi$ , then  $(\Sigma, D, \varphi)$  has a bounded path.*

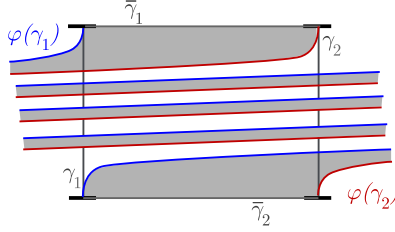
*Proof.* This is a restatement of the above discussion. □

Let  $\Sigma, D$ , and  $\varphi$  be given such that the pair  $\varphi(\gamma_1), \varphi(\gamma_2)$  is flat (and thus initially parallel) with respect to  $D$ . The remainder of this section is an exploration of what necessary conditions this places on elements of  $p.e.(\varphi)$ .

We start by observing that under these conditions (i.e. initially parallel and flat), the pair of trivial right positions whose vertical sets consist only of the arc boundary

FIGURE 37.  $P$  is a bounded path for type 1  $\varphi(\gamma_1)$  and  $\varphi(\gamma_2)$ .

points are consistent. Also, the entirety of each image  $\varphi(\gamma_i)$  is in the boundary of the bounded path (see Figure 38). In particular, such images are *parallel* in the sense of Definition 2.4. Now, for  $\alpha \in SCC(\Sigma)$ , it is clear that if all arcs  $\alpha \cap D$  are horizontal on  $D$  (Definition 4.1), then  $(D, \tau_\alpha^{-1}\varphi)$  is again initially parallel and flat, and so admits consistent right positions. Our interest then lies in  $\alpha$  such that  $\alpha \cap D$  contains diagonal arcs.

FIGURE 38. The bounded path of flat  $(D, \varphi)$ 

**Lemma 4.7.** *Let the pair  $\varphi(\gamma_1), \varphi(\gamma_2)$  be flat and initially parallel. Then  $\alpha \in p.e.(\varphi)$  only if:*

- (1):  $\alpha \cap \gamma_1 \neq \emptyset \Leftrightarrow \alpha \cap \gamma_2 \neq \emptyset$
- (2):  $\alpha \cap \varphi(\gamma_1) \neq \emptyset \Leftrightarrow \alpha \cap \varphi(\gamma_2) \neq \emptyset$

*Proof.* For statement (1), suppose  $\alpha$  is such that  $\alpha \cap \gamma_1 \neq \emptyset$  and  $\alpha \cap \gamma_2 = \emptyset$ . Referring to Figure 35, this means that arcs  $\alpha \cap D$  cannot be of type  $[2, 3]$ ,  $[1, 2]$  or  $[2, 4]$  on  $D$ , while any arc of type  $[1, 4]$  on  $D$  would result in  $\tau_\alpha^{-1} \circ \varphi$  not being right veering. Similarly, arcs  $\alpha \cap P$  cannot be of type  $[1, 2]$  or  $[1, 3]$  on  $P$ , while the right veering conditions eliminates  $[3, 4]$  and  $[1, 4]$ . Putting these together, we find that  $\alpha$  may be isotoped such that all intersections  $\alpha \cap P, D$  are along subarcs isotopic to one of the  $\rho, \rho', \rho''$  shown in the left side of Figure 40, and in particular that there is at least one along  $\rho$ .

Now, for such  $\alpha$ , the pair  $\tau_\alpha^{-1}(\varphi(\gamma_1)), \tau_\alpha^{-1}(\varphi(\gamma_2))$  is initially parallel, and so, if  $(\tau_\alpha^{-1} \circ \varphi)$  is positive, must contain a bounded path. Also, arcs along  $\rho', \rho''$  preserve the bounded path, so we may assume all intersections are along  $\rho$ . (Figure 39). It is immediate then that  $(D, \tau_\alpha^{-1}\varphi)$  has no bounded path.

The argument for statement (2) is nearly identical: We suppose  $\alpha \cap \varphi(\gamma_1) \neq \emptyset$  and  $\alpha \cap \varphi(\gamma_2) = \emptyset$ , and find that all intersections  $\alpha \cap P$  and  $\alpha \cap D$  are isotopic to one of the arcs  $\sigma, \sigma', \sigma''$  shown in the right side of Figure 40, and in particular that there is at least one along  $\sigma$ . Again,  $(D, \tau_\alpha^{-1}\varphi)$  has no bounded path.



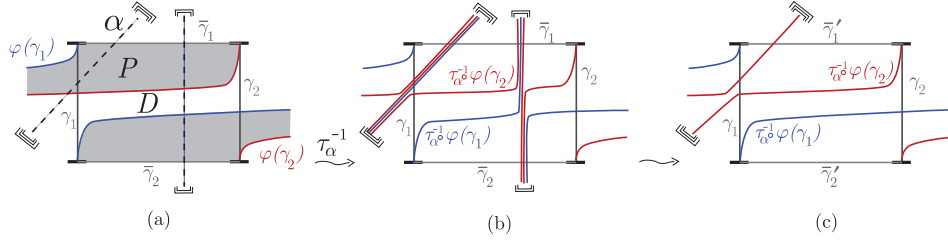


FIGURE 39. Illustration of the terminology of Lemma 4.7. (a) A typical  $\alpha$ , with one arc along  $\rho'$ , and one along  $\rho$ . (b) is the image under  $\tau_\alpha^{-1}$ . Notice that, to recover a standard picture of the associated  $D$ , we must ‘normalize’ the picture as in (c), thereby justifying the assertion that arcs along  $\rho'$  and  $\rho''$  may be ignored. It is clear that there is no bounded path.

Note that this is a slight generalization of the second example of Example 3.9. □

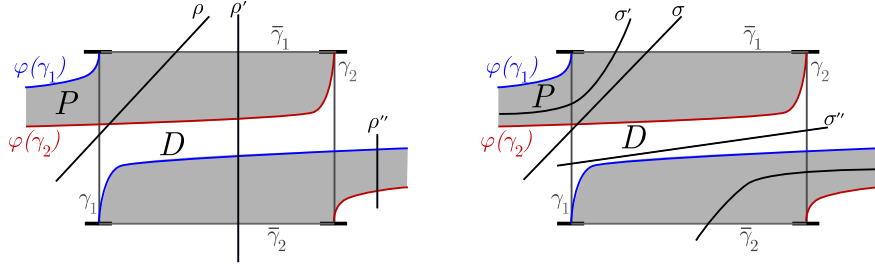


FIGURE 40.

We have one final application of the bounded path construction. Note that, for  $\alpha$  and  $D$  as above, an orientation of  $\alpha$  gives a derived orientation on each arc in  $D \cap \alpha$ . Thus, given a pair of upward arcs, we can ask whether their derived orientations agree, independently of the actual orientation of  $\alpha$ .

**Lemma 4.8.** *Let  $\varphi(\gamma_1)$  and  $\varphi(\gamma_2)$  be flat and initially parallel. Let  $\alpha$  be type 1 on  $D$ , such that  $\alpha \cap D$  has exactly 2 diagonal (so necessarily upward) arcs  $s_1$  and  $s_2$ . Then  $\alpha \in p.e.(\varphi)$  only if the derived orientations on  $s_1$  and  $s_2$  agree.*

*Proof.* Note firstly that, by Lemma 4.7,  $s_1$  and  $s_2$  must be as in Figure 41(a); i.e. one cuts the upper left corner of  $D$ , the other the lower right corner. We show that  $(D, \tau_\alpha^{-1}\varphi)$  has a bounded path if and only if the derived orientations on  $s_1$  and  $s_2$  agree, which, by Lemma 4.6 gives the result.

Note that if  $\alpha \cap D$  has a horizontal arc, it cannot have a vertical arc, and vice-versa. We distinguish the two cases:

- (1)  $\alpha \cap D$  has no vertical arcs. The boundary of bounded path  $P$  must include the initial segments of each arc  $\tau_\alpha^{-1}(\varphi(\gamma_i))$  from  $c_i$ ,  $i = 1, 2$ . We can then start from either corner  $c_i$  and follow the initial segment around  $\alpha$ . Figure

- 41 illustrates this for  $c_1$ . It is clear then that these initial segments will close up to bound  $P$  if the orientations match (Figure 41(b)). If, on the other hand, the orientations do not match, the segments do not form the boundary of a bounded path (Figure 41(c)).
- (2)  $\alpha \cap D$  has no horizontal strands. If there are vertical strands, we must adjust  $D$  such that the diagonal is given by  $\tau_\alpha^{-1}(\Delta)$ . Again, as in case (1), there is a bounded path if and only if the derived orientations on  $s_1$  and  $s_2$  agree.

□

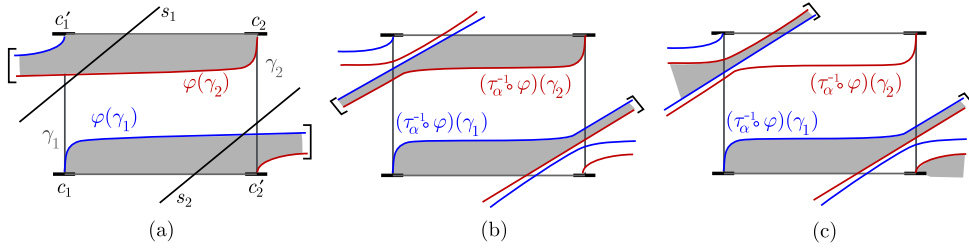


FIGURE 41. (a)  $\alpha \cap D$  has exactly 2 diagonal arcs  $s_1$  and  $s_2$ . (b) Orientations agree. (c) Orientations disagree.

**4.2. Restrictions from the full set of horizontal segments.** To summarize the previous subsection, for flat  $(D, \varphi)$ ,  $\alpha \in p.e.(\varphi)$  only if  $\alpha$  is type 1 on  $D$ , and satisfies the intersection conditions of Lemma 4.7. Furthermore, if  $\alpha \cap D$  has only two diagonal arcs, it must satisfy the orientation conditions of Lemma 4.8. We now wish to utilize the results of Section 3 to extend these results to the sets of horizontal segments of consistent right positions of the arc/monodromy pairs, and thus to obtain stronger necessary conditions on arbitrary type 1  $\alpha$  for inclusion in  $p.e.(\varphi)$ .

**4.2.1. Motivating examples.** We begin with a pair of examples, meant to motivate the various definitions to come.

*Example 4.9.* Consider a flat  $(D, \varphi)$ , where  $\varphi \in Dehn^+(\Sigma)$ , with consistent right positions  $\mathcal{P}_1$  and  $\mathcal{P}_2$  for the edges  $\gamma_1$  and  $\gamma_2$  of  $D$  (Figure 42(a)). The segments  $h_{c_1}$  and  $h_{c_2}$  are of course initially parallel, so completed by some  $v \in \mathcal{P}_1$  and  $w \in \mathcal{P}_2$  (it is easiest to keep in mind the simplest case in which  $v$  and  $w$  are the opposite endpoints of  $\gamma_1$  and  $\gamma_2$ , as in the Figure). Let  $\alpha$  be a type 1 simple closed curve such that  $\alpha \cap D$  has exactly two diagonal arcs, and satisfies the intersection conditions of Lemma 4.7 and orientation conditions of Lemma 4.8. It is straightforward to verify that any consistent positions  $\mathcal{P}'_i$  for  $((\tau_\alpha^{-1} \circ \varphi), \gamma_i)$ ,  $i = 1, 2$ , must contain uniquely determined points  $v_2 \in \mathcal{P}'_1$  and  $w_2 \in \mathcal{P}'_2$  which complete the initially parallel initial segments, and further that these points define initially parallel segments  $h_{v_2}$  and  $h_{w_2}$  which are then completed by the original completing points  $v$  and  $w$ , which are preserved by  $\tau_\alpha^{-1}$ . Furthermore, the corners of the regions are each fixable (indicated by circles in the Figure). The regions and points involved are illustrated in Figure 42(b).

Consider then a slightly more complicated configuration, in which  $\alpha$  has 4 diagonal arcs, arranged as in Figure 42(c). Again, one may verify that any consistent right positions for  $((\tau_\alpha^{-1} \circ \varphi), \gamma_i)$  must contain one of the two positions indicated in Figure 42(e) and (f). Again, each of these determines a sequence of regions and points which ends with the original completions. The goal of the remainder of this section is to show that for *any* type 1  $\alpha$ , any pair of consistent right positions for  $((\tau_\alpha^{-1} \circ \varphi), \gamma_i)$  must contain a similar sequence, which then determines necessary conditions on  $\alpha \in p.e.(\varphi)$  which generalize those of Lemmas 4.7 and 4.8.

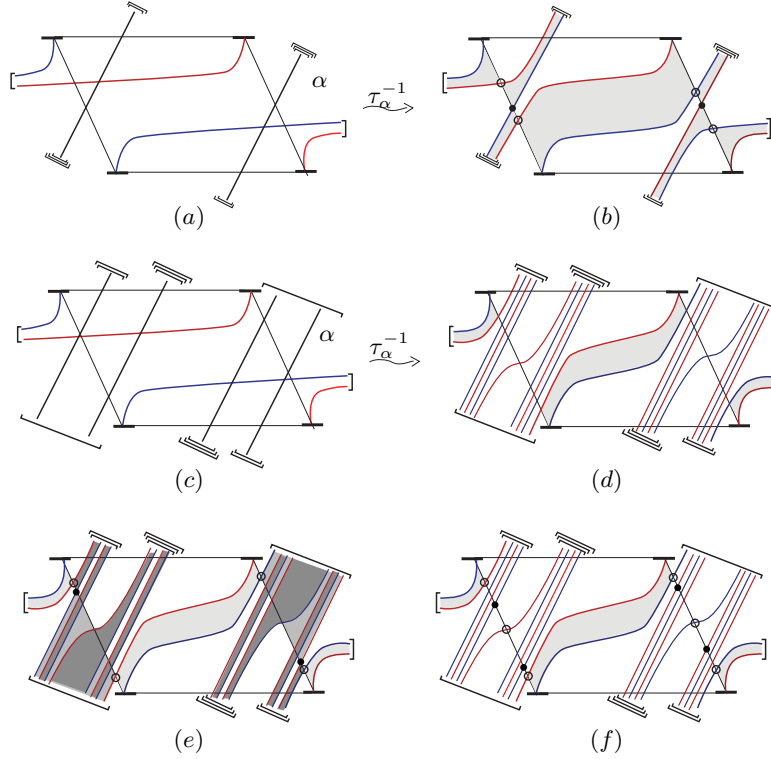


FIGURE 42.

4.2.2. *Notation and conventions.* Given flat  $(D, \varphi)$ , and a type 1 curve  $\alpha$ , we label the upward sloping arcs  $s_i \in \alpha \cap D$  as in Figure 43. A subarc  $s_i$  is thus defined only in a neighborhood of the point  $x_i$ . Let  $a_1, a_2, \dots, a_m$ , where  $a_1 = 1$ , be the indices of the  $x_i$  with order given by the order in which they are encountered traveling along  $\alpha$  to the right from  $x_1 \cap \gamma_1$ . We associate to  $\alpha$  the list  $\pi_\alpha = (a_1, a_2, \dots, a_m)$ , defined up to cyclic permutation. We decorate an entry with a bar,  $\overline{a_j}$ , if the derived orientations of  $s_{a_j}$  and  $s_1$  do not agree.

Given a pair  $x_i \in \alpha \cap \gamma_2$  and  $x_j \in \alpha \cap \gamma_1$  (so  $i$  is even,  $j$  odd), the pair splits  $\alpha$  into two disjoint arcs. If the orientations of  $s_i$  and  $s_j$  agree, we label these arcs  $\eta_{i,j}$  and  $\eta_{j,i}$  (where for even  $i$ ,  $\eta_{i,j}$  refers to the arc connecting  $x_i$  and  $x_j$  and initially exterior to  $D$  at each endpoint, so for odd  $j$ , a neighborhood of each endpoint of  $\eta_{j,i}$  is contained in  $D$ ). We refer to each such arc as a *path* of the pair  $(\alpha, D)$ . We say paths  $\eta$  and  $\eta'$  are *parallel* if, after sliding endpoints along the  $\gamma_i$  so as to

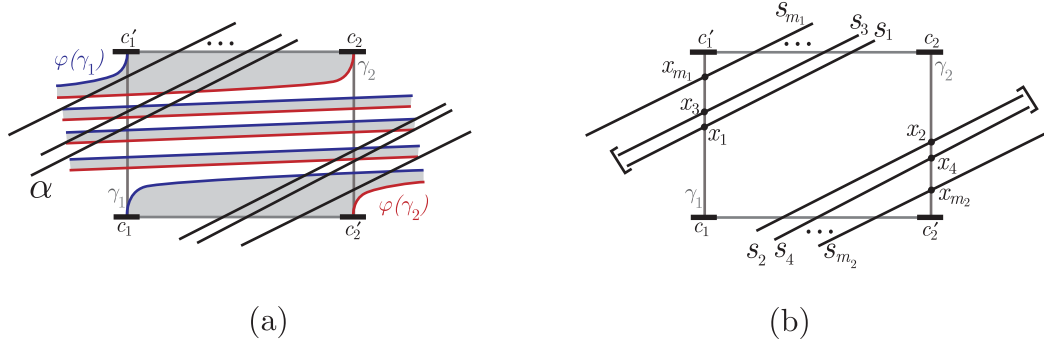


FIGURE 43. (a) The diagonal arcs of  $\alpha \cap D$ . (b) Labeling of arcs and intersections. The paths  $\eta_{2,3}$  and  $\eta_{4,1}$  are components of a symmetric multipath.

coincide, they are isotopic as arcs (relative to their endpoints). Then a *multipath* of  $(\alpha, D)$  is a collection of more than one pairwise parallel path (Figure 43).

Of particular interest will be the following special case:

**Definition 4.10.** A multipath as described in the previous paragraph is *symmetric* if its components are  $\eta_{a_1, b_1}, \eta_{a_2, b_2}, \dots, \eta_{a_r, b_r}$ , where each pair  $\{a_i, b_{r+1-i}\}$  is  $\{j, j-1\}$  for some even  $j$ . So, for example, any symmetric *path* is  $\eta_{j, j-1}$  or  $\eta_{j-1, j}$  for some even  $j$ .

We may now state the main definitions of this subsection, which generalize the conditions of Lemmas 4.7 and 4.8:

**Definition 4.11.** Let  $\alpha \in SCC(\Sigma)$  be type 1 on a region  $D$ . We say  $\alpha$  is *nested* with respect to  $D$  if its associated  $\pi_\alpha$  can be reduced to the trivial by successive removals of pairs  $(i, j)$  of consecutive entries, where  $\eta_{i, j}$  is a symmetric path or component of a symmetric multipath. We call  $\alpha$  *balanced* (with respect to  $D$ ) if each  $x_i$  is an endpoint in a symmetric path or component of a symmetric multipath.

Note that, in the absence of symmetric multipaths of more than one component, these properties are encoded in  $\pi_\alpha$ . For example,  $(1\bar{4}5632)$  is nested but not balanced,  $(135462)$  is balanced but not nested, and  $(1\bar{4}56\bar{3}2)$  is both nested and balanced. Also note that either condition requires the number of intersections  $|\alpha \cap \gamma_1|$  to equal  $|\alpha \cap \gamma_2|$ ; i.e.  $m_1 + 1 = m_2$ .

We will want to characterize these conditions in terms of paths of  $\alpha$ . We need:

**Definition 4.12.** Let  $\eta_{a, b}, \eta_{c, d} \subset \alpha$  be paths. We refer to the pair as *nested* if either one contains the other, or they are disjoint. Otherwise, the pair is *non-nested*.

It is then immediate that balanced  $\alpha$  is nested if and only if each pair of components of symmetric multipaths is nested.

The motivation for these definitions becomes clear with the following:

**Theorem 4.13.** Let  $(D, \varphi)$  be flat and parallel. Then  $\alpha \in p.e.(\varphi)$  only if  $\alpha$  is nested and balanced with respect to  $D$ .

We will postpone the proof so as to introduce even more terminology and a couple of helpful lemmas. The basis of the argument is that, if  $\alpha \in p.e.(\varphi)$ , then

$\tau_\alpha^{-1} \circ \varphi$  admits a positive factorization, and so by Theorem 3.1 there are consistent right positions  $\mathcal{P}_i$  of  $((\tau_\alpha^{-1} \circ \varphi), \gamma_i)$ . By Lemma 4.6 the arcs  $\tau_\alpha^{-1}(\varphi(\gamma_i))$  are initially parallel, and so the  $\mathcal{P}_i$  must include completing points which we label  $v_2$  and  $w_2$ . As noted in Example 4.9, the horizontal segments  $h_{v_2}$  and  $h_{w_2}$  are also initially parallel, and so for consistency must be completed by some  $v_3$  and  $w_3$ . In fact, for  $1 \leq j \leq p$ , where  $p$  depends on the number of symmetric paths of  $(\alpha, D)$ , there are points  $v_j$  and  $w_j$  such that each pair of horizontal segments  $h_{v_j}, h_{w_j}$  is initially parallel, and completed by the pair  $v_{j+1}, w_{j+1}$ . This in turn will require  $\pi_\alpha$  *balanced* for this sequence to continue to the opposite endpoints of the  $\gamma_i$ , and *nested* for overall consistency of the right positions. The situation for the simplest case ( $\pi_\alpha = (1, 2)$ ) is illustrated in Figure 44.

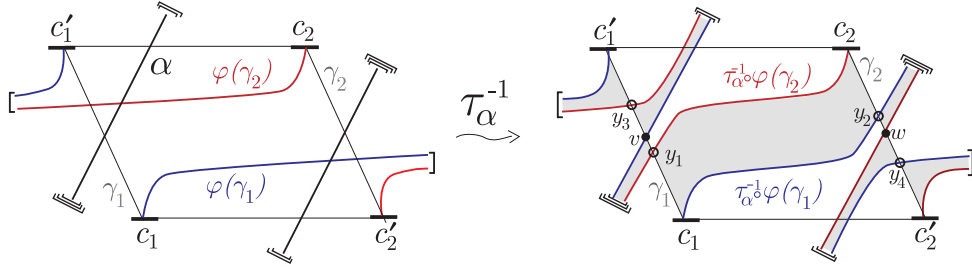


FIGURE 44. The simplest possible nested and balanced  $\alpha$  (where  $\pi_\alpha = (1, 2)$ ), and the regions involved in the minimal consistent right positions on  $\tau_\alpha^{-1}(\varphi(\gamma_i))$ .

For the more general case, we will refer to Figure 45, in particular restricting  $\tau_\alpha^{-1}$  to a neighborhood  $U(\alpha)$  of  $\alpha$ . We must keep track of subarcs of  $\tau_\alpha^{-1}(\varphi(\gamma_j))$  in a neighborhood of each point  $\alpha \cap \gamma_i$ . Each neighborhood will contain exactly  $m$  subarcs (which we will call *strands*), each of which is a subarc of one of the subarcs  $[y_k, y_{k+2}]$  of one of the  $\tau_\alpha^{-1}(\varphi(\gamma_j))$  (Figure 45 makes this clear). The entire (inverse) image then is determined by the ‘local pictures’ given these point-neighborhoods along with the information of how they fit together. We will refer to such a point-neighborhood as  $N_j$ . In particular, as each such subarc has a unique intersection point with a  $\gamma_i$ , we may refer to it by way of a coordinate system on  $U(\alpha)$ : denote the intersection of the subarc  $[y_k, y_{k+2}]$  (in the inverse image) with the point-neighborhood  $N_j$  as  $s_k^j$  (Figure 45 gives an example). Each point of  $\gamma_i \cap \tau_\alpha^{-1}(\varphi(\gamma_i))$  may then be uniquely identified by the  $s_k^j$  on which it lies.

**Definition 4.14.** Given a pair of complementary paths  $\eta_{a,b}$  and  $\eta_{b,a}$ , where  $a$  is even, let  $B_{a,b}$  and  $B_{b,a}$  be the rectangular regions bounded by  $\gamma_1, \tau_\alpha^{-1}(\varphi(\gamma_1)), \gamma_2$ , and  $\tau_\alpha^{-1}(\varphi(\gamma_2))$ , where  $B_{a,b}$  has corners  $y_a$  and  $y_b$ ,  $B_{b,a}$  has corners  $y_{b+2}$  and  $y_{a+2}$ , and  $B_{a,b} \cup B_{b,a}$  retracts to  $\alpha$  (Figure 46 (a)). We refer to each region as *basic*. Observe that, using our coordinates on  $U(\alpha)$ , each  $B_{p,q}$  contains exactly the points  $\{s_r^l \mid x_r \in \eta_{p,q}, x_l \in \eta_{q,p}\}$ . We refer to basic regions  $B_{a,b}$  and  $B_{c,d}$  as *nested* or *non-nested* if the associated paths  $\eta_{a,b}$  and  $\eta_{c,d}$  are nested or non-nested. From the definitions, we see that, if  $B_{a,b}$  and  $B_{c,d}$  are nested, they are either disjoint, or intersect in ‘strips’ as in Figure 46 (b). Conversely, if the regions are non-nested, they intersect in a ‘corner overlap’ as in Figure 46 (c).

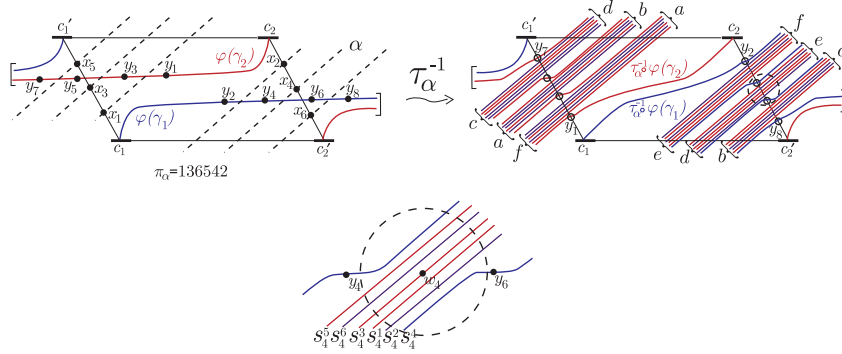


FIGURE 45. Above left, the various points of  $\alpha \cap \gamma_i$  and  $\alpha \cap \varphi(\gamma_i)$ . Above right, the inverse image  $\tau_\alpha^{-1}(\varphi(\gamma_i))$ , for  $\alpha$  with  $\pi_\alpha = 136542$  (strands terminating in brackets with like letters are meant to be identified). Below, a detail of a point-neighborhood  $N_4$ .

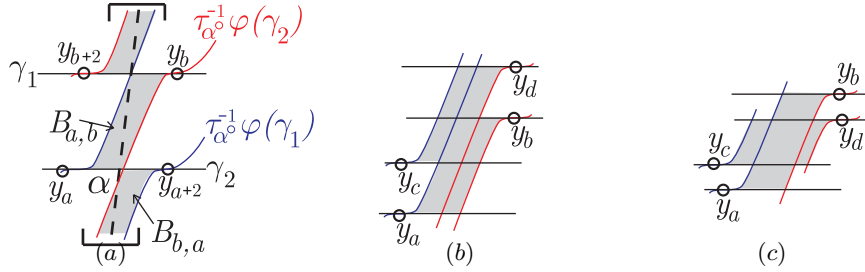


FIGURE 46. (a) The region  $B_{a,b}$  corresponding to the path  $\eta_{a,b}$ , and complementary  $B_{b,a}$  corresponding to  $\eta_{b,a}$ . The curve  $\alpha$  is the dashed line. (b) Non-nested, and (c) nested regions.

Throughout the rest of this section, all notation will be as in Figures 45 and 46. We will further assume that  $m_1 \geq m_2 - 1$ ; i.e. that there are at least as many upward intersections  $\alpha \cap \gamma_1$  as there are upward intersections  $\alpha \cap \gamma_2$ .

4.2.3. *The positions  $\mathcal{P}_1^*$  and  $\mathcal{P}_2^*$ .* Our immediate goal is to show that, if  $(\tau_\alpha^{-1} \circ \varphi, \gamma_i), i = 1, 2$  admit consistent right positions, then any such pair of positions extends non-trivially along the entire length of each arc, as described above. Theorem 4.13 will then follow from various properties of these positions.

**Lemma 4.15.** *Let  $(D, \varphi)$  be flat and parallel,  $\alpha \in p.e.(\varphi)$ , and  $\mathcal{P}_i, i = 1, 2$  consistent right positions of  $(\tau_\alpha^{-1} \circ \varphi, \gamma_i)$ . Then there are  $\{v_j\}_{j=1}^n \subset \mathcal{P}_1, \{w_j\}_{j=1}^n \subset \mathcal{P}_2$ , and  $\{e_k\}_{k=1}^{2n} \subset \mathbb{N}$  such that*

- (1) *Each of the sets  $\{v_j\}$  and  $\{w_j\}$  is a right position (i.e.  $v_1 = c_1$  and  $v_n = c'_1$ , and  $w_1 = c_2$  and  $w_n = c'_2$ ), and the indices  $1, \dots, n$  increase along each of  $\gamma_i$  and  $\tau_\alpha^{-1}(\varphi(\gamma_i))$ .*
- (2) *For each  $j < n$ , segments  $h_{v_j, v_{j+1}}$  and  $h_{w_j, w_{j+1}}$  are initially parallel along a region  $B_j$ , and completed along a region  $B'_j$  with endpoints  $v_{j+1}$  and  $w_{j+1}$ . Furthermore, the set of midpoints for these regions are fixable, and the*

midpoints of the completing pair  $B_j, B'_j$  are  $y_{e_{2j-1}}$  and  $y_{e_{2j}}$  (in the set  $\{y_k\}$  of fixable points indicated in Figure 45).

(See Figure 47 for a schematic illustration.)

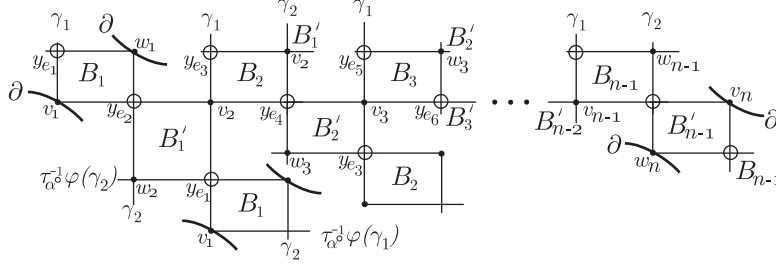


FIGURE 47. A schematic overview of the positions  $\mathcal{P}_1^*$  and  $\mathcal{P}_2^*$  constructed in Lemma 4.15. The picture is of the universal cover of  $\Sigma$ , along a lift of  $\tau_\alpha^{-1}(\varphi(\gamma_1))$ . As usual, all lifts of an object are given the same label as the original object. The circled vertices are the fixable points  $\{y_k\}$ .

*Proof.* By assumption,  $y_1$  and  $y_2$  (as in Figure 45) are midpoints of an initially parallel region  $B_1$ , which for consistency must be completed by some region  $B'_1$  with endpoints  $v_2$  and  $w_2$ . We need then to show that the horizontal segments  $h_{v_2, c'_1}$  and  $h_{w_2, c'_2}$  are themselves initially parallel along a region with midpoints again in the fixable point set  $\{y_k\}$ . The result will then follow, as we may repeat the construction until we hit one of the opposite endpoints.

Using the ‘coordinate’ notation introduced above, recall that  $v_2$  can be uniquely described by the strand  $s_r^l$  on which it lies. This also determines  $w_2$  as lying on  $s_{r+1}^{l-1}$  (Figure 48(a)). Observe that it cannot be the case that both  $r > 1$  and  $l > 2$ ; in particular this would imply that the arcs  $[y_2, y_4], [y_4, y_6] \subset \tau_\alpha^{-1}(\varphi(\gamma_1))$  are parallel, and thus that  $\alpha$  is not connected (Figure 48(b)). We distinguish 3 cases:

- (1) Suppose firstly that  $r = 1, l = 2$ , so  $v_2$  lies in the intersection of the arc  $[y_2, y_4]$  with  $N_1$ , and thus  $w_2$  lies in the intersection of the arc  $[y_1, y_3]$  with  $N_2$ . It follows from Lemma 4.8 that  $v_2$  and  $w_2$  are completing points if and only if  $\eta_{2,1}$  is a symmetric path of  $\alpha, D$ , in which case  $h_{v_2}$  and  $h_{w_2}$  will be initially parallel along a region with midpoints  $y_3$  and  $y_4$  (this is the case illustrated in Figure 44. For later reference, we note that  $B'_1$  and  $B_2$  are (respectively) exactly the basic regions  $B_{2,1}$  and  $B_{1,2}$  defined earlier.
- (2) We next consider the case  $r > 1$ . Then  $v_2$  in  $N_r$  and  $w_2$  in  $N_{r+1}$  define a completing region  $B'_1$ , which in turn implies existence of a symmetric multipath of  $\alpha, D$  with  $(r+1)/2$  components  $\eta_{2,r}, \eta_{4,r-2}, \dots, \eta_{r+1,1}$  (the case  $r = 5$  is illustrated in Figure 49(a)). So  $l = 2$ , and  $h_{v_2}$  and  $h_{w_2}$  are initially parallel along a region  $B_2$  as in the Figure. Observe that  $B'_1$  contains each of the basic regions  $B_{2,r}, B_{4,r-2}, \dots, B_{r+1,1}$ , arranged in a ‘row’ between  $\gamma_1$  and  $\gamma_2$ , while  $B_2$  contains each of the complementary basic regions  $B_{r,2}, B_{r-2,4}, \dots, B_{1,r+1}$ , arranged in a ‘column’ between  $\tau_\alpha^{-1}(\varphi(\gamma_1))$  and  $\tau_\alpha^{-1}(\varphi(\gamma_2))$ .

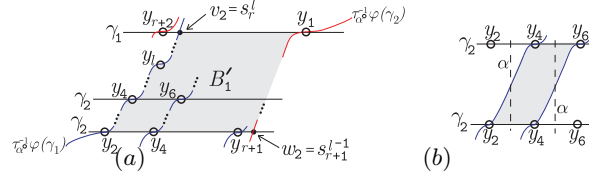


FIGURE 48. (a) The general situation for the completing disc  $B'_1$ . If both  $r > 1$  and  $l > 2$ , then there is a rectangular subregion of  $B'_1$  with edges  $[y_2, y_4] \subset \gamma_2$ ,  $[y_2, y_4] \subset \tau_\alpha^{-1}(\varphi(\gamma_1))$ ,  $[y_4, y_6] \subset \gamma_2$ ,  $[y_4, y_6] \subset \tau_\alpha^{-1}(\varphi(\gamma_1))$  as in (b). Observe then that  $\alpha$  (the dashed lines) cannot be a connected curve.

- (3) Finally, suppose  $l > 2$ . By case (2), this implies  $r = 1$ . The configuration is complementary to that of case (2), in that  $h_{v_2}$  and  $h_{w_2}$  are now initially parallel along a region  $B_2$  determined by a symmetric multipath with  $l/2$  components,  $\eta_{1,l}, \eta_{3,l-2}, \dots, \eta_{l-1,2}$ . Again, Figure 49(b) illustrates the situation (for the case  $l = 6$ ). Again  $B'_1$  contains each of the basic regions  $B_{2,l-1}, B_{4,l-3}, \dots, B_{l,1}$ , but they are now arranged in a column, while the complementary basic regions of  $B_2$  are in a row.

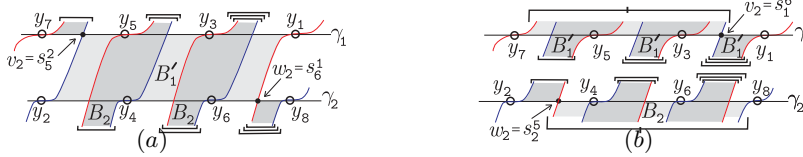


FIGURE 49. Figures for Lemma 4.15. (a) The case  $r = 5$ , so  $v \in N_5$  and  $w \in N_6$ . The completing region  $B'_1$  for  $h_{c_1}$  and  $h_{c_2}$  is lightly shaded, while the initially parallel region  $B_2$  for  $h_{v_2}$  and  $h_{w_2}$  is darkly shaded.  $B'_1$  contains basic regions  $B_{2,5}, B_{4,3}$ , and  $B_{6,1}$ , while  $B_2$  contains  $B_{5,2}, B_{3,4}$ , and  $B_{6,1}$ . Though irrelevant to our argument, for intuition it is perhaps worth noting that the paths taken by the basic regions of  $B_2$ , which are here represented with our usual bracket notation, will each cross  $B'_1$  exactly  $r - 3$  times (compare with Figure 42(e)). (b) The ‘complementary’ case  $l = 6$ .

Continuing in this fashion, then, we obtain a sequence of points  $\{v_j\}$  and  $\{w_j\}$  satisfying condition (2), which continues until we hit an endpoint; i.e.  $w_n = c'_2$  (recall that we are assuming  $m_1 \geq m_2 - 1$ ). Condition (1) will then be satisfied if  $m_1 = m_2 - 1$ , so that the corresponding  $v_n$  is the other endpoint  $c'_1$ . This however follows using the argument of Lemma 4.7; replacing  $\varphi(\gamma_1)$  and  $\varphi(\gamma_2)$  in that Lemma with the segments  $h_{v_{n-1}, c'_1}$  and  $h_{w_{n-1}, c'_2}$ , we see that these segments are initially parallel, and completed only if  $v_n = c'_1$ . Figure 50 shows the relevant regions.  $\square$

We have the following immediate corollary, giving us ‘half’ of Theorem 4.13:

**Corollary 4.16.** *Let  $(D, \varphi)$  be flat and parallel. Then  $\alpha \in p.e.(\varphi)$  only if  $\alpha$  is balanced with respect to  $D$ .*  $\square$



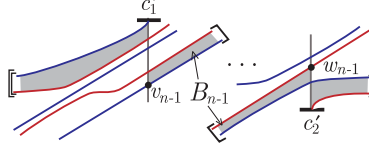


FIGURE 50.

4.2.4. *Nestedness.* The proof of the remainder of Theorem 4.13, that *nestedness* is a further necessary condition for consistency, in fact also follows easily from this lemma, but keeping track of everything involved requires quite a bit of notation. We begin by using Lemma 4.15 to characterize nestedness in terms of regions and endpoints.

Firstly, denote by  $\mathcal{R}(\mathcal{P}_1, \mathcal{P}_2)$  the set of initially parallel / completed regions in a pair of right positions  $\mathcal{P}_1$  and  $\mathcal{P}_2$ . As in the proof of Lemma 4.15, we associate to each region  $B_j$  (or  $B'_j$ ) of  $\mathcal{R}(\mathcal{P}_1^*, \mathcal{P}_2^*)$  a collection of basic regions which it contains. Using our rather cumbersome notation, regions  $B_{2, e_3-2}, B_{4, e_3-4}, \dots, B_{e_4-2, 1}$  are the basic regions of  $B'_1$ , while the complementary set gotten by switching each pair of indices is associated to  $B_2$ . In general of course,  $B_{e_{2j}, e_{2j+1}-2}, \dots, B_{e_{2j+2}-2, e_{2j-1}}$  are the basic regions of  $B'_j$ , their complements the basic regions of  $B_{j+1}$ . It is sufficient to keep in mind Figure 49.

We can thus characterize nestedness in terms of regions as follows:

*Observation 4.17.* A balanced curve  $\alpha$  is nested if and only if, for any two regions  $A, B \in \mathcal{R}(\mathcal{P}_1^*, \mathcal{P}_2^*)$ , any pair consisting of a basic region of  $A$  and a basic region of  $B$  is nested (Figure 46).

Finally, again using the proof of Lemma 4.15, if  $B_{a_1, b_1}, B_{a_2, b_2}, \dots, B_{a_l, b_l}$  are the regions associated to  $B'_j$ , where  $a_{i+1} > a_i$  for each  $i$ , then the endpoints  $v_{j+1} \in \mathcal{P}_1^*$  and  $w_{j+1} \in \mathcal{P}_2^*$  are either  $\{s_{a_l}^{b_l}, s_{a_1}^{b_1}\}$  or  $\{s_{b_1}^{a_1}, s_{b_l}^{a_l}\}$ .

We need:

**Definition 4.18.** Given a pair of right positions  $\mathcal{P}_1$  and  $\mathcal{P}_2$ , we call a region  $B \in \mathcal{R}(\mathcal{P}_1, \mathcal{P}_2)$  *empty* (in  $(\mathcal{P}_1, \mathcal{P}_2)$ ) if neither the interior of  $B$  nor the interior of the edges which form  $\partial B$  contain any points of either  $\mathcal{P}_i$ . Conversely, any point  $y$  in the fixable point set  $\{y_k\}$  is *isolated* (in  $\mathcal{R}(\mathcal{P}_1, \mathcal{P}_2)$ ) if, for each  $B \in \mathcal{R}(\mathcal{P}_1, \mathcal{P}_2)$ ,  $y$  is not in the interior of  $B$  nor the interior of the edges which form  $\partial B$ .

**Lemma 4.19.** Let  $\mathcal{P}_1^*$  and  $\mathcal{P}_2^*$  be as in Lemma 4.15. Suppose for some  $j$  the region  $B'_j$  is empty in  $\mathcal{R}(\mathcal{P}_1^*, \mathcal{P}_2^*)$ , and that the midpoints  $y_{e_{2j-1}}, y_{e_{2j}}$  is isolated in  $\mathcal{R}(\mathcal{P}_1^*, \mathcal{P}_2^*)$ . Then

- (1)  $B_{j+1}$  is empty in  $(\mathcal{P}_1^*, \mathcal{P}_2^*)$
- (2) The midpoints  $y_{e_{2j+1}}$  and  $y_{e_{2j+2}}$  are also isolated in  $\mathcal{R}(\mathcal{P}_1^*, \mathcal{P}_2^*)$ .
- (3) For any  $B \in \mathcal{R}(\mathcal{P}_1^*, \mathcal{P}_2^*)$ , each pair consisting of a basic region of  $B$  and a basic region of  $B'_j$  is nested.

*Proof.* This is clear once one has the correct picture in mind. We will consider the case  $j = 1$ , from which the general case will follow. We will draw the situation as in Figure 51(a), so that the  $t$  basic regions of  $B'_1$  are lined up as indicated, so that we may refer to them by their relative positions within the figure. In particular,  $B_{2, 2t-1}$  is the ‘leftmost’ region,  $B_{2t, 1}$  the ‘rightmost’. Consider then a

region  $B \in \mathcal{R}(\mathcal{P}_1^*, \mathcal{P}_2^*)$ . We will assume for notational sake that  $B = B'_k$  for some  $k$ , so that the associated basic regions are  $B_{p,p+q+1}, \dots, B_{p+q,p-1}$  for some even  $p$  and  $q$ . We consider two cases:

- (1) There are non-nested  $B_{a,b}$  associated to  $B'_1$  and  $B_{c,d}$  associated to  $B'_k$ . Without loss of generality, we may assume the entries  $a, c, b, d$  occur in that order in  $\pi_\alpha$ . Observe then that  $B_{a,b}$  and  $B_{c,d}$  intersect as in Figure 46 (b); i.e. the upper left corner of  $B_{a,b}$  is in the interior of  $B_{c,d}$ , while the lower right corner of  $B_{c,d}$  is in the interior of  $B_{a,b}$ . Now, as  $y_1$  is isolated, the ‘rightmost’ basic region  $B_{p+q,p-1}$  of  $B'_k$ , of which  $v_{k+1}$  is a corner, also overlaps one of the basic regions of  $B'_1$  (Figure 51 (a)). As  $B'_1$  is assumed empty, this implies that  $v_{k+1} = s_{p-1}^{p+q}$ , so that  $B'_k$  is a ‘column’ (as described in the proof of Lemma 4.15). But then as  $y_2$  is isolated, it follows that the leftmost region,  $B_{p,p+q-1}$ , also overlaps a basic region of  $B'_1$ . But then (Figure 51 (b)) we have  $w_{k+1} = s_p^{p+q-1}$  in the interior of  $B'_1$ , a contradiction. Property (3) is thus verified.
- (2) In the absence of non-nested regions, recall that any intersections among the basic regions are in ‘strips’ as in Figure 46. It is simple to see then (from e.g. Figure 49) that if either the upper left or lower right corner of a basic region of  $B'_k$  lies in  $B_2$ , it lies in  $B'_1 \cap B_2$ , a contradiction. In particular, neither endpoint of  $B'_k$  lies in  $B_2$ . Property (1) is thus also verified.

Finally, we must show property (2), that  $B$  contains neither of  $y_{e_3}, y_{e_4}$ . Suppose otherwise, say  $y_3$  lies in  $B$ . Then, as by construction no basic region contains any  $y_k$ , the point  $y_{e_3}$  must lie in the complement of the basic regions of  $B$ . But then  $B'_1$  and  $B$  contain non-nested regions, contradicting (1) above.

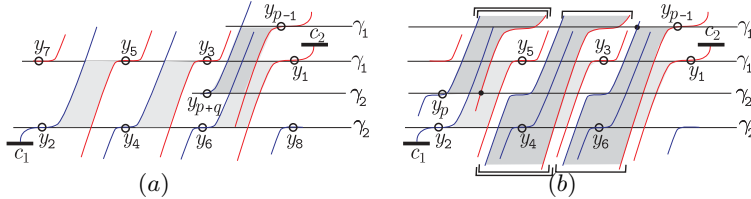


FIGURE 51. Figures for Lemma 4.19 (the case  $t = 3$ , so  $e_3 = 7, e_4 = 8$ ).

For the general case we simply adjust indices. □

Similarly,

**Lemma 4.20.** *Suppose the region  $B_j$  is empty in  $(\mathcal{P}_1, \mathcal{P}_2)$ , and the midpoints  $y_{e_{2j-1}}$  and  $y_{e_{2j}}$  isolated in  $\mathcal{R}(\mathcal{P}_1, \mathcal{P}_2)$ . Then  $B'_j$  is also empty in  $(\mathcal{P}_1, \mathcal{P}_2)$ .*

*Proof.* Suppose that  $B_j$  is empty,  $v \in B'_j$ . Then  $v$  is the endpoint of an initially parallel region  $B \subset B'_j$  (Figure 52). However, such a region may only be completed by a region whose boundary contains one of the pair  $y_{e_{2j-1}}, y_{e_{2j}}$ , a contradiction. □

Observe then that, if  $B_1$  is empty, Lemma 4.20 implies that  $B'_1$  is empty, and so by Observation 4.17 it follows that the collection of entries of  $\pi_\alpha$  up to the largest index of a basic region of  $B'_1$  (i.e.  $\{1, 2, \dots, e_3-1\}$ ) appear in  $\pi_\alpha$  as a nested subword.

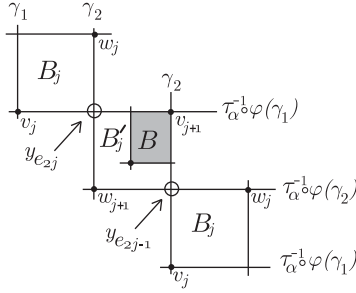


FIGURE 52. Figure for Lemma 4.20

Our strategy is then to proceed by modifying the surface  $\Sigma$  via a sequence of punctures, which will have the effect of removing all regions  $\mathcal{R}(\mathcal{P}_1, \mathcal{P}_2) \setminus \mathcal{R}(\mathcal{P}_1^*, \mathcal{P}_2^*)$ , and isolating each of the fixed points  $y_{e_j}$ . This will allow us to generalize Lemma 4.19 to apply to each region of  $\mathcal{R}(\mathcal{P}_1^*, \mathcal{P}_2^*)$ , and then show that the ‘overlapping regions’ which characterize the non-nested case are an obstruction to consistency.

We begin by defining our sequence of modifications. Given  $\mathcal{P}_i^*$  as in Lemma 4.15, let  $\Sigma^j$  be the surface given by deleting a pair of points from a neighborhood of each of the midpoints  $\{y_{e_k} \mid e_k \leq 2j\}$  as in Figure 53. To be precise, we chose a neighborhood about each such point such that the restriction of  $\{\gamma_1, \gamma_2, \tau_\alpha^{-1}(\varphi(\gamma_1)), \tau_\alpha^{-1}(\varphi(\gamma_2))\}$  to this neighborhood is a pair of arcs with a single intersection point, so these arcs divide the neighborhood into 4 ‘quadrants’, two of which are filled by  $B_j$  and  $B'_j$ . We then delete a neighborhood of a point in the interior of each of the other two quadrants (Figure 53). Note that this has the effect of removing from  $\mathcal{R}(\mathcal{P}_1, \mathcal{P}_2)$  each region which contains either of these points, so that each midpoint is isolated in the new region set.

Observe that our arcs  $\gamma_i$  as well as their images are preserved by this construction, so may be viewed as lying on each of the  $\Sigma^j$ , and similarly the mapping class  $\tau_\alpha^{-1} \circ \varphi$  can be viewed as an element of each  $\Gamma_{\Sigma^j}$ .

We then inductively define a sequence of right-positions  $\mathcal{P}_i^j$  for the pairs  $(\tau_\alpha^{-1} \circ \varphi, \gamma_i)$  for each surface  $\Sigma^j$ , where each  $\mathcal{P}_i^j$  is obtained from  $\mathcal{P}_i^{j-1}$  by removing any point either in the interior of  $B_j$  or in the interior of its boundary.

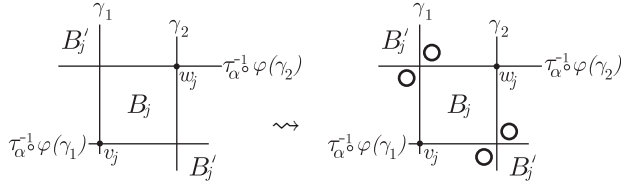


FIGURE 53. Modification  $\Sigma^{j-1} \rightsquigarrow \Sigma^j$ . The thick circles indicate boundary components.

Finally:

**Lemma 4.21.** *The above modification process is such that, for each  $\Sigma^j$ , the pair  $\mathcal{P}_1^j$  and  $\mathcal{P}_2^j$  is consistent, and furthermore  $\mathcal{R}(\mathcal{P}_1^*, \mathcal{P}_2^*) \subset \mathcal{R}(\mathcal{P}_1^j, \mathcal{P}_2^j)$ .*

*Proof.* The proof is by induction on  $j$ : The base step, that on  $\Sigma$  the original positions  $\mathcal{P}_i$  satisfy the conditions, is trivial. Suppose then that the conditions hold for  $\Sigma^{j-1}$ ,  $\mathcal{P}_1^{j-1}$ , and  $\mathcal{P}_2^{j-1}$ . Observe that, as the deletion process ensures that for each  $k < j$ ,  $B_k$  is empty, and each pair  $y_{e_{2k-3}}, y_{e_{2k-2}}$  isolated, it follows from Lemma 4.20 that each region  $B_1, B'_1, B_2, \dots, B_{j-1}, B'_{j-1}$  is empty in  $(\mathcal{P}_1^{j-1}, \mathcal{P}_2^{j-1})$ . Consider then  $\Sigma^j$ ,  $\mathcal{P}_1^j$  and  $\mathcal{P}_2^j$ .

We first show that the pair  $(\mathcal{P}_1^j, \mathcal{P}_2^j)$  is consistent: there is an obvious inclusion of  $\mathcal{R}(\mathcal{P}_1^j, \mathcal{P}_2^j)$  in  $\mathcal{R}(\mathcal{P}_1^{j-1}, \mathcal{P}_2^{j-1})$ , so we must show that, if  $B \in \mathcal{R}(\mathcal{P}_1^{j-1}, \mathcal{P}_2^{j-1})$  does not survive the deletion process (i.e.  $B$  has an endpoint in  $B_j$  or contains one of  $y_{e_{2j-1}}, y_{e_{2j}}$ ), then the same is true for any completing region  $B'$ . Figure 54 indicates the setup. Observe that  $B$  cannot contain  $B_j$ , as each such region either has an endpoint in  $B'_{j-1}$  or contains one of the points  $\{y_{e_k} \mid k \leq 2j-2\}$ . Suppose then  $B$  is a region with endpoint  $v$  in  $B_j$  (Figure 54(a)). Then, as  $B'_{j-1}$  is empty, and the pair  $y_{e_{2j-3}}, y_{e_{2j-2}}$  isolated,  $B$  has a midpoint in  $B_j$ . But then any completing region  $B'$  either contains one of the points  $\{y_{e_{2j-1}}, y_{e_{2j}}\}$ , or has an endpoint in  $B_j$ . In either case  $B'$  does not survive. If, on the other hand,  $B$  has no endpoint in  $B_j$ , then  $B$  must contain one of the points  $\{y_{e_{2j-1}}, y_{e_{2j}}\}$  (Figure 54(b)), and again have a midpoint in  $B_j$ , so any completing  $B'$  again does not survive.

It is left then to show that no region of  $\mathcal{R}(\mathcal{P}_1^*, \mathcal{P}_2^*)$  is removed through the deletion process, but this follows from the argument of Lemma 4.19. Indeed, in the triple  $(\Sigma^{j-1}, \mathcal{P}_1^{j-1}, \mathcal{P}_2^{j-1})$ , the region  $B'_{j-1}$  is empty, and the points  $\{y_{e_{2j-3}}, y_{e_{2j-2}}\}$  are isolated. Thus by Lemma 4.19,  $B_j$  contains no point of  $\mathcal{P}_1^* \cap \mathcal{P}_2^*$ , and the points  $\{y_{e_{2j}}, y_{e_{2j-1}}\}$  are isolated in  $\mathcal{R}(\mathcal{P}_1^*, \mathcal{P}_2^*)$ .  $\square$

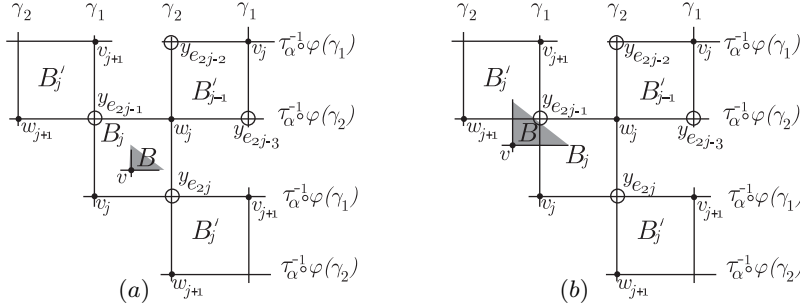


FIGURE 54. The setup for the argument of Lemma 4.21. As usual, the figure illustrates the situation in the universal cover of the surface; lifts of a common object are labeled identically.

We are now able to complete Theorem 4.13:

*Proof.* (of Theorem 4.13) By Lemma 4.16, we only need to show that, for  $\alpha$  balanced with respect to  $D$ ,  $\alpha \in p.e.(\varphi)$  only if  $\alpha$  is nested with respect to  $D$ . So, given balanced  $\alpha \in p.e.(\varphi)$ , let  $\mathcal{P}_i$  be consistent right positions for  $(\tau_\alpha^{-1} \circ \varphi, \gamma_i)$ ,  $i = 1, 2$ , and let  $\mathcal{P}_i^* \subset \mathcal{P}_i$  be as in Lemma 4.15. But by Lemma 4.21, each midpoint of each region  $B \in \mathcal{R}(\mathcal{P}_1^*, \mathcal{P}_2^*)$  is isolated in  $\mathcal{R}(\mathcal{P}_1^*, \mathcal{P}_2^*)$ , and so by Observation 4.17,  $\alpha$  is nested.  $\square$

## 5. NON-POSITIVE OPEN BOOKS OF STEIN-FILLABLE CONTACT 3-FOLDS

In this section we prove Theorem 1.1 by constructing explicit examples of open book decompositions which support Stein fillable contact structures yet whose monodromies have no positive factorizations. We first introduce a construction, based on a modification of the lantern relation, which allows us to introduce essential left-twisting into a stabilization-equivalence class of open book decompositions. As, by Giroux, elements of such an equivalence class support a common contact manifold, proving the essentiality of this left-twisting (accomplished here using the methods of the previous sections) is sufficient to produce examples of non-positive open books which support Stein-fillable contact structures.

**5.1. Immersed lanterns.** For our construction, we start out on the surface  $\Sigma_{0,4}$  of genus zero with 4 boundary components, and a mapping class with factorization  $\tau_{\epsilon_1}\tau_{\epsilon_2}$  as in Figure 55(a). It is easy to see that this defines an open book decomposition of  $S^1 \times S^2$  with the standard (and unique) Stein fillable contact structure. We use the well known lantern relation to give a mapping class equivalence between the words indicated in Figure 55(a) and (b), thus introducing a (non-essential) left twist about the curve  $\alpha$  into the positive monodromy. To make room for what is to come, we must enlarge the surface by adding a 1-handle (Figure 55(c)) to the support of the lantern relation, so that the associated open book decomposition is of  $\#^2(S^1 \times S^2)$ , with its (also unique) Stein fillable contact structure (recall that stabilization-equivalence to an open book with positive monodromy is sufficient to show Stein fillability of the supported contact manifold). Note in particular that this operation does not change the property of Stein fillability. We then stabilize by plumbing a positive Hopf band, use this stabilization curve to braid two of the lantern curves into a new configuration in which the lantern relation does not apply, and then destabilize to a book in which, as the lantern is unavailable, the left twist about  $\alpha$  can no longer be canceled. The steps are indicated clearly in the remainder of Figure 55. As none of the steps (c) through (f) affect the supported contact structure, we have obtained an open book decomposition, supporting a Stein-fillable contact structure, which has no obvious positive factorization. We refer to this construction as an *immersed lantern* relation. To motivate this terminology, observe that the surface and curves of Figure 55(f) are obtained from those of Figure 55(c) by a self plumbing of the surface. Figure 56 summarizes the construction.

The remainder of this section uses the results of Section 4 to demonstrate that the left-twisting introduced by the ‘immersed lantern’ is in fact essential. We also show how this result generalizes to give similar examples of other open books with the same page.

**5.2. The positive extension of  $\varphi'$ .** Our method of demonstrating essentiality of the left twisting introduced by the immersed lantern is as follows: Let  $\varphi = \tau_{\delta_1}\tau_{\delta_2}\tau_{\beta_1}\tau_{\beta_2}\tau_{\alpha}^{-1}$ , where all curves are as in Figure 55, and define  $\varphi' := \tau_{\alpha} \circ \varphi = \tau_{\delta_1}\tau_{\delta_2}\tau_{\beta_1}\tau_{\beta_2}$  (note that  $\alpha$  has no intersection with any of the other curves, so  $\tau_{\alpha}$  commutes with each twist). Suppose that  $\varphi$  has positive factorization  $\tau_{\alpha_n} \cdots \tau_{\alpha_1}$ . Then we may factorize  $\varphi' = \tau_{\alpha}\tau_{\alpha_n} \cdots \tau_{\alpha_1}$ . Our goal is then to derive a contradiction by showing that  $\alpha \notin p.e.(\varphi')$ . This subsection comprises of two steps. Firstly, we show that  $\alpha$  has trivial intersection with each curve in  $p.e.(\varphi')$ , and secondly use this to conclude that  $\alpha \notin p.e.(\varphi')$ .

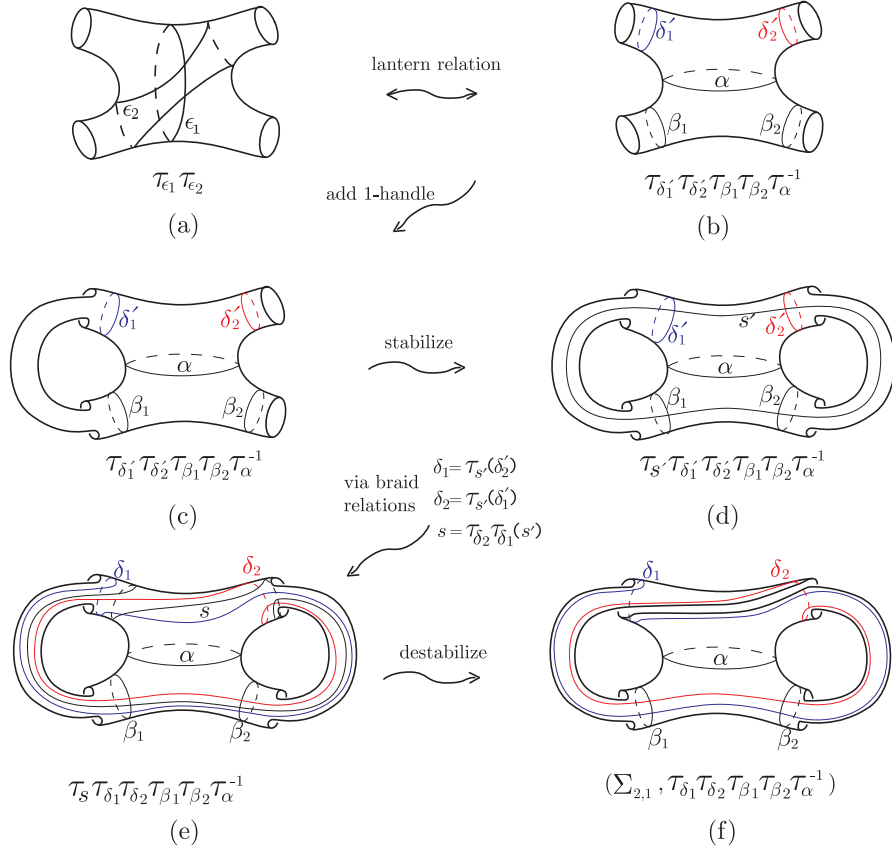


FIGURE 55.  $(\#^2(S^1 \times S^2), \xi_{st}) = (\Sigma_{2,1}, \tau_\alpha^{-1} \tau_{\delta_1} \tau_{\delta_2} \tau_{\beta_1} \tau_{\beta_2})$ .

For the first step, we wish to show that  $p.e.(\varphi')$  lies entirely on  $\Sigma \setminus \alpha$  by applying the results of Section 4 to the pair  $\gamma_1, \gamma_2$  shown in Figure 57. Observe firstly that  $\Sigma \setminus \{\gamma_1, \gamma_2\}$  is a pair of pants bounded by  $\beta_1, \beta_2$ , and  $\alpha$ , and so these three curves are the only elements of  $SCC(\Sigma)$  which have no intersection with  $\{\gamma_1, \gamma_2\}$ . The region  $(D, \varphi')$  is flat (Definition 4.3), and so by the results of Section 4, and in particular Theorem 4.13, each curve  $\epsilon \in p.e.(\varphi') \setminus \{\beta_1, \beta_2, \alpha\}$  is type 1, nested, and balanced. This brings us to:

**Lemma 5.1.** *Let  $\Sigma$ ,  $\alpha$  and  $D$  be as in Figure 57, and  $\epsilon \in SCC(\Sigma)$  be type 1, nested, and balanced on  $D$ . Then  $\epsilon \cap \alpha = \emptyset$*

The remainder of this subsection will bring together the necessary information to prove this Lemma. We will assume throughout that  $\epsilon \cap D$  has no vertical segments (if this were not the case, then  $\epsilon \cap D$  would have no horizontal segments, and we would simply exchange  $\gamma_i$  and  $\tilde{\gamma}_i$  throughout the proof).

So as to simplify our view of the situation, we begin by cutting  $\Sigma$  along  $\tilde{\gamma}_i, i = 1, 2$ , keeping track of the points  $\epsilon \cap \tilde{\gamma}_i$  (see Figure 58). The resulting surface is a pair of pants  $\Sigma'$  with points  $\epsilon \cap \tilde{\gamma}_i$  labeled as in Figure 58, which are connected by  $m$  embedded, nonintersecting arcs  $\epsilon \cap \Sigma'$ . Examples are given in Figure 59.

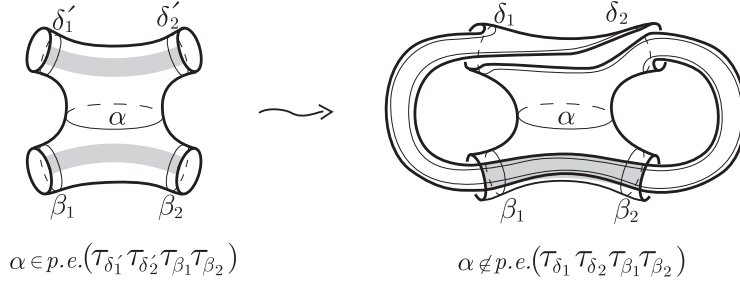


FIGURE 56. Immersing a lantern: To the left, curves of the lantern relation. In particular, a positive twist about each boundary parallel curve is sufficient to cancel a negative twist about the curve  $\alpha$ . To the right, the curves in an ‘immersed’ configuration for which the cancellation no longer holds. Topologically, one obtains the immersed configuration by a self-plumbing of the surface; i.e. an identification of the shaded rectangles via a  $90^\circ$  twist as in the figure. As open book decompositions, one gets from one picture to the other by the steps of Figure 55. The effect on the contact manifold is a connect sum with  $S^1 \times S^2$ , with the standard (Stein-fillable) contact structure.

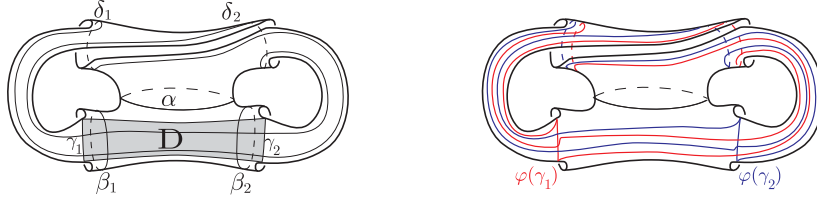


FIGURE 57. To the left, the arcs  $\gamma_i, \bar{\gamma}_i$ , and the region  $D$ . To the right, the images  $\varphi'(\gamma_1), \varphi'(\gamma_2)$

Observe that each arc in  $\epsilon \cap \Sigma'$  corresponds to a pair  $(i, j)$  of consecutive entries in  $\pi_\epsilon$ , where  $i, j$  are the indices of the arc endpoints (so, e.g., if there is an arc with endpoints  $\{p_4, r_3\}$ , then 3, 4 appear consecutively in  $\pi_\epsilon$ ). Also recall that the first and last entries of  $\pi_\epsilon$  are considered consecutive. We call a set of parallel arcs a *multiarc*. We call a multiarc *symmetric* if it is a symmetric multipath in  $\epsilon$  (Definition 4.10). Observe that each symmetric multiarc is contained in a (necessarily symmetric) multipath, while a symmetric multipath may be broken into multiple multiarcs, of which only one is symmetric.

Recall (Definition 4.11) that  $\pi_\epsilon$  is nested if and only if it may be reduced to the trivial by successive removal of consecutive pairs  $a, b$  of entries, where each such pair is the indices of the endpoints of a component of a symmetric (multi)path of  $\epsilon, D$ .

As a final observation, the *balanced* property is equivalent to the requirement that each component of each symmetric multiarc either has each endpoint on  $\partial_1$ , or one endpoint on each of  $\partial_2$  and  $\partial_3$ .

We summarize various observations concerning arcs  $\epsilon \cap \Sigma'$  in the following:

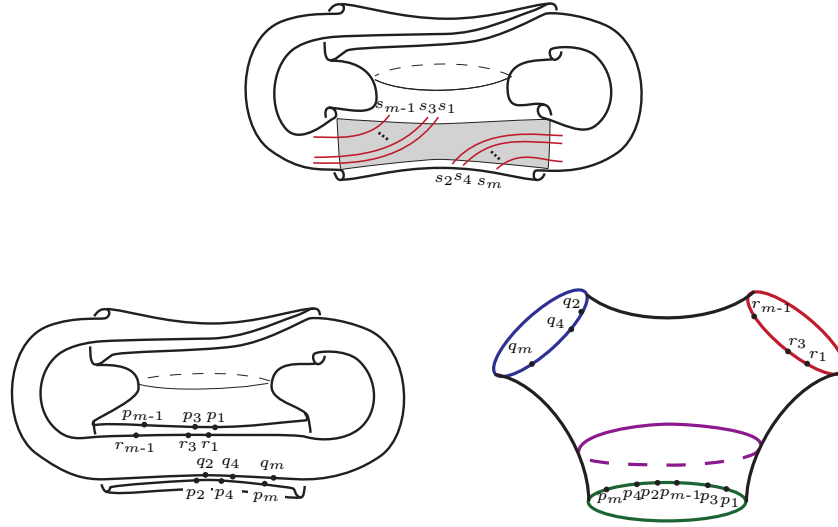


FIGURE 58. (a) indicates the diagonal arcs  $\{s_i\} = \epsilon \cap D$  on  $\Sigma$ , while (b) and (c) illustrate the construction of  $\Sigma'$  by cutting  $\Sigma$  along two edges of  $D$ , as well as indicating the notation for the various boundary points used in the Lemma.

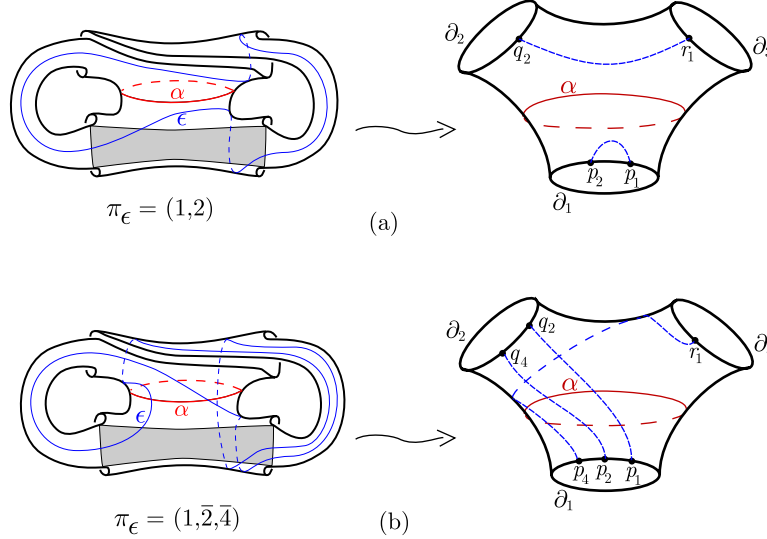


FIGURE 59. (a) A nested, balanced curve  $\epsilon$  in  $\Sigma$ , and the result of cutting  $\Sigma$  as in Lemma 5.1. As demonstrated in Theorem 4.13, such  $\epsilon$  cannot intersect  $\alpha$ . Note that each arc  $\epsilon \cap \Sigma$  is symmetric. (b) A curve  $\epsilon$  which is neither nested nor balanced. None of the arcs are symmetric.

**Lemma 5.2.** *Let  $\Sigma, \Sigma', \alpha$  and  $D$  be as above, and components of  $\partial\Sigma'$  labeled  $\partial_i$ ,  $i = 1, 2, 3$ , where  $\partial_1$  is parallel to the curve  $\alpha$ . Then if  $\epsilon$  is a balanced and nested curve on  $D$ ,*



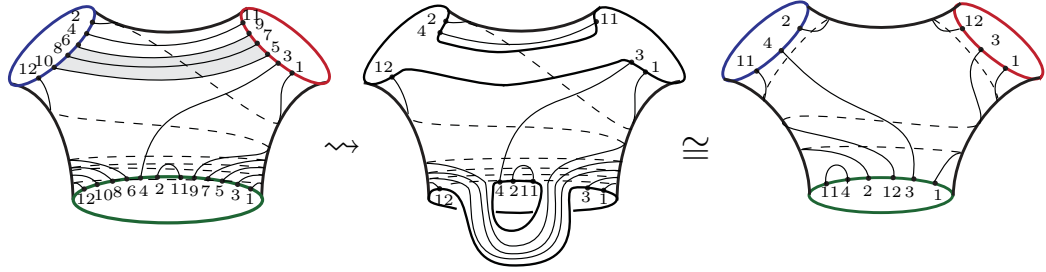


FIGURE 60. Reduction of a symmetric multipath. The multiarc in  $\Sigma'$  is shaded. Here  $\pi_\epsilon = (1, 12, 9, 6, 7, 8, 5, 10, 3, 4, 11, 2)$ . The curve  $\epsilon$  is neither nested nor balanced. Note that we are now suppressing the  $q, r$  and  $p$ 's.

- (1) No component of  $\epsilon \cap \Sigma'$  has both endpoints in  $\partial_2$  or both endpoints in  $\partial_3$ .
- (2) Any component of  $\epsilon \cap \Sigma'$  with both endpoints in  $\partial_1$  is boundary-parallel.

*Proof.* Each of these can be seen from Figure 58. For (1), suppose there is some arc  $\gamma \in \epsilon \cap \Sigma'$  with each endpoint on  $\partial_2$ . Now if  $\gamma$  is boundary-parallel, then it corresponds to either a bigon bounded by  $\epsilon$  and one of the  $\bar{\gamma}_i$ , contradicting intersection minimality, or a downward arc  $\epsilon \cap D$ , so  $\epsilon$  is not type 1, a contradiction. The same argument shows that there is no boundary parallel arc with both endpoints on  $\partial_3$ . If however  $\gamma$  is *not* boundary parallel, it separates  $\Sigma'$  into two annulus components, one of which contains a proper subset of  $\epsilon \cap \partial_2$  on one boundary component, while the other boundary component is the original  $\partial_3$ . This annulus must then contain some boundary parallel arc connecting points of  $\partial_3$ , a contradiction.

For (2), any arc with each endpoint on  $\partial_1$  which is not boundary-parallel would separate  $\Sigma'$  into two annuli so that one annulus has the points  $\epsilon \cap \partial_2$  on one component, and some subset of the points  $\epsilon \cap \partial_1$  on the other, while the other annulus has the points  $\epsilon \cap \partial_3$  on one component, again some subset of the points  $\epsilon \cap \partial_1$  on the other. But there are a total of  $m - 2$  remaining points of  $\epsilon \cap \partial_1$ , while  $\epsilon \cap \partial_i$  for  $i = 2, 3$  contains  $m/2$  points. This would then necessitate some arc parallel to  $\partial_2$  or  $\partial_3$ , contradicting (1). □

5.2.1. *The un-nesting sequence.* Now, given a balanced and nested  $\epsilon$ , by definition there is a sequence of ‘un-nestings’, i.e. deletions of pairs of consecutive entries corresponding to symmetric multipaths, which reduce  $\pi_\epsilon$  to the empty word. We write this sequence as  $\pi_\epsilon =: \pi_1 \rightsquigarrow \pi_2 \rightsquigarrow \dots \rightsquigarrow \pi_n = \emptyset$ , where each  $\rightsquigarrow$  represents removal of all entries associated to some multipath.

For the initial un-nesting, let  $R \subset \Sigma'$  be a disc-neighborhood of the multiarc corresponding to the entries to be removed. Observe that, by deleting  $R$  from  $\Sigma'$ , and then reattaching  $R$  to the resulting surface(s) as a one-handle in the obvious way, we obtain a new (possibly disconnected) subsurface of  $\Sigma$  such that  $\epsilon$  intersects the boundary of the new subsurface in  $2w$  fewer points, where  $w$  is the number of components of the multiarc (Figure 60 illustrates the construction). We continue to obtain a sequence  $\Sigma' =: \Sigma'_1 \rightsquigarrow \Sigma'_2 \rightsquigarrow \dots \rightsquigarrow \Sigma'_n$  such that each arc  $\epsilon \cap \Sigma'_j$  corresponds to a pair of consecutive entries in  $\pi_j$ . In particular,  $\epsilon$  is a simple closed curve in the interior of  $\Sigma'_n$ .

The key observation then is that, if the multiarc corresponding to the initial un-nesting connects boundary components  $\partial_2$  and  $\partial_3$ , then  $\Sigma'_2$  will again be a pair of pants, and contain  $\alpha$ . Moreover, this process preserves certain properties of the configuration (listed in Definition 5.3) which allow us to iterate the process until we arrive at a pair of pants containing both  $\alpha$  and  $\epsilon$ , so that the two can have no non-trivial intersection.

**Definition 5.3.** A pair  $\Sigma'_j, \pi_j$  in the above reduction sequence is *standard* if:

- (1)  $\Sigma'_j$  is a pair of pants containing  $\alpha$ . We label the boundary component parallel to  $\alpha$  as  $\partial_1(\Sigma'_j)$ .
- (2) Each symmetric multiarc either has all endpoints on  $\partial_1$ , or connects the remaining two boundary components.
- (3)  $\partial_1(\Sigma'_j)$  contains each entry of  $\pi_j$ , ordered such that there can be at most one symmetric multiarc with endpoints on this boundary component.
- (4) Each pair of entries  $k, k + 1$ , for  $k$  odd, of  $\pi_j$  has one entry in each of the remaining boundary components, ordered such that there can be at most two symmetric multiarcs connecting the two components.

Figure 61 outlines a slightly different characterization of these conditions.

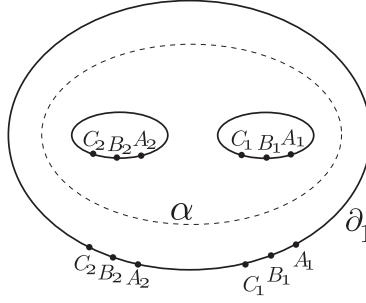


FIGURE 61. An illustration of the conditions of Definition 5.3. Suppose  $\{1, 2, \dots, m\} / \sim$ , where  $j \sim k \Leftrightarrow j$  and  $k$  are entries in a common symmetric multipath, has exactly three classes  $[A], [B]$ , and  $[C]$ . As  $\epsilon$  is nested, each class has an even number of elements, split into pairs as endpoints of components of symmetric multipaths. We divide each class as  $[A] = A_1 \cup A_2$  (similarly for  $[B]$  and  $[C]$ ), such that each element of  $A_1$  is connected to an element of  $A_2$  by a component of a symmetric multipath. Then condition (2) of the definition simply states that no symmetric multiarc crosses  $\alpha$  exactly once, while (3) and (4) are satisfied if and only if the splitting can be done such that in addition the classes are distributed as drawn. The figure generalizes in the obvious way to the case of arbitrarily many classes.

**Lemma 5.4.** *The reduction sequence can be chosen such that each pair  $\Sigma'_j, \pi_j$  is standard.*

*Proof.* By induction on  $j$ . For  $j = 1$ , condition (1) is trivial, condition (2) is an immediate consequence of the *balanced* condition, and conditions (3) and (4) follow

from construction of  $\Sigma'$  along with condition (2). Suppose then that  $\Sigma_j$  is adapted to  $\pi_j$ . We will show that the same is true for  $\Sigma_{j+1}$  and  $\pi_{j+1}$ . There are two cases:

- (1)  $\Sigma'_j \cap \epsilon$  contains a symmetric multiarc with no endpoints on  $\partial_1(\Sigma'_j)$ . The effect on the configuration of a reduction via this multiarc is most easily seen through the characterization given in Figure 61. In particular, one of the equivalence classes of indices is removed, and the indices of some of the splittings of equivalence classes are permuted (Figure 62 gives an example). Neither of these affect the conditions.

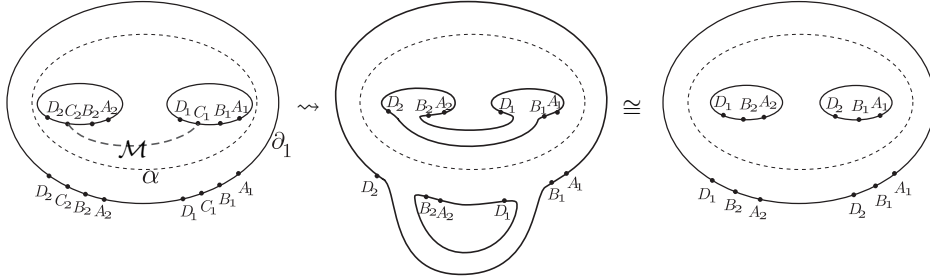


FIGURE 62. Effect of reduction in the case of a multipath  $\mathcal{M}$  with no endpoint on  $\partial_1$ .

- (2) Otherwise, the configuration contains a unique symmetric multiarc  $\mathcal{M}$ , as the conditions ensure that there can be at most one with endpoints on  $\partial_1$ . Observe then that any symmetric multiarc of the pair  $\Sigma'_{j+1} \cap \epsilon$  must be an extension of (possibly a sub-multiarc of)  $\mathcal{M}$ . Our goal is to show that any two such extensions must be components of a common symmetric multiarc, which is therefore the *unique* symmetric multiarc of  $\Sigma'_{j+1} \cap \epsilon$ , and use this to derive a contradiction.

So, let  $\eta_{a,b}$  and  $\eta_{c,d}$  be components of  $\mathcal{M}$ , and suppose these extend to symmetric  $\eta_{a',b'}$  and  $\eta_{c',d'}$  in  $\Sigma'_{j+1}$ . The extensions  $[a, a']$ ,  $[b, b']$ ,  $[c, c']$  and  $[d, d']$  are thus arcs in the initial configuration  $\epsilon \cap \Sigma'$ .

Consider then the original surface  $\Sigma'$ , and the collection of arcs consisting of the innermost symmetric multiarc  $\mathcal{M}_0$  of the multipath  $\mathcal{M}$  (i.e. the multiarc whose endpoints are first removed by the un-nesting sequence) and the extension arcs  $[a, a']$ ,  $[b, b']$ ,  $[c, c']$  and  $[d, d']$ . There are again two cases:

- (a) The innermost multiarc  $\mathcal{M}_0$  has all endpoints on  $\partial_1$ . By Lemma 5.2,  $\mathcal{M}_0$  must be boundary parallel in  $\Sigma'$ . So, following property (3) of Definition 5.3,  $\mathcal{M}_0$  separates a disc  $D$  of  $\Sigma'$  such that each pair of entries  $a, b$  with the property that  $\eta_{a,b}$  is a component of a symmetric multiarc other than  $\mathcal{M}_0$  has exactly one element in  $\partial(D)$  (Figure 63(a)). In particular, one of the extension arcs (say  $[a, a']$ ) has an endpoint in  $D$ , so it is contained in  $D$  and extends in parallel fashion with  $[c, c']$ , and thus for symmetry the same is true of  $[b, b']$  and  $[d, d']$ .
- (b)  $\mathcal{M}_0$  connects  $\partial_2$  and  $\partial_3$  (Figure 63(b)). Then the complement of  $\mathcal{M}_0$  is an annulus. Suppose that some extension arc (again  $[a, a']$ ) is boundary parallel in this annulus. Then for symmetry the same is true of  $[b, b']$ , which then forces one (and therefore, for symmetry, both) of

$[c, c']$  and  $[d, d']$  to be boundary parallel, so that they extend as a common multipath. If, on the other hand, none of the arcs are boundary parallel, observe that the arcs  $[a, a']$  and  $[b, b']$  cut the complement of  $\mathcal{M}_0$  into a pair of discs, one containing both arcs  $[c, c']$  and  $[d, d']$ , which thus must be parallel to  $[a, a']$  and  $[b, b']$ .

Thus each  $\Sigma'_l$ , for  $l > j$ , will again contain a unique symmetric multiarc. This then gives a contradiction, as for nestedness  $\Sigma'_{n-1}$  must contain exactly two symmetric multiarcs. □

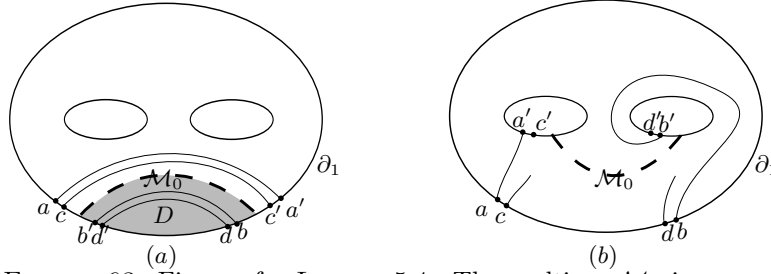


FIGURE 63. Figures for Lemma 5.4. The multiarc  $\mathcal{M}_0$  is represented by the dashed arc in the figures.

The proof of Lemma 5.1 then follows immediately, as  $\Sigma'_n$  is a pair of pants containing both  $\alpha$  and  $\epsilon$ , so these can have no non-trivial intersection.

We bring all of this together with:

**Theorem 5.5.** *The monodromy of the open book decomposition  $(\Sigma, \varphi)$  of  $(\#^2(S^1 \times S^2), \xi_{st})$  shown in Figure 55(f), where  $\xi_{st}$  is the unique Stein-fillable structure, has no factorization into positive Dehn twists.*

*Proof.* Suppose that  $\varphi$  is positive, so  $\tau_\alpha^{-1} \tau_{\delta_1} \tau_{\delta_2} \tau_{\beta_1} \tau_{\beta_2} = \tau_{\alpha_n} \cdots \tau_{\alpha_1}$ . Then  $\varphi' := \tau_{\delta_1} \tau_{\delta_2} \tau_{\beta_1} \tau_{\beta_2} = \tau_\alpha \tau_{\alpha_n} \cdots \tau_{\alpha_1}$ ; i.e.  $\alpha \in p.e.(\varphi')$ . Then, by Lemma 5.1, each  $\alpha_i$  has trivial intersection with  $\alpha$ . But then  $\alpha$  must be an element of the step-down (Definition 2.3)  $\mathcal{C}_{\tau_\alpha \tau_{\alpha_n} \cdots \tau_{\alpha_1}}(\gamma) = \mathcal{C}_{\varphi'}(\gamma)$  for any properly embedded arc  $\gamma$  which intersects  $\alpha$  exactly once. The choice of  $\gamma$  shown in Figure 64 then gives a contradiction. □

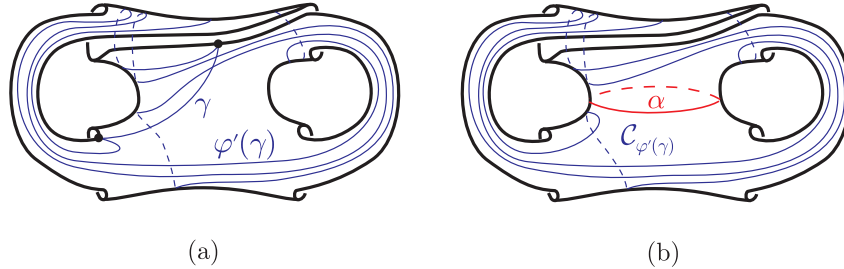


FIGURE 64. (a) The arc  $\gamma$ , and its image  $\varphi'(\gamma)$ . (b) The stepdown  $\mathcal{C}_{\varphi'}(\gamma)$ , and the curve  $\alpha$ ; clearly  $\alpha \notin \mathcal{C}_{\varphi'}(\gamma)$

**5.3. Further examples.** We conclude with some observations allowing immediate generalizations of Theorem 5.5.

*Observation 5.6.* Let  $\psi \in \Gamma_{\Sigma_{2,1}}$  have a factorization  $\psi' \circ \varphi'$ , where  $\psi'$  is positive, and  $\varphi'$  as in the previous subsection. Then  $\psi \circ \tau_\alpha^{-1} = \psi' \circ \varphi' \circ \tau_\alpha^{-1}$ , and so, following the notation of Figure 55, the open books  $(\Sigma_{2,1}, \psi \circ \tau_\alpha^{-1})$  and  $(\Sigma_{2,2}, \psi' \circ \tau_{\epsilon_1} \tau_{\epsilon_2} \tau_{s'})$  are stabilization-equivalent, and in particular each support a Stein-fillable contact structure.

*Observation 5.7.* Let  $\psi \in \Gamma_{\Sigma_{2,1}}$  be such that  $(\psi, D)$  is flat and parallel (where  $D$  is as in Figure 58), and  $\alpha \notin \mathcal{C}_{\psi(\gamma)}$  (where  $\gamma$  is as in Figure 64). Then the proof of Theorem 5.5 holds for  $\varphi'$  replaced by  $\psi$ ; i.e. the monodromy  $\psi \circ \tau_\alpha^{-1}$  has no positive factorization.

For example,  $\psi := \tau_{\delta_1}^{e_1} \tau_{\delta_2}^{e_2} \tau_{\beta_1}^{e_3} \tau_{\beta_2}^{e_4}$  clearly satisfies these conditions for any positive integers  $e_i$ , so that the resulting open book decomposition  $(\Sigma_{2,1}, \tau_\alpha^{-1} \circ \psi)$  is stabilization-equivalent to  $(\Sigma_{2,2}, \tau_{\delta_1}^{e_1-1} \tau_{\delta_2}^{e_2-1} \tau_{\epsilon_1} \tau_{\epsilon_2} \tau_{s'} \tau_{\beta_1}^{e_3-1} \tau_{\beta_2}^{e_4-1})$ , thus supports a Stein-fillable structure, yet its monodromy has no positive factorization. As a simple example, for the case  $e_1 = e_2 = e_3 = 1$ , we obtain an open book decomposition of  $(S^1 \times S^2) \# L(e_4 - 1, e_4 - 2)$  for each  $e_4 \geq 2$  (Figure 65).

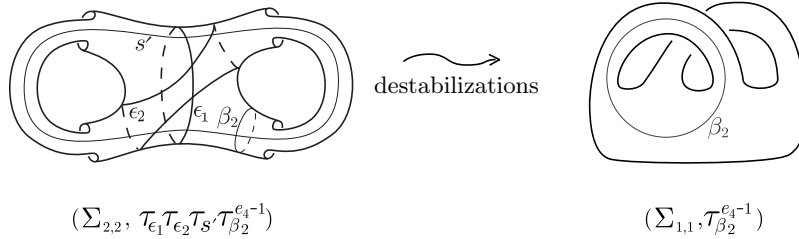


FIGURE 65.  $(\Sigma_{2,2}, \tau_{\epsilon_1} \tau_{\epsilon_2} \tau_{s'} \tau_{\beta_2}^{e_4-1}) = ((S^1 \times S^2) \# L(e_4 - 1, e_4 - 2), \xi_{st})$

REFERENCES

[AO] S. Akbulut, B. Ozbagci, *Lefschetz fibrations on compact Stein surfaces*, *Geom. Topol.* 5 (2001), 319334.  
 [BEV] K. Baker, J. Etnyre, J. Van Horn Morris, *Cabling, contact structures, and mapping class monoids*, 2010, arXiv:1005.1978v1  
 [CH] V. Colin, K. Honda, *Reeb vector fields and open book decompositions*, 2008. arXiv:0809.5088  
 [EO] J. B. Etnyre and B. Ozbagci, *Invariants of contact structures from open books*, *Trans. Amer. Math. Soc.* 360 (2008), no. 6, 3133–3151. arXiv:math/0605441v1  
 [E1] J. B. Etnyre, *Planar open book decompositions and contact structures*, *IMRN* 79 (2004), 4255–4267. arXiv:math/0404267v3  
 [FM] B. Farb, D. Margalit *A Primer on Mapping Class Groups*, Princeton University Press 2011.  
 [Gi] E. Giroux, *Géométrie de contact: de la dimension trois vers les dimensions supérieures*, *Proceedings of the International Congress of Mathematicians (Beijing 2002)*, Vol. II, 405–414. arXiv:math/0305129v1  
 [HKM] K. Honda, W. Kazez and G. Matic, *Right-veering diffeomorphisms of compact surfaces with boundary I*, *Invent. Math.* 169 (2007), no. 2, 427–449. arXiv:math/0510639v1  
 [L] Y. Lekili, *Planar open book with four binding components*, 2010 arXiv:1008.3529v2

- [LP] A. Loi, R. Piergallini, *Compact Stein surfaces with boundary as branched covers of  $B^4$* , Invent. Math. 143 (2001), 325348. arXiv:math/0002042v1
- [TW] W. Thurston and H. Winkelnkemper, *On the existence of contact forms*, Proc. Amer. Math. Soc. **52** (1975), 345–347.

